UNITED NATIONS
UNIVERSITY

UNU-GTP

ORKUSTOFNUN

Silica rich waters in Köldulaugagil, Hengill area, SW-Iceland

Ngereja Myabi Mgejwa

SUB-SURFACE GEOLOGY, PETROCHEMISTRY AND HYDROTHERMAL ALTERATION OF WELLS MW-03, MW-09 AND MW-20 FROM MENENGAI GEOTHERMAL FIELD, KENYA

Report 4
December 2016

SUB-SURFACE GEOLOGY, PETROCHEMISTRY AND HYDROTHERMAL ALTERATION OF WELLS MW-03, MW-09 AND MW-20 FROM MENENGAI GEOTHERMAL FIELD, KENYA

MSc thesis
School of Engineering and Natural Sciences
Faculty of Earth Sciences
University of Iceland

by

Ngereja Myabi Mgejwa
Ministry of Energy and Minerals
P.O. Box 2000
Dar es Salaam
TANZANIA
ngereja.mgejwa@mem.go.tz

INTRODUCTION

The Geothermal Training Programme of the United Nations University (UNU) has operated in Iceland since 1979 with six month annual courses for professionals from developing countries. The aim is to assist developing countries with significant geothermal potential to build up groups of specialists that cover most aspects of geothermal exploration and development. During 1979-2016, 647 scientists and engineers from 60 developing countries have completed the six month courses, or similar. They have come from Africa (38%), Asia (36%), Latin America (14%), Europe (12%), and Oceania (1%). There is a steady flow of requests from all over the world for the six-month training and we can only meet a portion of the requests. Most of the trainees are awarded UNU Fellowships financed by the Government of Iceland.

Candidates for the six-month specialized training must have at least a BSc degree and a minimum of one-year practical experience in geothermal work in their home countries prior to the training. Many of our trainees have already completed their MSc or PhD degrees when they come to Iceland, but many excellent students with only BSc degrees have made requests to come again to Iceland for a higher academic degree. From 1999 UNU Fellows have also been given the chance to continue their studies and study for MSc degrees in geothermal science or engineering in co-operation with the University of Iceland. An agreement to this effect was signed with the University of Iceland. A similar agreement was also signed with Reykjavik University in 2013. The six-month studies at the UNU Geothermal Training Programme form a part of the graduate programme.

It is a pleasure to introduce the 49th UNU Fellow to complete the MSc studies under a UNU-GTP Fellowship. Ngereja Myabi Mgejwa, BSc in Geology from the Ministry of Energy and Minerals in Tanzania, completed the six-month specialized training in Borehole Geology in 2011. His research report was entitled: *Borehole geology and hydrothermal alteration of well HE-55 at Hellisheidi geothermal field, SW–Iceland.* After three years of geothermal work in Tanzania, he came to Iceland for MSc studies at the University of Iceland, School of Engineering and Natural Sciences, starting in August 2014. In May 2016, he defended his MSc thesis presented here, entitled: *Sub-surface geology, petrochemistry and hydrothermal alteration of wells MW-03, MW-09 and MW-20 from Menengai geothermal field, Kenya.* His studies in Iceland were financed by the Government of Iceland through a UNU-GTP Fellowship from the UNU Geothermal Training Programme. We congratulate him on his achievements and wish him all the best for the future. We thank the School of Engineering and Natural Sciences, Faculty of Earth Sciences at University of Iceland for the co-operation, and his supervisors for the dedication.

Finally, I would like to mention that Ngereja's MSc thesis with the figures in colour is available for downloading on our website *www.unugtp.is*, under publications.

With warmest greetings from Iceland,

Lúdvík S. Georgsson, Director
United Nations University
Geothermal Training Programme

ACKNOWLEDGEMENTS

DEDICATION

This work is dedicated to my parents Hellena and Samson Mgejwa.

ABSTRACT

The Menengai geothermal field is one of the high temperature geothermal systems in Kenya. It is seated within the Great East Africa Rift System in the Central Kenyan Rift Valley and covered by Quaternary volcanics. The study wells, MW-03, MW-09 and MW-20, were drilled inside the Menengai caldera, which is characterized by ring faults, the Molo TVA which trends NNW-SSE and the Solai TVA which trends NNE-SSW direction. The volcano formed about 200,000 years ago and the prominent 12 x 8 km caldera about 8000 years ago. Binocular and petrographic microscopes, XRD-analysis, ICP analysis and temperature logs were applied for the research. In the study wells, fine-coarse grained trachytes, pyroclastics, tuffs, basalts and intrusives (syenite) were observed. Based on Al_2O_3 concentration and total K_2O + Na_2O, the analysed rocks are metaluminous compared to the neighbouring wells MW-04, MW-06 and MW-07. The geochemical evolution of Menengai rocks seems to be mainly controlled by fractional crystallization. However, more than one process is involved. The relationship between trace elements with depth in wells MW-03, MW-09 and MW-20 depict four volcanic episodes which may be related to Menengai caldera formation.

The study defined seven hydrothermal alteration zones; Unaltered, zeolite-smectite (40-180°C), quartz (above 180°), illite (220°C), chlorite (above 230°C), epidote (240°C) and wollastonite-actinolite zone (above 280°C). Chlorite was noted in MW-03 and MW-20, illite zone was defined in MW-09 and MW-20. In MW-03, illite and actinolite occur at the bottom of the well and wollastonite-actinolite zone is thinning towards MW-03. Based on the alteration minerals and formation temperatures, the wells show indications of heating, where MW-03 appears heating from approximately 1800m. Nine aquifers/feed zones were identified in MW-03, eight in MW-09 and six in MW-20. These feed zones are linked to lithological boundaries, fractures and faults and permeable formations.

Calcite looks to be the dominant alteration mineral in the wells and tends to deposit later than higher temperature alteration minerals at some depths. Calcite forms by; replacing primary minerals such as feldspar, pyroxene and volcanic glass; boiling of the reservoir fluid that causes to the loss of CO_2 leading to calcite precipitates in veins or open spaces and calcite precipitates in veins or fractures when hotter fluid mixes with circulating ground water. Epidote appears to be a rare alteration mineral in the Menengai geothermal field, which could be due to high concentrations of CO_2, low contents of iron in the rocks and thermal fluids which are important for epidote formation.

PREFACE

The author of this thesis will utilize the knowledge, skills and experience gained from this research on Menengai geothermal wells back home in Tanzania. As for now, geothermal exploration in Tanzania is on-going, and drilling is expected to commence in the near future. Menengai geothermal field is within the East African Rift System and most of the geothermal sites in Tanzania are also located in the rift, and may share the same geological settings in some areas.

This thesis was done as part of the partial fulfilment of the degree of Master of Science in Geology and submitted to the University of Iceland, accounting for the 60 ECTS needed for the 120 ECTS required for the degree, and contributes additional input to the existing Menengai geothermal conceptual model.

Ngereja Myabi Mgejwa

TABLE OF CONTENTS

LIST OF FIGURES

LIST OF TABLES

ABBREVIATIONS

GEARS	Great East African Rift System
ISOR	Iceland GeoSurvey
ICP-OES	Inductively Coupled Plasma-Optical Emission Spectroscopy
Ma	Million years
m a.s.l.	Metres above sea level
m b.s.l.	Metres below sea level
MW	Menengai well
Molo TVA	Molo tecto-volcanic axis
TAS	Total alkali vs. silica
Solai TVA	Solai Tecto-Volcanic Axis
TGDC	Tanzania Geothermal Development Company
ppm	parts per million
XRD	X-ray diffractometry

x

1. INTRODUCTION

1.1 Background information

The Menengai geothermal field is one of the high temperature geothermal systems in Kenya. The geothermal field is located a few kilometres south of the equator, and about 10 km north of Nakuru City (Figure 1). The field comprises three main features; the Menengai Caldera, Ol'rongai volcano in the northwest and part of the Solai graben in the northeast. It is seated within the Great East Africa Rift System in the Central Kenyan Rift Valley.

The first detailed study of the Menengai caldera was carried out by McCall (1957a, b, 1964, 1967) describing different features of its geology. The caldera is partly filled by young rugged lava flows and covers an area of about 77km². The rim is marked by a single vertical cliff that varies between 0 and 300 m. The caldera is estimated to be formed at about 0.2 Ma ago and seems to form part of central Kenya Peralkaline field as described by Macdonald et al, (2011). Detailed studies on the Menengai geothermal area started in the 1960s, as shown, for example, by the early work of McCall (1967).

The existence of geothermal energy resources has been evidenced by deep geothermal wells which have been drilled within the caldera (Figure 2).
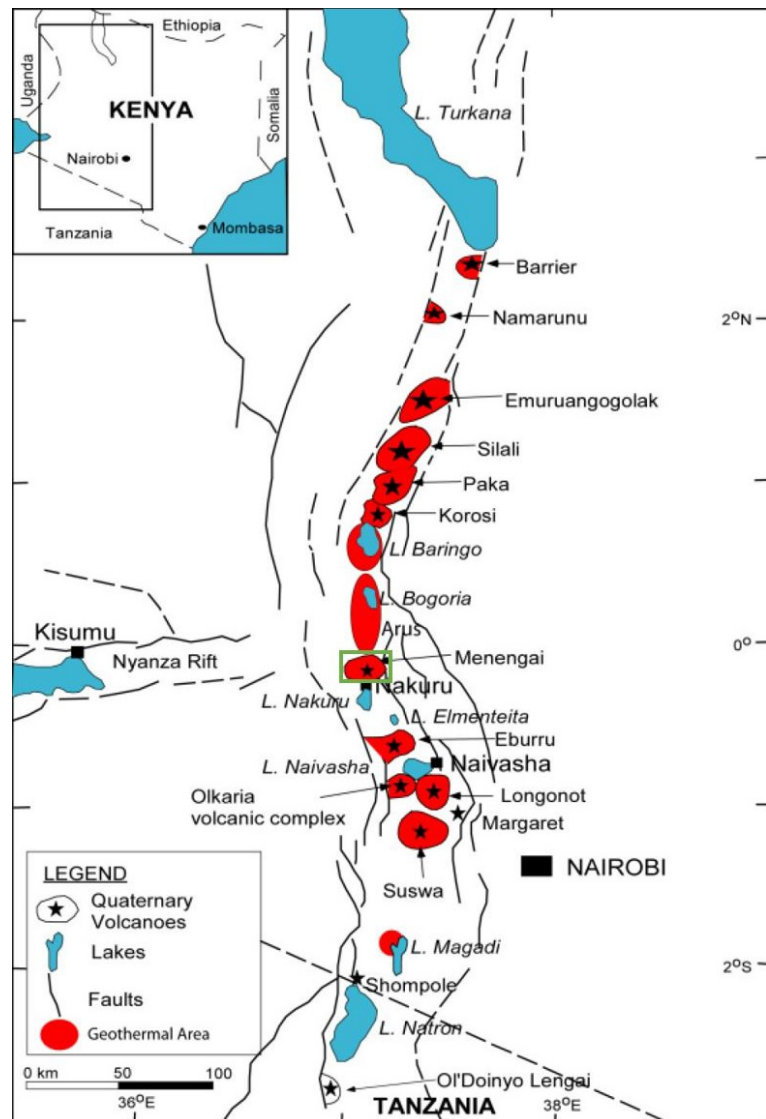
FIGURE 1: Major volcanic centres (Menengai shown by a green rectangle) on the Kenya Rift floor (GDC, 2010)

1.2 Purpose statement

Geothermal resources have been pointed out in Kenya as an important contributor to the nation´s energy mix. By 2020, geothermal resources are expected to supply 2000 MWe, whereby part of this will come from Menengai geothermal field. The field is developed by Geothermal Development Company (GDC). Since 2011 several deep geothermal wells have been drilled and power plant construction is underway for the first 105 MWe. Therefore, more intensive scientific studies at Menengai field are of paramount importance to facilitate further understanding of the geothermal system and ensure constant updates. It is anticipated that results from this study will add more information to the existing conceptual model which will ensure optimum resource utilization.
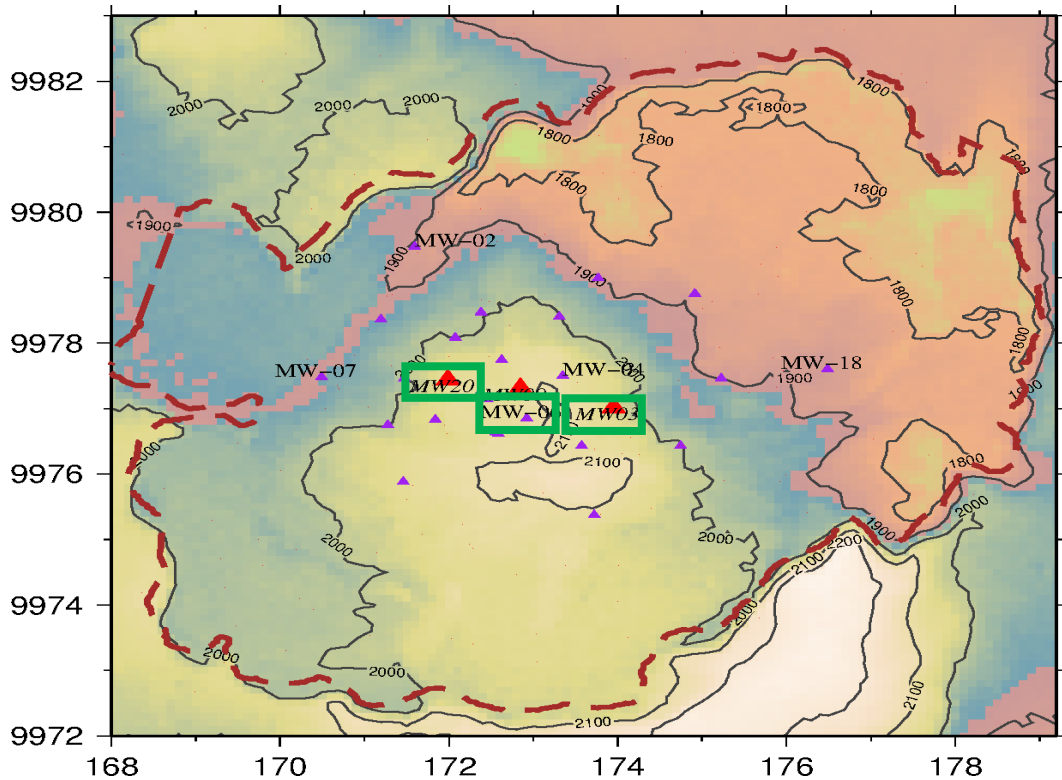
FIGURE 2: Menengai caldera showing study wells (green boxes) and other drilled wells
(modified from GDC, 2014b)

1.3 Objectives of the study

The main objectives of studying Menengai geothermal wells MW-03, MW-09 and MW-20 are to:

- Identify the various rock types in the wells which will lead to the understanding of the lithology and structure in which the geothermal resource is located.
- Identify the hydrothermal alteration and alteration history. This is very important, i.e. with regards to whether the area is in equilibrium or if it is heating or cooling.
- Identify the nature of aquifers and their relationship with lithology and alteration.
- Relate the subsurface results to surface structures such as faults.
- Identify the occurrence of calcite and epidote in Menengai geothermal system and the implication of calcite to permeability.
- Interpret in greater detail the factors that control the geothermal system, including upflow/downflow and permeability in the area surrounding the study wells.
- Ascertain the effect of hydrothermal processes on rock chemistry.

1.4 Geological and structural setting

1.4.1 The Great East African Rift System

The Great East African Rift System (GEARS) is an active intracontinental rift, with suggestively greater volumes of volcanic products on Earth than any other recently active rifts of similar nature. The rift started to form during Miocene about 25 million years ago (Ebinger, 2005). It forms a divergent tectonic plate boundary, in such a way that the African plate tends to split into two plates, the Nubian and Somali protoplates (Figure 3). From the Ethiopian segment southwards, the rift splits into the eastern and western branches. In the Late Tertiary to Recent, the rift has undergone massive volcanism.
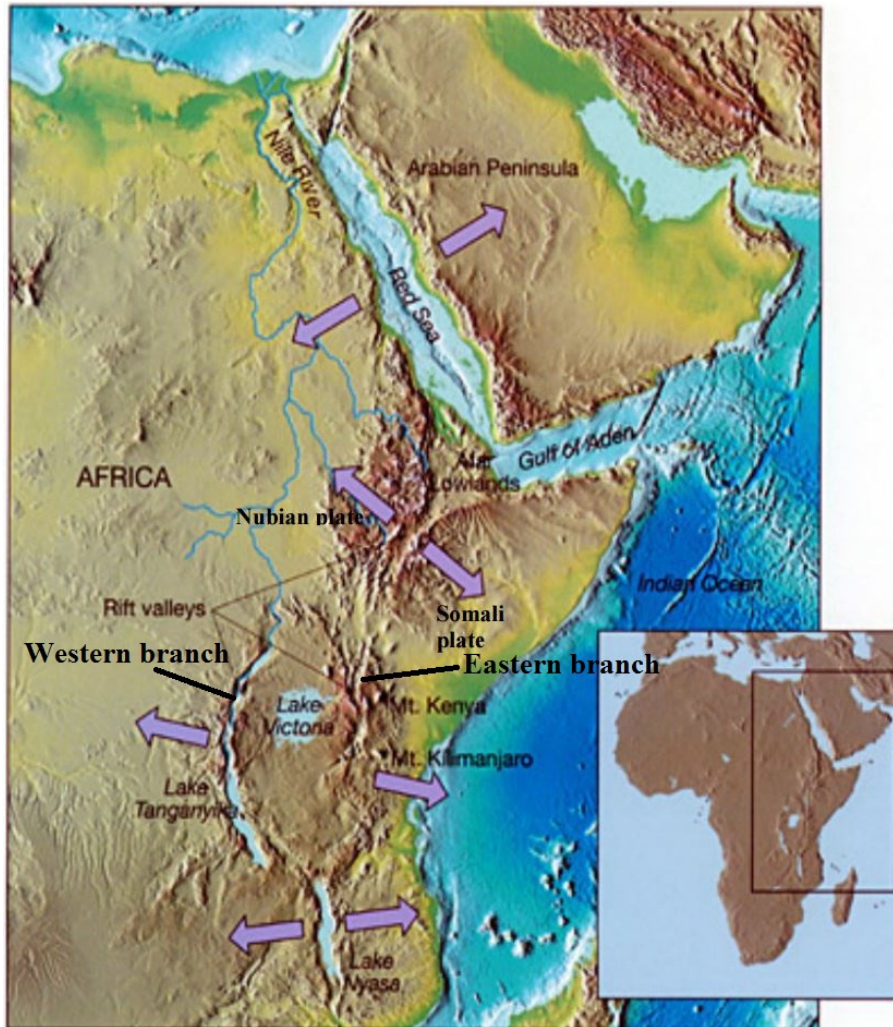
FIGURE 3: East African Rift System; arrows show the directions of
rifting (modified from GDC, 2010)

It runs more than 5,000 km from the Gulf of Aden to Mozambique (e.g. Baker et al., 1972, Leat, 1983; Macdonald, 2002; Omenda, 1997) before reaching Mozambique. The Western and Eastern branches of the rift meet in Mbeya - Tanzania and form a triple junction. The Great East African Rift System is in the process of splitting the African plate into two plates at a rate of about 6.9 mm annually in each direction in the northern part while decreasing to the south to about 1.9 mm annually as noted by Fernandes et al., 2004.

The Kenyan rift forms part of the eastern branch of EARS and is volcanically very active. The Kenyan rift extends from Lake Turkana to northern part of Tanzania and started to open in the early Miocene in the north around Lake Turkana and subsequently migrated southwards (Omenda, 2007). It formed mainly within the basement of the Mozambique belt and close to the margin of the Tanzania craton, particularly at the Eastern margin (Hetzel and Strecker, 1994; Smith and Mosely, 1993). Rogers et al. (2000) pointed out that the Kenyan rift is a volcano-tectonic feature that transects the country extending from Lake Turkana - Kenya in the north to Lake Natron - Tanzania in the south. The tectonics led to the formation of a graben structure with an average width of 40-80 km followed by fissure eruptions and form flood lavas within the axis of the rift, 2-1 Ma, which is the reason for the development of massive large shield volcanoes along the fissures and axes of the rift (Figure 1).

The volcanism that started 35-30 Ma in the Turkana region was followed by normal faulting and extension, estimated currently to be 35-40 km (Rogers et al., 2000). The magmatism has consequently propagated southwards with time, reaching northern Tanzania at 5-8 Ma (Macdonald et al, 2002) since its initiation.

1.4.2 Regional geology

Menengai is mostly composed of Late Quaternary Volcanics on the surface which is related to the development of the Kenyan rift. The lava fields located along N-S trending fissures are composed of trachytic and trachy - phonolitic composition (GDC 2010, Jones 1985, Leat 1983), observed at the scarp walls beyond the Ol'banita swamps, Lomolo and Kisanana areas (Figure 4A and B). These lavas underlie ignimbrites and pyroclastics, possibly originating from Menengai eruptions to the south.
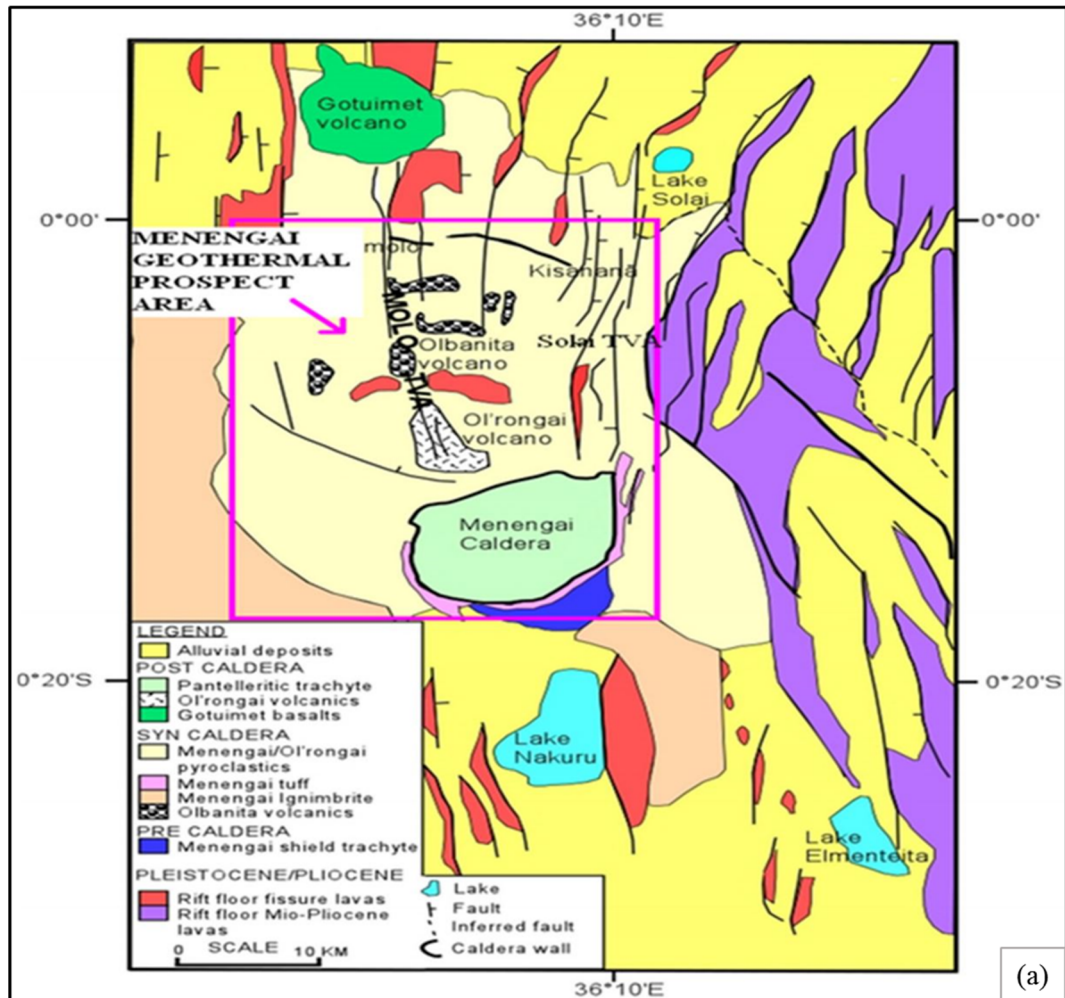
FIGURE 4A: Menengai geological map with its surroundings (GDC, 2010)

Volcanism associated with the rifting started during the Miocene, and continued in the Pliocene. In Pliocene, the volcanism produced the Bahati trachytes and tuffs in the east between 5.1-2.0 ma (Baker et al, 1988) and Kinangop tuffs to the south of 3.4-3.7 ma. The ignimbrite eruptions converted an earlier half graben into a graben. Eruption of Limuru flood trachyte (1.8-2.0 ma) was initiated by the progressive inward migration of fault zones. Between 1.65-09 ma, eruptions of basalts and basaltic trachy-andesites respectively were triggered by faulting that followed the formation of the Limuru flood trachytes (Baker et al., 1988). According to Baker et al. (1988), the faulting was triggered by a convecting mantle, opening up fractures which acted as conduits for volcanic activity (Quaternary volcano) and the development of many large shield volcanoes of silicic composition.

4
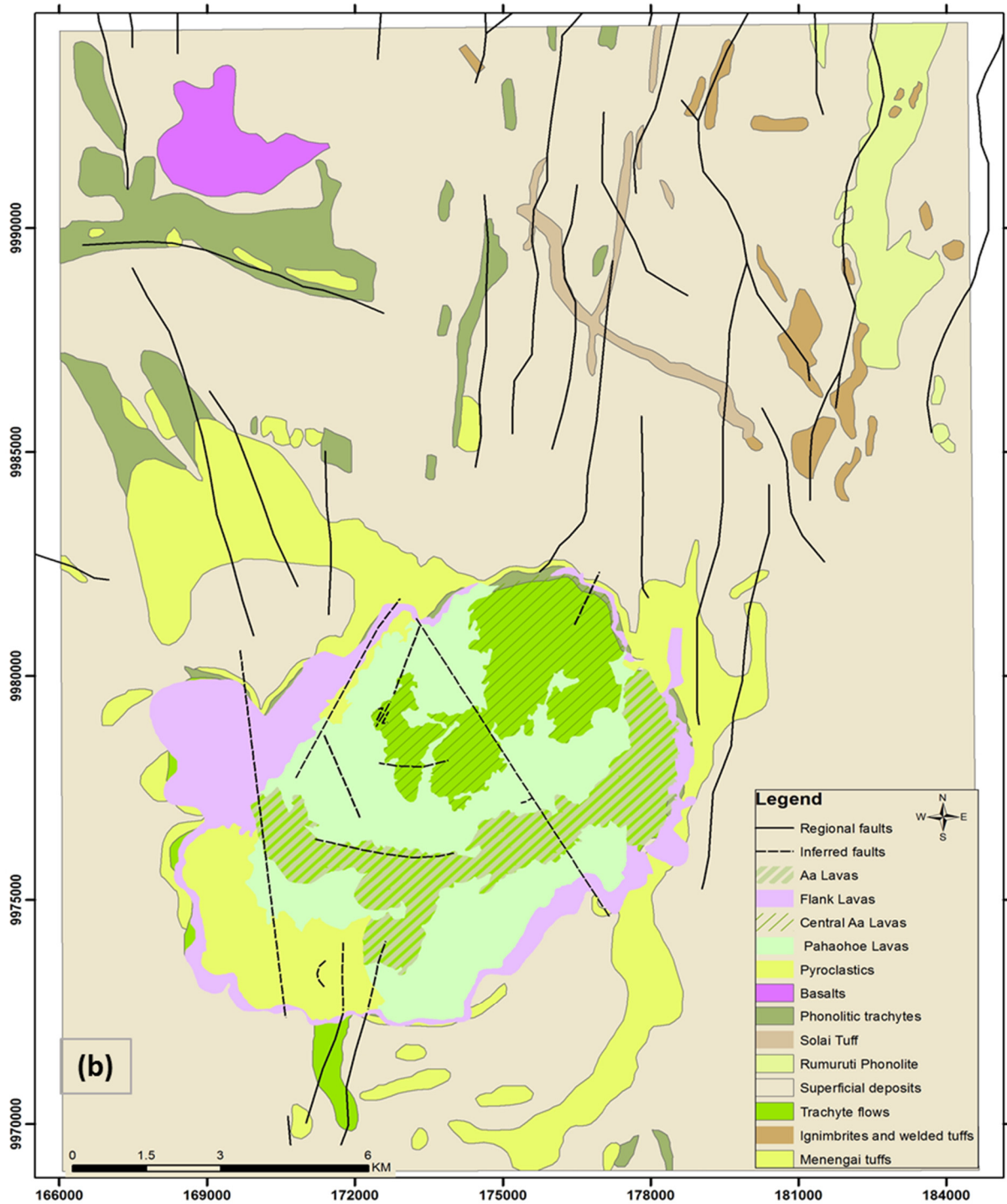
FIGURE 4B: Menengai geological map with its surroundings (GDC, 2010)

1.4.3 Local geology

From a geological point of view, Menengai is a relatively young (<0.2 Ma) caldera volcano seated in the south-central Kenya Rift Valley (Figure 5). The rocks are classified into three main groups which formed in 3 different volcanic phases; the Menengai massif lavas correspond to pre-caldera formations, the pyroclastics that formed during the caldera collapse (syn-caldera) and the glassy lavas that erupted after the collapse. These rocks are exposed in and around Menengai (e.g. GDC, 2010; Leat, 1984). The age and composition of Menengai volcano is similar to Quaternary volcanoes like Suswa, Longonot, Naivasha-Olkaria and Eburru, which accumulated on the floor of Rift Valley south of Menengai (Leat, 1984).
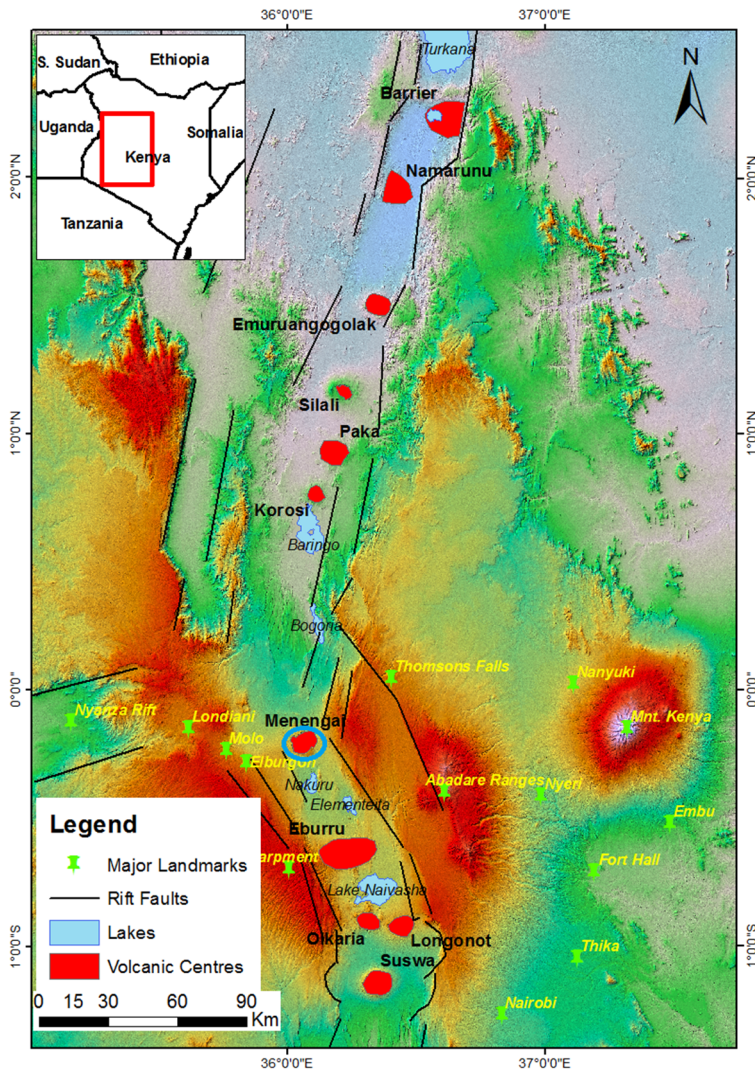
FIGURE 5: Digital elevation model showing volcanic centres including Menengai (blue circle) and the south-central Kenya Rift Valley (modified from Ofwona, 2002)

The pre-caldera volcanics are exposed in the caldera wall from Lion´s Head (Figure 6) west towards West Cliff (Leat, 1984) and the West tuffs form most of the pre caldera pile. In the south, West Cliff shows a transition between pre-caldera successions composed of lavas and tuffs (Figure 6). The tuffs in the NW are mostly coarse and contain poorly vesicular pumice according to Leat (1984). The pre-caldera lavas have been dated to be about 0.18- .01 ma (Leat, 1983) and the lavas are described as mainly of trachytic composition and containing over 95% of sanidine crystallites with insignificant amounts of riebeckite/arfvedsonite.

Two ash flow tuffs represent the Syn-caldera activity and these tuffs were both preceded by pumice falls (Leat, 1984, 1991). The first (representing about 20 km^3 of magma) is separated from the second (representing about 30 km^3 of magma) by sediment beds up to 4 m thick. Both ash flows were emplaced as single flow units and have outflow sheet aspect ratios of about 1:4,000. Half the volume of the combined ash flow sheet was ponded in the caldera (Leat, 1984, 1991). During the syn-caldera, huge volumes of magma (50km^3) erupted, suggesting the presence of a high

level magma chamber under Menengai caldera (Leat, 1984).

The post caldera activity produced mainly air fall pumice deposits and cinder cones by Strombolian eruption(s) (Leat, 1984). Therefore, the older flows are covered with these deposits in the caldera. Most of the eruptions are separated by soil horizons indicating a hiatus between individual eruptions. The total volume of magma erupted during post caldera volcanism is estimated to be approximately 25km^3, according to Leat (1984).

1.4.4 Subsurface geology and geothermal manifestations

The subsurface geology of Menengai geothermal field has been studied since the start of drilling in 2011 by Omondi (2011), Mibei (2012), Kipchumba (2013), Lopeyok (2013), Kahiga (2014), Mbia (2014), and Mutua (2015). The studies concentrated on analysing drill cuttings and provided crucial information on the geothermal system, particularly stratigraphy, hydrothermal alteration and history of the system. From these studies, characteristic alteration zones in Menengai are recognized based on distribution of

6

key index minerals such as zeolites, smectites, chlorite, quartz, epidote and actinolite. Furthermore, different rocks such as trachyte, pyroclastics, trachy-basalt, phonotephrite, trachyte andesite, tuff, phonolite, rhyolite, and basalt and syenite intrusives in Menengai have been identified in many wells.

The apparent indicators of geothermal activity include the young volcanism represented by the numerous recent eruptions both inside and outside the caldera, the large caldera collapse and significant tectonics resulting in intense faulting of the area. The hydrothermal activity at Menengai shows several surface expressions like fumaroles, steaming ground, and geothermal grass scientifically known as Fimbristylis exilis. Occurrence of all manifestations mentioned above signifies hydrothermal activity and the existence of geothermal reservoirs in the area.

1.4.5 Structural geology of Menengai

Menengai area consists of three main structures, the Menengai caldera or ring faults, the Molo TVA which trends NNW-SSE and the Solai TVA, which trends NNE-SSW
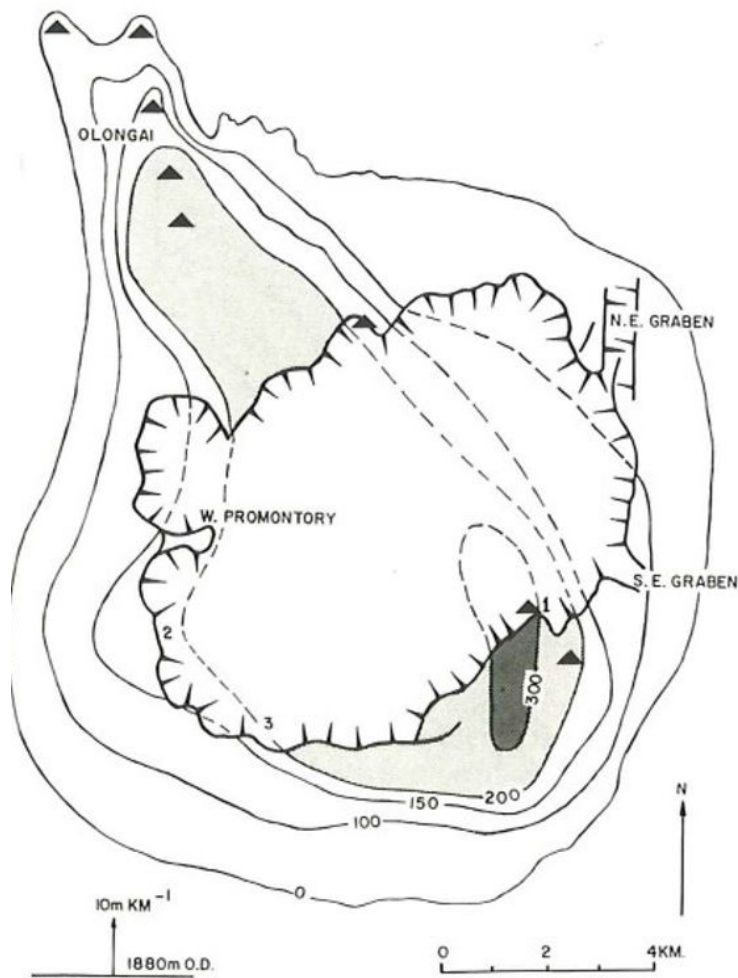
FIGURE 6: Isopach map for the pre caldera volcanics of Menengai. Solid triangles indicate probable or possible pre – caldera vents, point 1 shows Lion's Head Cliff, point 2 shows the West Cliff and point 3 stands for the Southwest Cliff (Leat, 1984)

direction (Figures 4A and 7). The Ol'Rongai structural system marks the larger Molo TVA that has experienced volcanic activity which resulted in the build-up of a NNW-SSE trending ridge. The latter cuts the Menengai caldera at the Northern end and indicates that these faults are younger than the caldera. However, these faults are poorly exposed within the caldera floor but they have a southern extension under the Menengai volcanic pile. The Solai TVA system follows the orientation of the Menengai caldera. Menengai can be explained as a pre-caldera low-angle volcanic shield, which has nearly vertical embayed caldera walls up to 300 m high (Leat, 1983; Macdonald, 2002).

1.4.5.1 The Menengai caldera and ring faults

The Menengai caldera, or ring faults, forms an elliptical depression with minor and major axes measuring about 8 and 12 km (GDC, 2010; Leat, 1983) formed 8000 years ago. Several vents are situated near to the caldera wall, the location of these vents was probably controlled by the ring fracture of the caldera and indicates that magma came up through the caldera fault. Leat (1983) suggested that the ring fracture volcanism is a common feature in GEARS, another example being the Longonot caldera, a few kilometres south of the Menengai caldera.
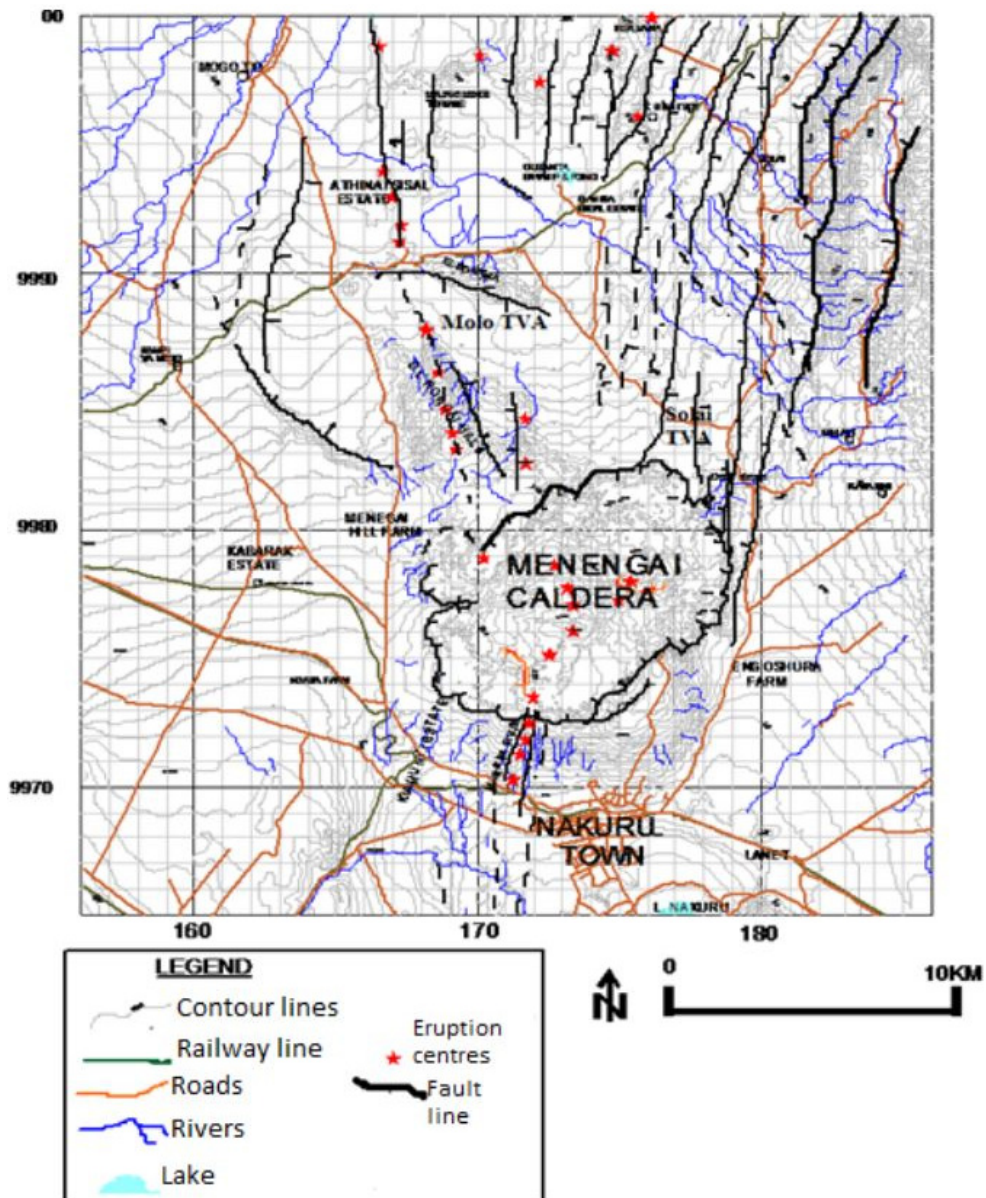
FIGURE 7: Structural map of Menengai showing the orientation of tectonic axes (GDC, 2010)

1.4.5.2 The Molo tectono-volcanic axis (TVA)

The Molo tectono-volcanic axis (TVA) is a prominent volcano-structural feature, represented on the surface by a concentrated zone of faults and fractures along which volcanic eruptions took place in the early Pleistocene (Geotermica Italiana, 1987). The Ol'rongai structural system (Figures 4A and 6) marks a part of the larger Molo TVA that has undergone substantial volcanic activity, which resulted in a build-up of a NNW-SSE trending ridge referred to as the Ol'rongai volcanoes. The apparent strong volcanism indicated by several eruption centres in the western part of Menengai caldera is perhaps due to the intersection of the caldera structures and the Molo TVA or Ol'Rongai fracture system (Kipchumba, 2013).

In the Ol'rongai area, the structure is manifested by intense volcanic activity including an explosive crater (Figure 6). The surface expression of this volcano has been significantly eroded, perhaps by ponding of volcanic materials from Menengai volcano, erosion and sedimentation. However, Simiyu and Keller (1997) noted that gravity highs are present in this area and could reveal the roots or plugs that are remnants of an old magma chamber. Leat (1984) pointed out that the Menengai pre-caldera shield had the same orientation with NW-SE structures and was probably influenced by these faults.

8

Therefore, the Ol'rongai faults seem to be older than the ones in the Solai system which cut into the caldera. The Ol'rongai system extends northwards (Figure 7) through Lomolo and past the Gotuimet volcanic centre on a regional scale (Leat, 1983).

1.4.5.3 The Solai graben (TVA)

The Solai tectonic system is a narrow graben which includes structures that extend NE-SW from the Solai area towards Lake Nakuru, south of the caldera (Figure 7). The system comprises several faults/fractures and strikes in NE-SW and NNE-SSW directions. The western boundary of the graben is associated with the Makalia faults (Mibei and Lagat, 2011), considered to be younger than the Menengai caldera. At the northern end of the caldera, the Menengai pyroclastics seem to be cut only by the Solai system (e.g. Leat, 1991). The Ol'rongai and the Solai TVA appear to converge inside the caldera which may have led to enhanced permeability at that location on the caldera floor (Figures 7 and 8).
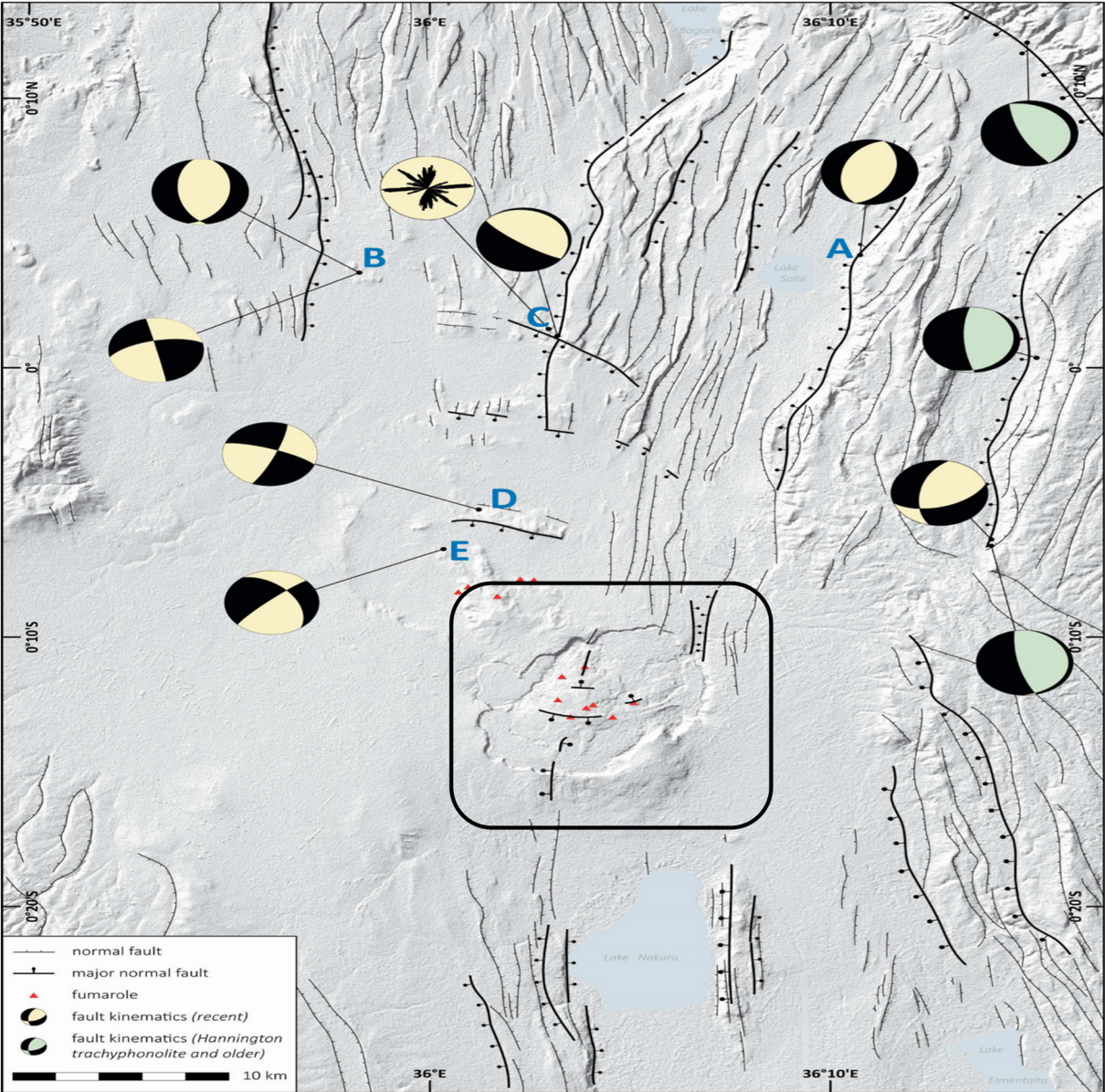
FIGURE 8: Structural overview of the region north of Nakuru (Rectangle showing Menengai caldera) A = East of Lake Solai, B = Alfega quarry, C = road to Kisanana, D = south of Olobanita swamp and E = north of Olongai. Hillshade based on SRTM-X DEM (DLR 2010) and ASTER DEM (NASA 2001) (Modified from GDC, 2013)

1.5 Hydrogeological setting

The Menengai caldera is situated on the floor of the Rift valley and bordered by the Bahati escarpment, Rusinga and Marmanent – Olarabe Rift cliffs to the east and Mau escarpment with the Pekerra River and Kilombe volcano to the west (Figure 9) (Mbia, 2014). The rift floor drainage is mainly from Menengai caldera northwards with the exception of the drainage from the southern rim, or slopes, of the Menengai caldera into Lake Nakuru, as noted by Mungania (2004). Hence, the location of the Menengai caldera is lower in terms of altitude compared to the high rift scarps that form the recharge areas.
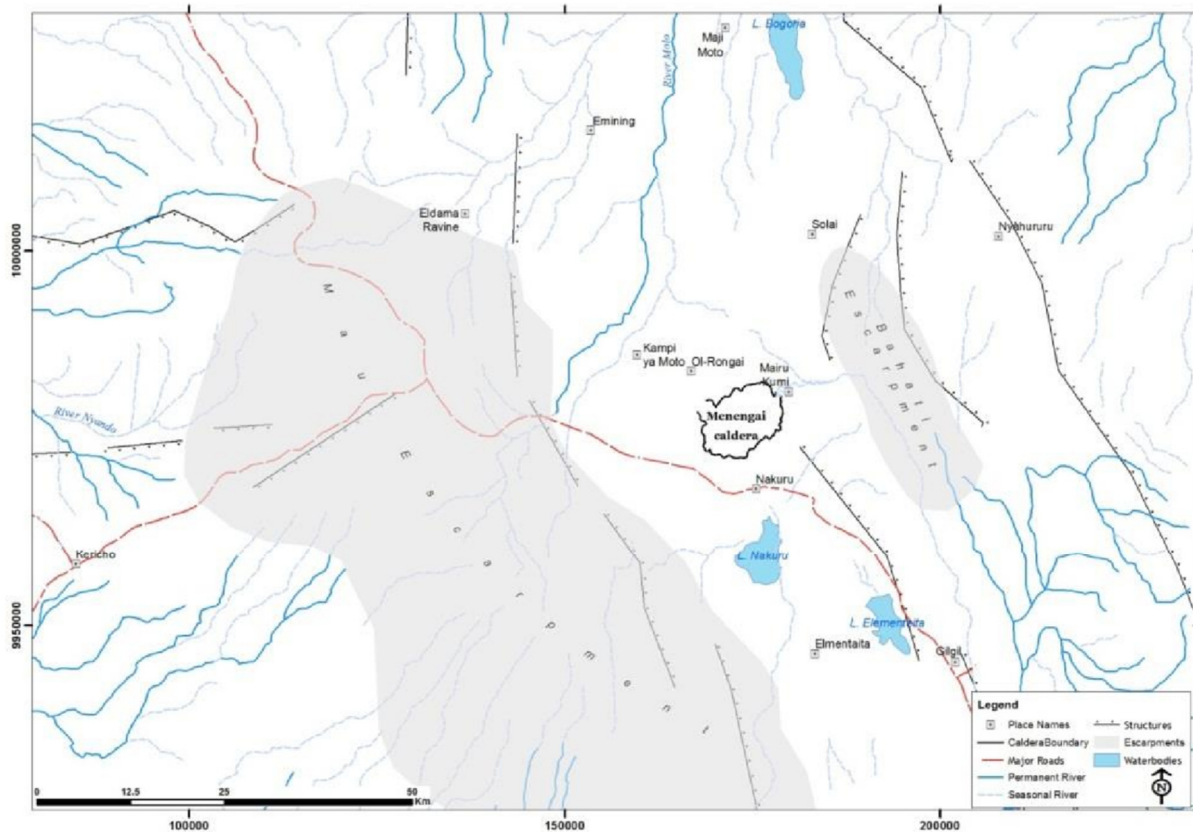
FIGURE 9: Regional hydrogeological map with Menengai area (adapted from Mbia, 2014)

Lake Nakuru is among the highest lakes on the central Kenya dome of the Rift Valley, sitting at 1,760 m a.s.l. which has hydrological implications for the regional water flow pattern. The area comprises permanent rivers such as Molo and Rongai in the NW area (Figure 9). Rivers Njoro and Lamuriak are semi-permanent and flow from the Mau Hills into Lake Nakuru (Figure 9).

The caldera rings faults/fractures and the tectonic volcanic axes provide good recharge channels into the subsurface (Figure 10), from western escarpment (Mau) and eastern escarpment (Aberdare). Intense rift floor fractures and/or faulting provide conducive environment for water to penetrate into the crust towards magma bodies (Lagat, 2011).

1.6 Geophysical Studies

Magnetotelluric (MT) and Transient electromagnetic (TEM) measurements show low resistivity at depth of about 5 km (Figure 11) within the centre of the caldera and extending towards the western margin of the caldera (GDC, 2010). This deeper low resistivity structure, could be envisaged as hot intrusions that could be related to the heat source for the geothermal system at Menengai (GDC, 2010). Geotermica Italiana (1987) showed a large positive gravity anomaly in the central part of the area. They described the anomaly to be related to a dense body located at 3.5-4 km deep having a density of 2.8 g/cm^3, which

could be a heat source for the system. The anomaly concurs within the Molo Volcanic Axis, which is intruded by a sequences of dikes as explained by Simiyu and Keller (1997) and Simiyu (1998). Also, gravity high of 40 mGal was noted from a regional profile across Menengai (Simiyu 1998), showing anomaly which was modelled as intrusive body.
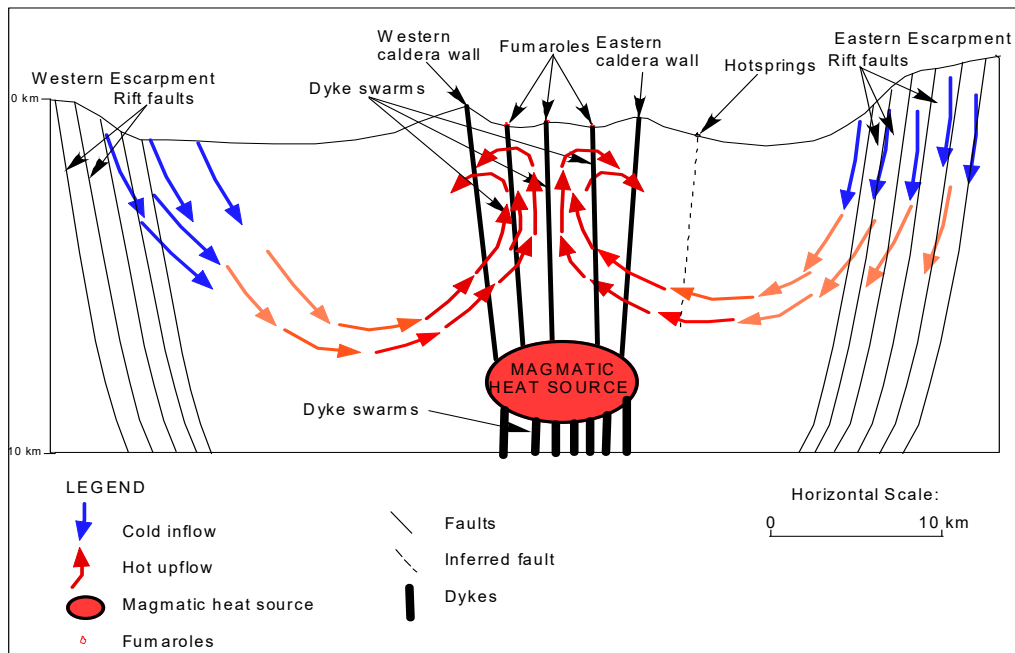
FIGURE 10: Menengai schematic model showing cold inflow and hot outflow
(Modified from GDC 2010)
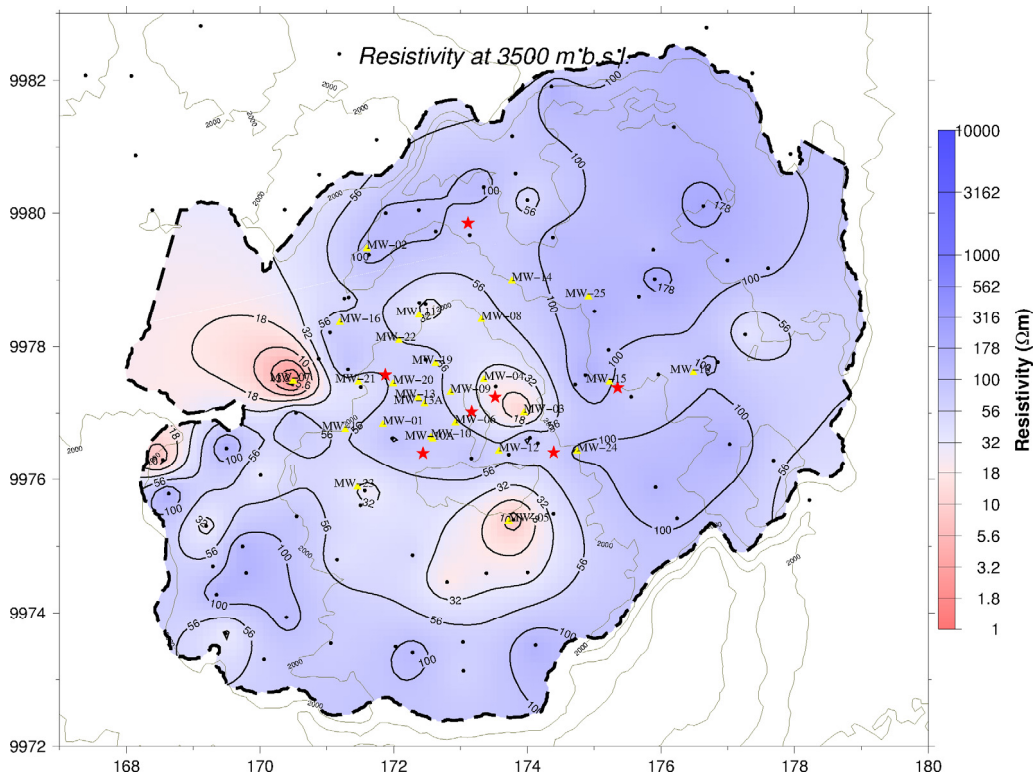
FIGURE 11: Iso-resistivity distribution at 3000 m below sea level in Menengai geothermal prospect. The black circles represent MT/TEM soundings, red stars are the fumaroles and the yellow triangles are the drilled wells (GDC, 2014b)

11

1.7 Geochemical studies

Several geochemical studies have been carried out in the Menengai geothermal field. Geothermal fluids from fumaroles and steaming ground have been sampled at the surface above the Menengai geothermal systems (Figure 12). The analyses indicate high CO_2 contents (>1.2%), particularly along the fractured zones. The CO_2 concentration is structurally controlled. Furthermore, according to GDC (2010), the fracture zones coincide with high Rn-222 activity (anomalous values in the range of 2002-3700 cpm) in the caldera and to the north and northwest out of the caldera.
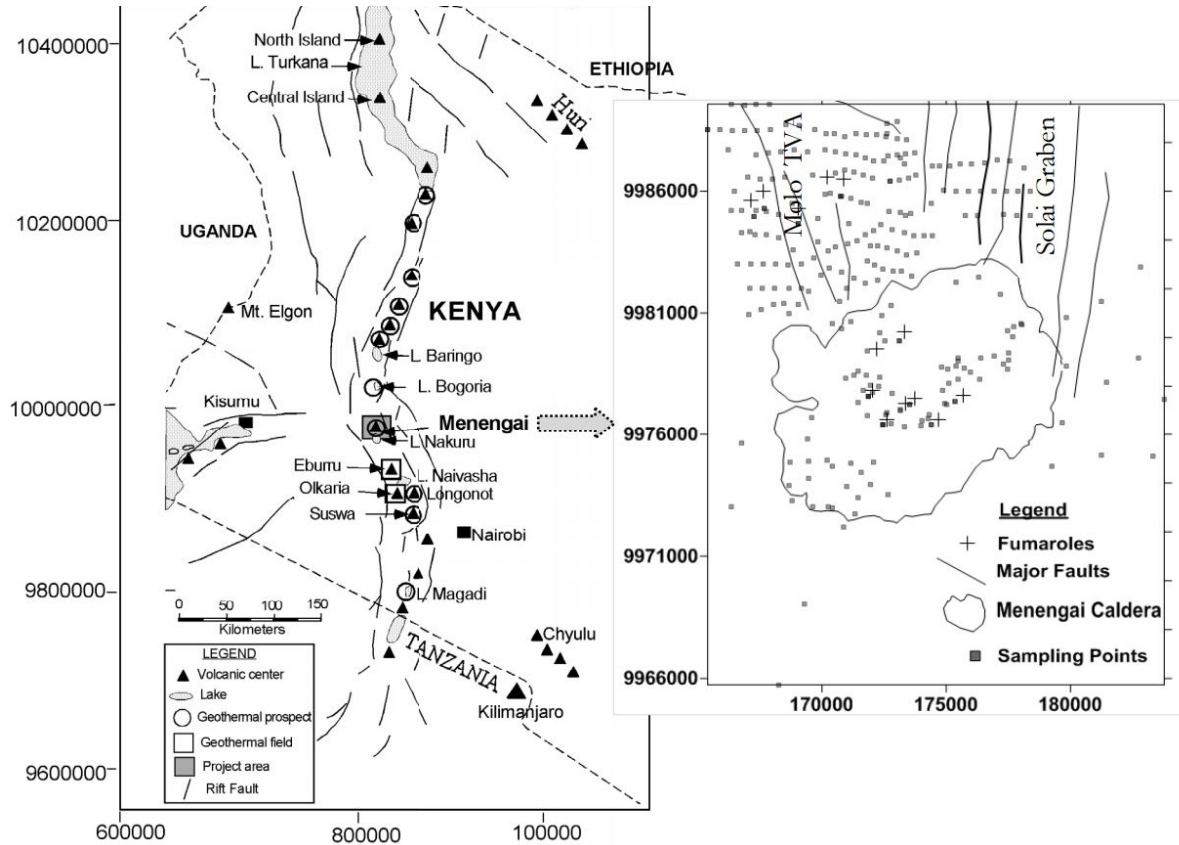
FIGURE 12: Location of Menengai geothermal prospect showing fumaroles,
major faults and sampling points (Kanda, 2013)

The ratio of the two gases Rn and CO_2 is a good indicator for a magmatic source of the gases. In Menengai the high ratios are noted inside the caldera, towards the north and north western parts (Lagat, 2011) (Figure 13).

Based on the concentrations of CO_2, H_2S and H_2 temperatures of the fumaroles were calculated. TH_2S geothermometer gives temperatures in the range of 279-298°C while TH_2S-CO_2 ranges between 274 and 304°C (Kanda, 2013). Mungania et al. (2004) showed that gas geothermometry based on H_2S and CO_2 concentrations indicate reservoir temperatures greater than 250°C.
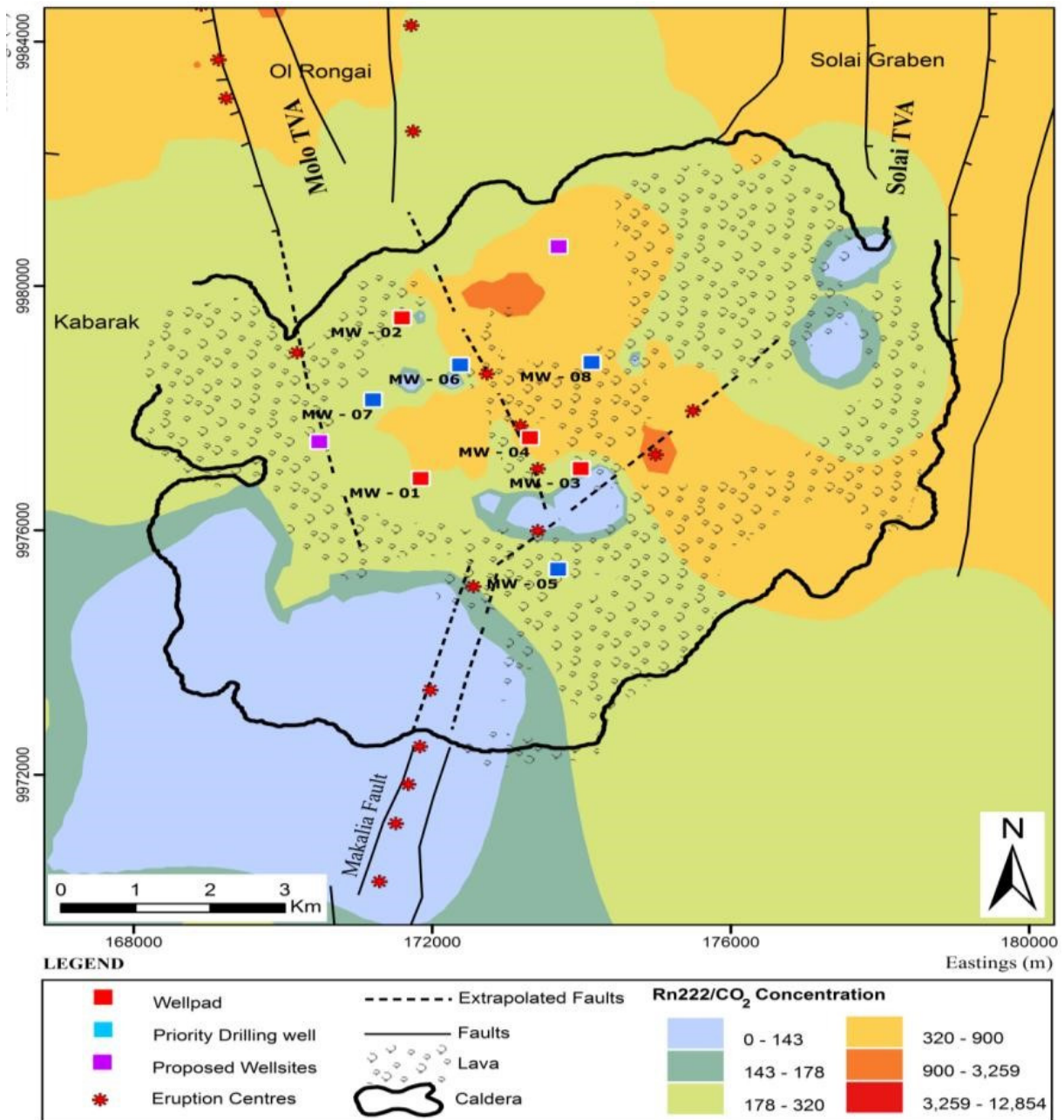
FIGURE 13: Radon/CO$_2$ ratios distribution map (GDC, 2010)

2. METHODOLOGY

2.1 Sampling

For this study drill cuttings were collected from Menengai geothermal wells; MW-03, MW-09 and MW-20. These boreholes have depths of 2106 m, 2077 m and 2461 m respectively. The wells were drilled for 100days from 1st June 2011 to 9th September 2011 for MW-03, 105days for MW-09 from 17th July 2012 to 29th October 2012 and MW-20 took 120days from 7th October 2013 to 3rd February 2014. In all wells the drill cuttings were sampled at every 2 m. The cuttings were analysed using binocular microscope. Representative sample cuttings were selected from different rock types for petrographic, XRD analysis and ICP-OES analysis. The results from binocular and petrographic microscopes, XRD analysis, ICP and previous information were plotted to show lithology, alteration minerals with depth using log plot software (Rock Ware, 2007).

TABLE 1: Information on MW-03, MW-09 and MW-20 of the Menengai geothermal field

Well name	Eastings	Northings	Elevation	Depth (TD) (m)	Production casing (m)	Liners (m)
MW-03	173993	9977009	2957.34	2106	1096.46	2070
MW-09	172848.48	9977331.37	2105	2077	858	2077
MW-20	171989	9977446	2075	2461	1211	2450

2.2 Analytical techniques

Analytical techniques used in this study includes binocular and petrographic microscope, XRD and ICP-OES analyses.

2.2.1 Binocular microscope analysis

The sample cuttings were analysed at the Iceland GeoSurvey (ISOR) laboratory. Washing the samples to remove dusts and impurities before analysing is of paramount importance to enhance the visibility. The washed samples were mounted on a binocular microscope (Wild Heerbrugg Binocular Microscope) to analyse different features such as colour, rock type(s), grain size, veins, oxidation, alteration intensity, alteration minerals, primary minerals and alteration stage and permeable zones. Also, mineral paragenetic sequence is determined with the use of the microscope if the vesicles or veins have not been destroyed by the drill bit, since crushing the rocks by the drill bit cause disappearance of some detailed geological features.

Drill cuttings were analysed carefully since some of the cuttings were mixed with foreign materials including previously drilled units. Most of the foreign materials in the studied wells are cement and mica. Therefore, logging went keenly to identify the actual rock penetrated. Hydrochloric acid was used at this stage to reveal whether the rock consists of or includes calcite. After this analysis, selected representative samples were prepared for petrographic analysis, XRD and ICP analyses.

2.2.2 Petrographic microscope analysis

The petrographic analyses were based on three wells MW-03, MW-09 and MW-20. Samples for thin sections were selected from different lithological units. About 40 thin sections were analysed using Leitz Wetzler petrographic microscope at ISOR, Icelandic GeoSurvey laboratories and Olympus BX51 petrographic microscope at University of Iceland, Earth Institute laboratory. The target was to confirm rock type(s), texture, porosity, vein fillings and alteration minerals. The method was also essential to identify additional minerals which were not observed with the binocular microscope and to study depositional sequences of secondary minerals. The results, of petrographic microscopy together with binocular microscopy, XRD and ICP analysis (for rock types) were presented in logs with the aid of LogPlot software.

2.2.3 X-ray diffraction analysis

The X-ray Diffractions (XRD) analysis technique is very important in identifying minerals like clays and zeolites in less than 4 micron fraction, subsequently providing information on alteration temperatures. Also, it is possible to use the method to identify other minerals such as feldspar, but this method was employed only for identifying clay minerals. During the process, the X-rays are diffracted by a powdered sample with specially oriented grains Yoshio et al (2011), noted that X-ray spectra that are characteristic for different clay minerals are deduced by slowly changing the diffraction angle based on Bragg's law. The representative samples were selected and placed in crucibles, 1/5 sample and 3/4 water and then shaken for 4 hrs in a shaker machine to separate the phyllo-silicates from the rock matrix. When finished, the samples were mounted on thin films on a glass plate. They were run in the range of 2 - 14° on the XRD machine. The analysis was carried out using Bruker AXS, D8 Focus Diffractometer at ISOR - Iceland GeoSurvey. The results with diffractograms are found in Tables 3 and 4, Appendices V and VI.

2.2.4 ICP – OES analysis

The whole-rock chemical analyses were done for the selected rock units from wells MW-03, MW-09 and MW-20 at various depths with 10, 8 and 10 samples respectively. It has to be noted that mixing of cuttings between different lithological units in the well can occur, in particular with increasing depth. Therefore, samples from relatively thicker lithological units that appeared to show minimal mixing, using binocular microscope. Also the external materials were removed and homogeneous samples remained for further steps. The samples were grounded to powder and weighed in with lithium metaborate and heated in graphite crucible for 30 min at 1000°C. The samples were dissolved in acidic solution after having been melted. The analyses were done at 2 ml sample/min with an argon plasma at 1200V in cross - flow nebulizer. After obtaining the data they were corrected and normalized to 100%. The analysis produced 10 major elements Si, Ti, Fe, Al, Mn, Mg, Ca, Na, K, and P; which were converted to oxides (SiO_2, Ti_2O, FeO, Al_2O_3, MnO, MgO, CaO, Na_2O, K_2O and P_2O_5) in percentage and 13 trace elements such as Sr, Ba, Zr, Y, Zn, Ni, Cu, Cr, Co, V, Sc, Rb, and La in ppm were analysed. The uncertainty for standard Si and Mg is ~1%, Ti <2%, Al, Fe, Ca, Na, K from 4-6%, Mn and P<8% whereas trace elements from 4-8%. The sample were analysed using Spectro Ciros 500 ICP-OES equipment at University of Iceland, Earth Institute Laboratory. See procedures are described in Appendix IV.

3. RESULTS

3.1 Lithology

Different rock types such as trachyte, pyroclastics, basalt and tuff were encountered in the study wells. Figure 16, shows graphical representation of the rock units observed in wells MW-20, MW-09 and MW-03 using the four analytical techniques with black lines showing the horizons in the wells deduced from trends of trace elements in the wells complemented by lithology (see Section 3.6.4). The main rock type dominating in the studied wells (MW-03, MW-09 and MW-20) is trachyte. This rock was further classified as fine, medium and coarse grained trachyte (Figure 14). The rocks are altered and some appear fresh, the rock alteration in this study are divided into less/slightlymedium/ moderately and highly altered (Figure 15). The rocks in study wells are mainly composed of feldspar particularly alkali feldspar as suggested by (Leat, 1983). The lithology is based on the binocular, petrographic and ICP-OES analyses. Detailed descriptions of the lithology in the wells is in Appendices I, II and III.

3.1.1 Pyroclastics

Pyroclastics were encountered at 514-536, 0-2 and 456-462 m in wells MW-03, MW-09 and MW-20 respectively. In wells MW-09 and MW-20, pyroclastics are unconsolidated and unaltered, look yellowish to brown in colour. In MW-20 the pyroclastics are mixed with volcanic glass and some trachytic fragments. In these two wells, this unit shows oxidation. In MW-03 the pyroclastics are dark grey to brownish grey in colour and altered. The unit exhibits pyrite, calcite and clay minerals as alteration minerals in wells MW-03 and MW-20.

FIGURE 14: Stereomicroscope photos (a, b and c) with magnification of ×2 showing fine (a), medium (b) and coarse grained (c) trachyte from study wells. The width of all pictures are 4 mm
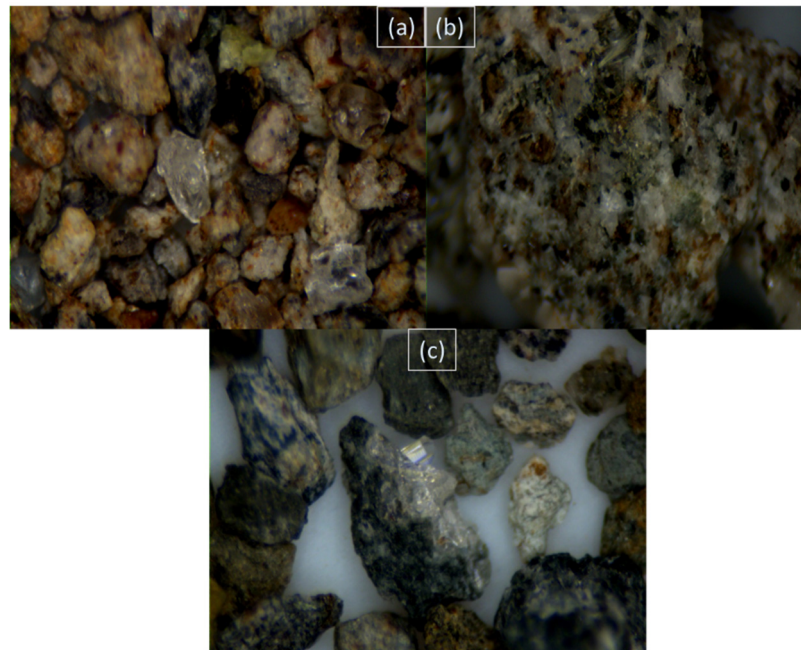
FIGURE 15: Stereomicroscope photos showing (a) little / slight, (b) medium/moderate and (c) high alteration in trachytes

3.1.2 Tuff

Tuff was observed in all wells, within the top unit at 250-272 m depth and occurs to 2058 m depth in well MW-03. In well MW-09, tuff is encountered at 118-132 m depth and appears regularly to 1552 m.

Tuff is noted at 4-6 and 380-386 m depth, but is appearing down to 1502 m in well MW-20. The rock is mainly light grey, brown and brownish grey in colour and in all the occurrences most of the tuffs is bleached and moderately altered. Microphenecrysts of feldspar are randomly oriented displaying pilotaxitic texture at 308-390 m in well MW-03. Some cuttings show vesicles filled by silica, clay minerals, zeolite, pyrite and calcite. In the top unit tuff, at 250-272 and 308-390 m in well MW-03 the vesicles are filled by silica and it is the same case to well MW-09 although in this well some vesicles are infilled with zeolites at 118-132 and 340-368 m. Some vesicles filled rarely with silica in well MW-20 from 380-386 m. Towards the bottom, vesicles seem to be filled by calcite, silica, pyrite and clay minerals in all wells. The rock appears to be mainly composed of alkali feldspar, plagioclase and pyroxene especially aegirine-augite as primary minerals. Secondary minerals in the rock are zeolites, calcite, pyrite and clay minerals. Tuff marker horizons were explained as a tool to mark the boundary/horizon between pre-, syn- and post caldera formations as were described by Mbia (2014) in wells MW-04, MW-06 and MW-07 and Mibei (2012) for wells MW-04 and MW-05.

3.1.3 Trachyte

Trachyte is dominant in all the study wells. It was classified according to grain sizes or texture, that is fine, medium and coarse grained as illustrated in Figure 14 (a and c). The rock is light to dark grey, brownish grey and greenish in colour. Some of the trachyte exhibits sanidine and plagioclase phenocrysts, embedded in a feldspar-rich groundmass. Pyroxene phenocrysts are infrequently present in the feldspar-rich matrix and rarely occur in rock matrix. Trachyte was first encountered at 72-156, 14-16 and 12-28 m in MW-03, MW-09 and MW-20, respectively, and seems to be medium grained and fine grained trachyte correspondingly. The rock continues to the bottom, alternating with tuff, pyroclastics and syenite. Different volcanic eruption episodes during the pre-, syn- and post caldera volcanic the activities could be the reason to textural disparities (GDC, 2014a). In all wells, trachyte is mainly composed of sanidine and pyroxene (augerine-augite) as primary minerals, abut blue amphiboles, glass, Fe-Ti oxides and olivine are also present in the rock. The above minerals tend to alter to secondary minerals, for instance, at 850 m in MW-20, pyroxene is altering to epidote. The hydrothermal alteration minerals in trachytes are zeolite, calcite, pyrite, clay minerals, epidote, wollastonite and actinolite.

3.1.4 Basalt

The rock is dark grey in colour. The rock unit is moderately to highly altered and exhibit vesicles, filled with calcite and clay minerals. Basalt was recognised in well MW-03 at 1458 m. It is nearly holocrystalline composed of plagioclase, pyroxene and Fe-Ti oxide as primary minerals. Basalt was not encountered in wells MW-09 and MW-20. The hydrothermal alteration minerals observed in the rock are calcite, clay minerals and epidote.

3.1.5 Syenite/ intrusion

The emplacement of magma into pre-existing rock is termed intrusion, and depending on the volume, intrusions can be major or minor. The intrusion (syenite) in the study wells is the plutonic equivalent to trachyte and occurs in all the wells as dykes. The rock is whitish in colour, medium to coarse grained composed mostly of alkali feldspar, less plagioclase, mafic minerals especially pyroxene, glass, amphiboles and Fe-Ti oxides as primary minerals.

As illustrated in Figure 16, syenite/intrusions were observed at 1394-1424 and 1510-1532 m in well MW-03, 1948-1980 m in MW-09 and 1322-1368, 1968-1980 and 2046-2092 m in well MW-20, while possible intrusions were encountered at 2050-2052 m in well MW-03 and 1688-1692 and 1300-1302 m in MW-09. These intrusions were noted in horizon 4 (Figure 16) which may indicate that it intruded the pre-caldera formations. Commonly, the intrusions look fresh whilst at some depths they appears altered and contain high temperature alteration minerals such as epidote, wollastonite and actinolite. These minerals were observed as infilling vugs. The intrusions in the wells seem to be associated with oxidation probably because of rapid loss of heat to the country rock.
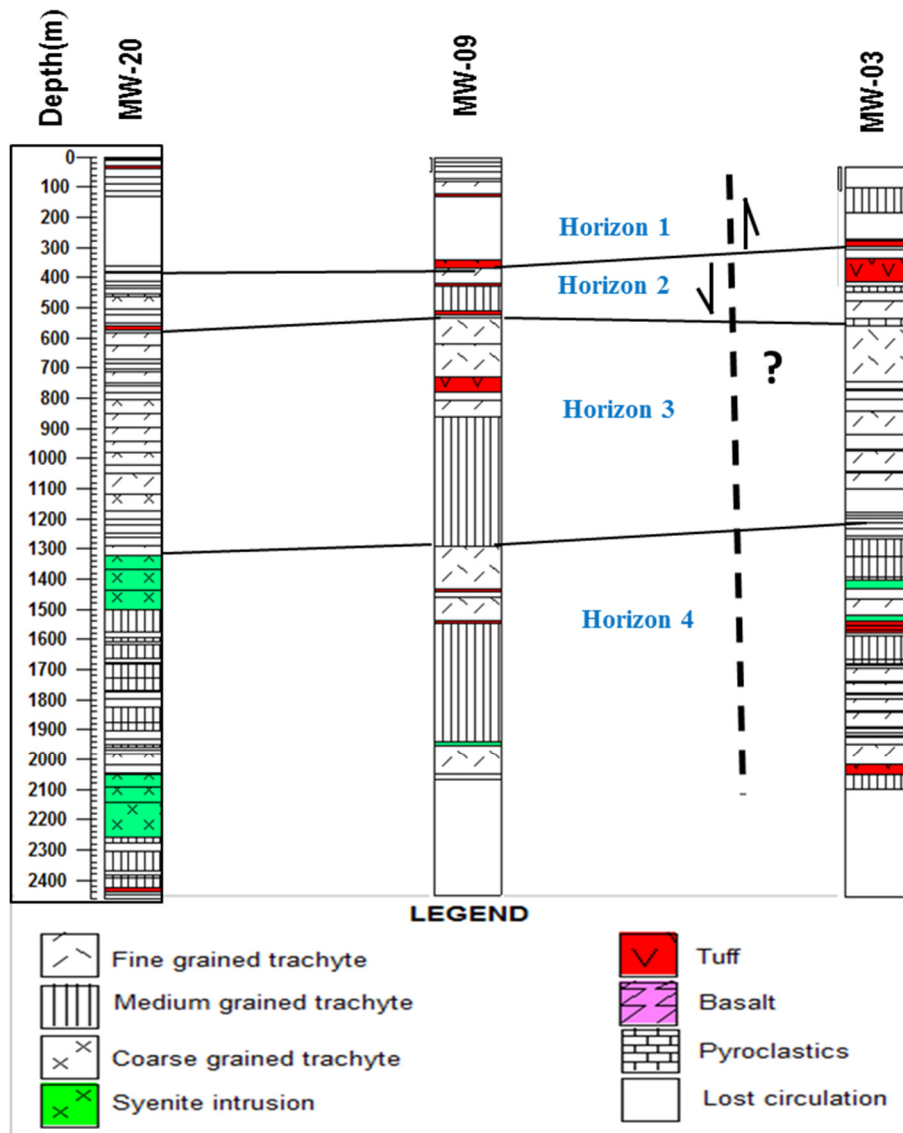
Figure 16: Graphical representation of the rock units observed in wells MW-20, MW-09 and MW-03 using the four analytical techniques with black lines showing different horizons in the wells and doted black line representing inferred fault.

3.1.6 Stratigraphic correlation

Trachytes are dominant in all study wells, while basalt found only in MW-03. From 250-386 m, a tuff marker horizon was noted in all the three wells (Figure 16), in the neighbouring wells MW-13 (Kahiga, 2014), MW-04 and MW-06 (Mibei, 2012) the horizon was noted from 320-400 m. In MW-04, MW-06 and MW-13, this tuff marker horizon have been interpreted as syn-caldera in age, which can relate to the study wells. The displacement of the tuff mark (Figure 16) horizon in the wells possibly is due to faults related to Molo TVA and Solai TVA. Ba, Sr, La and Y are showing trends in the study wells indicating four units in the wells which may show relationship with caldera stages. Syenitic intrusion occurs at 1322 m to the bottom in all wells, this may be related to the shallow magma chamber below the Menengai volcano, and this can be complemented by the presence of fresh glass in the bottom of well MW-03 at 2002 m. Also fresh glass was reported by Mibei, (2012) in well MW-04 and MW-06 at 2082 and 2174 m, respectively.

3.2 Aquifers / feed zones

The subsurface layers of water-bearing permeable rock or unconsolidated materials form aquifers. Existence of good vein/vesicle networks and high concentration of hydrothermal minerals in the rock indicate the presence of strong subsurface hydrological circulation. In addition, quartz, adularia, epidote, wairakite, illite, hyalophane, abundant pyrite and calcite are also positive signs of good permeability. But the precipitation of prehnite, pumpellyite, pyrrhotite and large quantities of laumontite and titanite can be attributed to a low-permeability zone as described by Reyes (2000).

The permeability of Menengai geothermal field are associated with fractures and faults in the trachytes, lithological contacts between formations, and permeable formations like tuffs (e.g. Mibei, 2012). In the study wells, inferred aquifers or feed zones, were identified using the following factors (Figure 17, 18 and 19);

- o Temperature logs and change in temperature;
- o Circulation losses;
- o Hydrothermal alteration;
- o Variation in the penetration rate;
- o Lithological boundaries and margins of intrusion.

In well MW-03 nine aquifers were identified at 268, 526, 790, 1080, 1234, and 1398, 1540 1600 and 1972 m (Figure 17).

Aquifer 1: Is a small aquifer hosted by tuff at 268 m, is noted by increase in temperature and rate of penetration.

Aquifer 2: Was identified increase in in rate of penetration 60 m/hr at 526 m. It is a small aquifer hosted by pyroclastics. Calcite deposition is observed.

Aquifer 3: Was identified by circulation loss at 790 m and increase in temperature at 700-800 m. It is considered a small aquifer.

Aquifer 4: Is at 1080 m, also a small aquifer. It was identified in fine grained trachyte. Above this formation, circulation losses occurred. Small increase in temperature is noted, and the formation is less altered with less calcite and pyrite.

Aquifer 5: This aquifer is at 1234 m. It is large, there is increase in temperature, and the aquifer is hosted by fine grained trachyte formation and medium altered. Above and below of this formation there is loss of circulation. Calcite and pyrite are deposited in this formation.

Aquifer 6: It is located at 1398 m, and is a small aquifer. At this depth there is decrease in temperature logs and rate of penetration. The aquifer is at the boundary between medium grained trachyte and syenite intrusion.

Aquifer 7: There is signature of temperature decrease at 1500 m and it is near the lithological boundary of intrusion and tuff. The aquifer is large and hosted by medium to highly altered rock with pyrite deposition.

Aquifer 8: This feed zone is large and is located in moderately altered medium grained trachytes at 1600 m. The temperature logs show an increase, and an increased rate of penetration from 8 m/hr to 15 m/hr at this depth. Deposition of calcite is observed.

Aquifer 9: It is at 1972 m and is a small aquifer in fine grained trachyte. At this depth, increase in temperature was observed. Less calcite and pyrite were deposited (Figure16).

In well MW-09, about eight aquifers were identified, five are small aquifers and large aquifers are three (Figure 18).
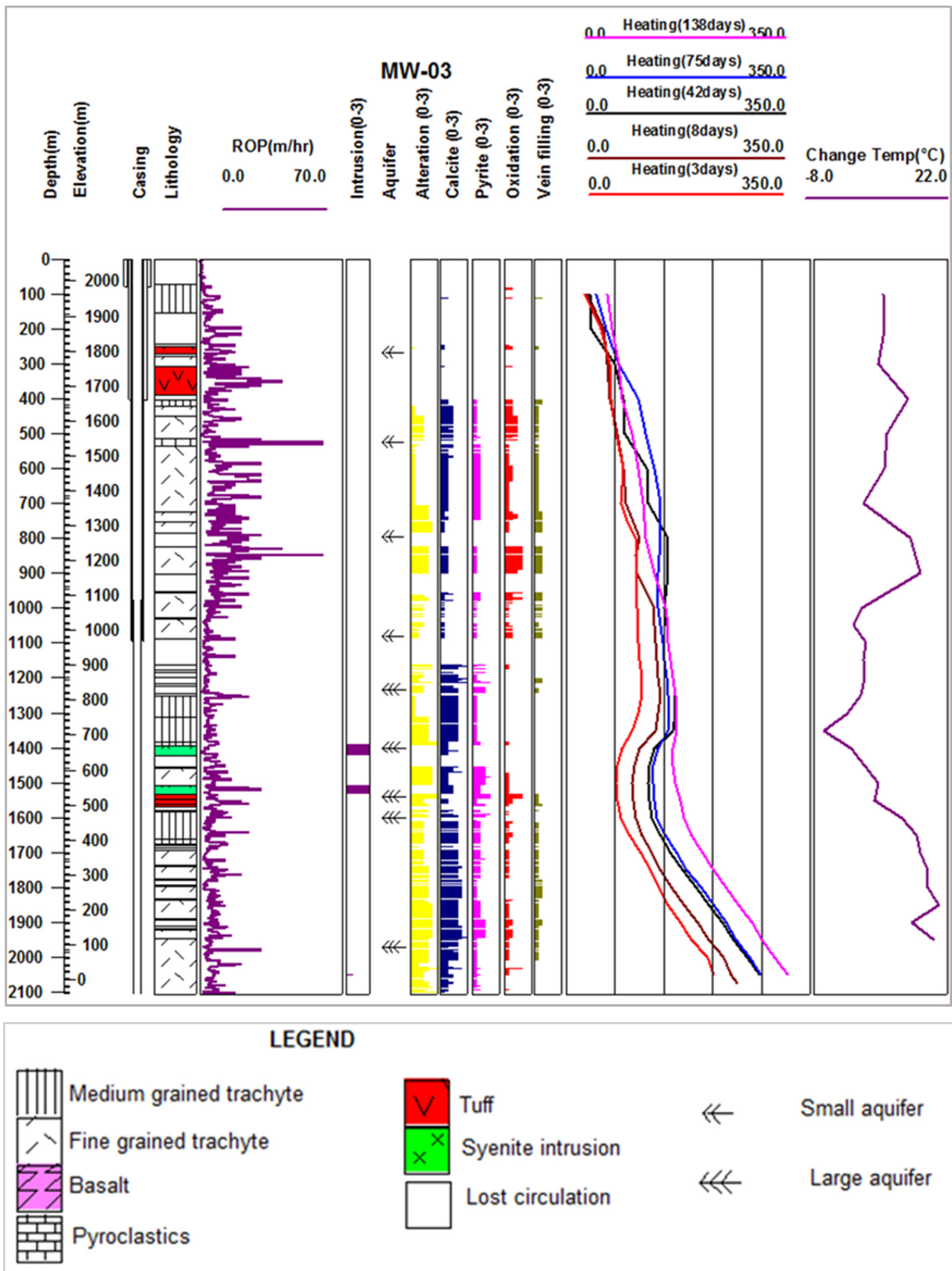
FIGURE 17: Lithology, aquifers and temperature logs in well MW-03

Aquifer 1 and 2: These are small aquifers at 216 and 530 m, respectively. Increase in rate of penetration and slight increase in temperature, complemented by loss of circulation were used to locate these aquifers. However, the two aquifers and aquifer 3 are cased off.

Aquifer 3: This is large aquifer is at 782 m. At this depth there is increase in rate of penetration, positive change in temperature and it is complemented by lithological boundary involving tuff and trachyte.
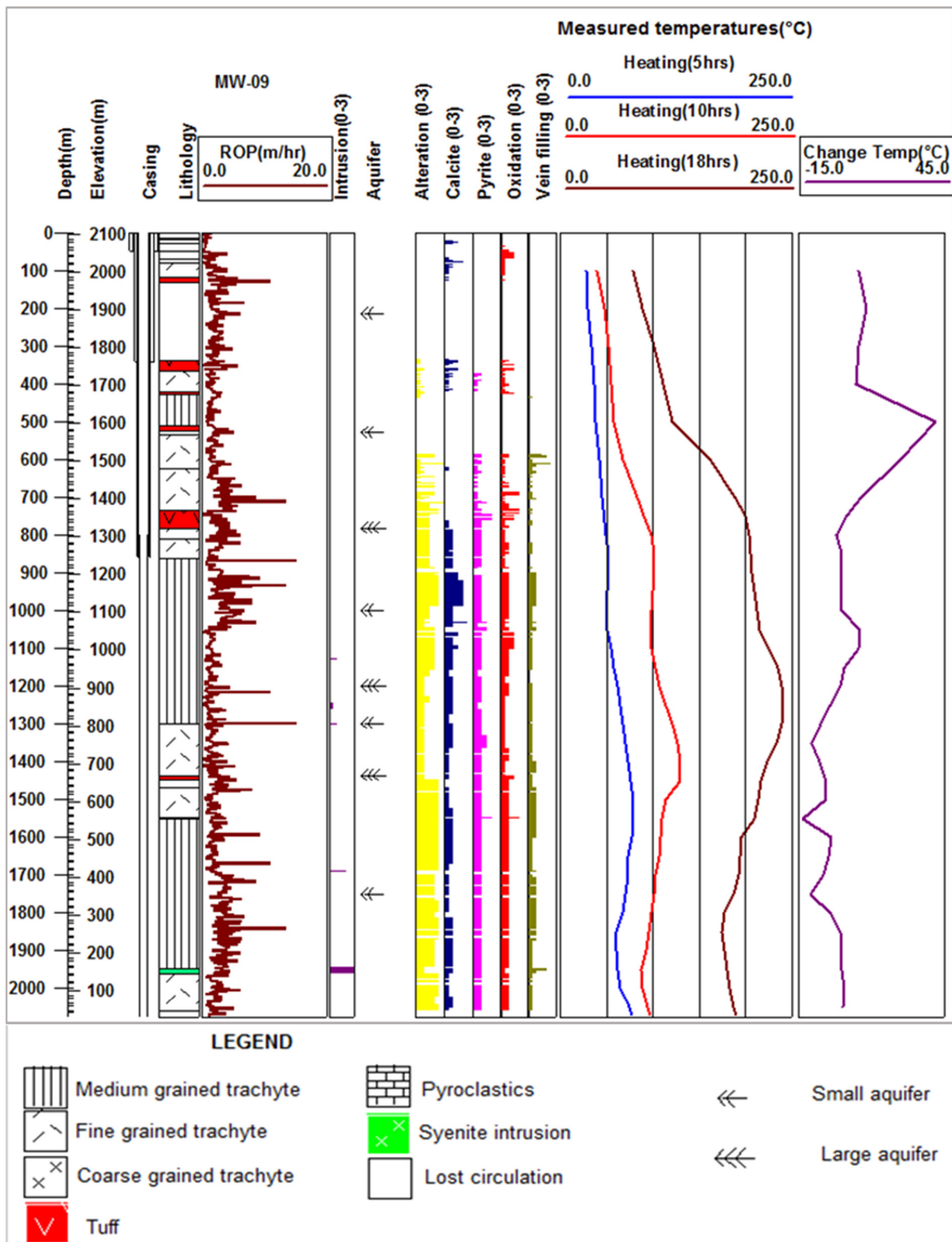
FIGURE 18: Lithology, aquifers and temperature logs in well MW-09

Aquifer 4: The feed zone is small and was noted at 1000 m, at this depth there is increase in rate of penetration, from 4.29 m/hr to 6.67 m/hr. Temperature logs show positive change in temperature. The aquifer is hosted by moderately altered medium grained trachyte.

Aquifer 5: It is a large aquifer and located at 1200 m in less altered medium grained trachyte. At this depth, slightly increase in temperature logs and rate of penetration were noted.
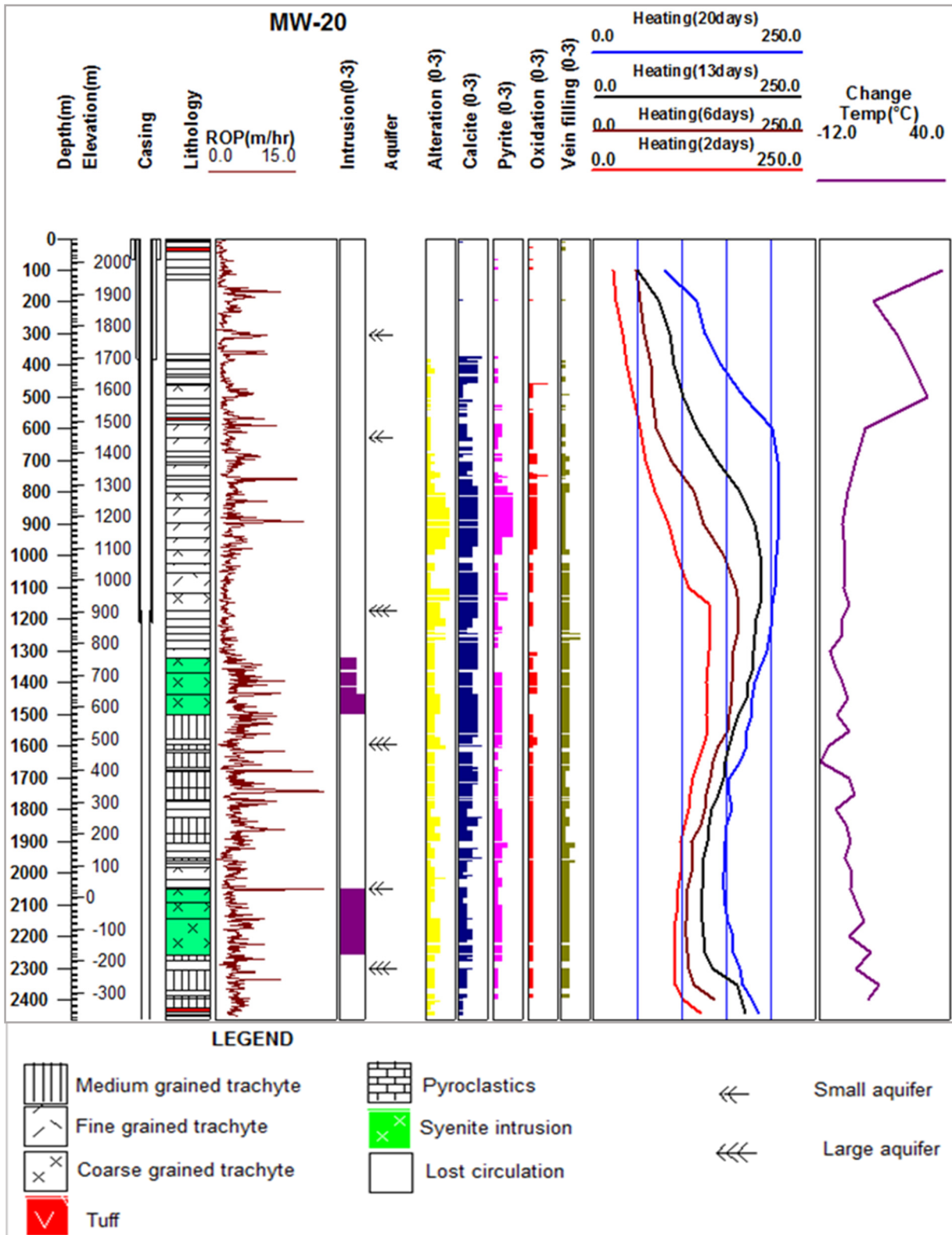
Figure 19: Lithology, aquifers and temperature logs in well MW-20

Aquifer 6: The aquifer was noted at 1298 m due to the increase in temperature logs and the rate of penetration is high. This aquifer is small and associated with a lithological boundary between fine grained trachyte and medium grained trachyte.

Aquifer 7: It was identified at 1436 m and it is a large aquifer. Moderate increase in rate of penetration and positive increase in temperature logs. Loss of circulation was also among the factors that contributed to locating this aquifer. The aquifer is hosted by fine grained trachyte that seems to be less altered.

Aquifer 8: This feed zone is located at 1750 m in moderately altered tuff. The feed zone was recognized by decrease in temperature log and slight increase in rate of penetration. There is less calcite and pyrite deposition.

The third well MW-20, exhibits six feed zones, three are small and the other three are large according to criteria described above (Figure. 19)

Aquifer 1: This feed zone is located in at 306 m. Temperature increase is seen at this depth. Also slight increase in rate of penetration and there is loss of circulation.

Aquifer 2: This feed zone is located in less altered fine grained trachyte at 626 m. Temperature increase is seen at this depth. Also slight increase in rate of penetration.

Aquifer 3 and 4: Both feed zones are large aquifers, the former is at 1174 m at the boundary between coarse grained trachyte and fine grained trachyte. Aquifer 4 is located at 1594 m and is associated with a lithological boundary of fine grained trachyte and medium grained trachyte. Rate of penetration increases at this depth and temperature shows slightly decrease to the bottom. All the aquifers are characterized by deposition of calcite and less pyrite.

Aquifer 5: The aquifer was recognized at 2050 m where temperature logs show a negative change and increase in the rate of penetration from 2.07 to 13.33 m/hr. However, the aquifer is small Aquifer occurs at the boundary of syenite intrusion and coarse grained trachyte, the two formations are less altered with little calcite and pyrite deposition.

Aquifer 6: The last feed zone in this well is small, noted at 2300 m. The zone is characterized by loss of circulation and slight increase in temperature logs.

3.3 Hydrothermal alteration

Hydrothermal alteration is the response of rock being subjected to thermal environments in the presence of hot fluids, which leads to rock changes in mineralogical and textural context.

In geothermal systems, hydrothermal alteration is very important in uncovering the history and the future of the system. The hydrothermal alteration can also be used in ore–deposit exploration. Hydrothermal alteration minerals are used to pinpoint the depth for production casing during drilling, so the minerals are useful as geothermometers. Also, the rocks at a specific area can be predicted whether is heating or cooling by comparing alteration temperatures of wells and formation temperatures. Reyes, 1990 described that hydrothermal minerals can also be used to estimate fluid pH, predicting scaling and corrosion tendencies of fluids, measure permeability, possible cold-water influx and as a guide to the hydrology.

Principally, when the rock heats up, particularly in volcanic active zones, the rock will tend to release some ions into the solution, after undergoing further heating, which will result in mineral rich fluid. Depending on temperature, rock type, pressure, permeability, fluid composition and duration of activity; the mineral rich fluid will crystallize alteration minerals out of the solution in open cavities or open structures. For example, in terms of temperature, epidote starts to appear at about 230°C and exists to over 300°C (e.g. Kristmannsdóttir, 1979; Franzson, 1998).

3.3.1 Alteration of primary mineral assemblages

Primary minerals are formed at the same time as the host rock and are termed rock forming minerals. Primary minerals crystallize from magma, dictated by chemical composition of the melt and physical conditions under which the magma solidifies. Given high permeability, elevated temperatures and intense fluid activity, primary minerals alter to secondary minerals, especially in geothermal environments. The secondary minerals form due to hydrothermal alteration that occurs after chemical

reactions between hydrothermal fluids and primary minerals. The Menengai geothermal field is composed of volcanic rocks of which more than 90% are of trachytic composition. The main primary minerals noted in the study wells are narrated below with decreasing susceptibility to hydrothermal alteration:

- o Glass (amorphous);
- o Olivine;
- o Sanidine
- o Plagioclase;
- o Pyroxene;
- o Amphiboles
- o Opaques (Fe-Ti Oxides)

Volcanic glass: Shows a vastly vitreous lustre and exhibits good conchoidal fractures. It is amorphous quenched magma and is the first component to be altered and replaced. The alteration of volcanic glass leads to the formation of zeolites such as mordenite, laumontite, cristobalite, quartz, calcite and clay minerals (Browne, 1978). Volcanic glass as primary constituent forms part of rock matrix at some depths. In the studied wells, this phase mostly alters to calcite, quartz and clay minerals (Table 2).

Olivine: This mineral is very susceptible to alteration. In thin section it can be identified by its high birefringence, distinctive irregular fracture pattern and lack of cleavage. It alters to clay minerals that form along rims and fractures. The mineral is rare in the study wells, however, where observed, it seems to be fresh.

Alkali feldspar: In the study wells the predominant alkali feldspar is sanidine. The mineral forms tabular or acicular crystals. Carlsbad twinning is common. Feldspar (sanidine) seen as rock groundmass and phenocrysts. The mineral alters to clay minerals.

Plagioclase: The low relief and conspicuous polysynthetic twinning of plagioclase makes it easy to be identified. Albite looks similar to quartz if is untwined. However, it does show incipient alteration, which is not common in quartz. As temperature increases the plagioclase is replaced by albite and calcite, chlorite and epidote. The mineral also occurs in the fine groundmass.

Amphiboles (riebeckite): They show deep blue colour and strong pleochroism and exhibits moderate relief in thin section. The deep blue colour suggest that they belong to the alkali amphibole group. The minerals alter to clay minerals, and at great depth to wollastonite, actinolite.

Pyroxene: The dominant pyroxene that occurs in the study wells is aegirine-augite. The mineral is dark green with strong pleochroism. Aegirine-augite occur as phenocrysts and as part of groundmass in some rock units. Pyroxene is noted to be replaced by clay minerals and actinolite at higher temperatures at depth.

TABLE 2: Primary rock-forming minerals and their alteration products
in wells MW-03, MW-09 and MW-20

Susceptibility	Primary minerals	Alteration mineral products
Decreasing ↓	Glass	Clay minerals, zeolite, calcite and quartz
	Olivine	Clay minerals, calcite, quartz
	Alkali feldspar	Clay minerals
	Plagioclase	Clay, calcite, albite, quartz, chlorite, epidote
	Amphiboles	Clay minerals, Wollastonite, actinolite
	Pyroxene	Pyrite, actinolite, calcite, chorite, epidote
	Opaque (Fe-Ti oxides)	Pyrite, Chalcopyrite and iron oxides (limonite/haematite)

Opaque (Fe-Ti Oxides): The minerals are opaque in both plane and crossed polarized light. The main minerals are ilmenite and magnetite, identified by reflected light in petrographic microscopy. They occasionally alter to pyrite, limonite/hematite and chalcopyrite.

3.3.2 Distribution and description of hydrothermal alteration minerals

As described below and illustrated in Figures 21, 22 and 23. The minerals were identified by using binocular, petrographic microscope and XRD analyses.

Limonite/haematite: The mineral is categorised by a reddish brown colour and it is hydrated iron oxide. This mineral is formed due to interaction between rock and cold groundwater. It was noted in MW-03 at 74 m down to 406 m within trachyte and tuff formations (Figure 21). Also the iron oxides noted in fractured cuttings and at contacts of syenite intrusions and host rocks at deeper depth, as a part of a contact aureal.

Zeolites: Over 40 naturally occurring zeolites exist and are often classified, due to shape such as fibrous/acicular, tabular/prismatic, and granular (e.g. Kristmannsdóttir, 1979; Koestono, 2007). These minerals are secondary minerals, and are hydrous sodium calcium aluminium silicates and do occur by filling cavities in rocks. Zeolites are temperature dependent and are used to determine the temperature at a given depth in geothermal systems. In the three wells, the following types of zeolites were found:

Analcime: This mineral occurs as isometric crystals. It was observed at depths from 92-322, 340-344 and 70-128 m in MW-03, MW-09 and MW-20, respectively. This is indicating minimum temperatures between 40 and 60°C.

Mesolite/scolecite: The two minerals can be classified as fibrous/ acicular. In thin section, scolecite occurs as radiating structures with 1st order yellow but mesolite is 1st order dark grey in colour. Occurs at a minimum of about 90°C and were noted to some depths from 310-372 m in MW-03, 120-126 m in MW-09 and 496 m in MW-20.

Thomsonite: This mineral occurs as acicular radiating crystals, spherical aggregates or clusters of prismatic crystals. It appears filling vesicles. The mineral was seen in well MW-03 at 258 and 298 m depth. The mineral was not seen in MW-09 and MW-20.

Cowlesite: This mineral appears to be colourless, radiating sprays of crystals as ball like structures. The minerals occur as low silica zeolite and fills cavities of the rocks. The mineral was observed at 536 m in MW-03. No cowlesite was noted in MW-09 and MW-20.

Opal: It looks pale yellow-brown in colour and fills cavities/vugs. This phase can be replaced/altered to quartz. Opal indicates temperatures less than 100°C. This phase is found between 126 and 132 m in MW-09.

Chalcedony: It shows a bluish colour under the binocular microscope and appears to fill vesicles uniformly. Chalcedony is a low-temperature silica mineral and it found in different depths from 74 m, 128 m and 364 m to 512 m, 752 m and 764 m in MW-03, MW-09 and MW-20 respectively. Chalcedony can be replaced/altered to quartz.

Quartz: The binocular and petrographic analyses show quartz depositing in vugs and veins. In cuttings the mineral showed an euhedral shape while in thin section it appears with no clear twinning. The refractive indices of quartz can be used to distinguish it from zeolites. Quartz can be used as indicator mineral for production casing because of its stability, however, it is required to show maturity with clear prismatic shape. It forms at temperatures of above 180°C as secondary minerals. Quartz was encountered in all the three wells. First appeared at 638, 712 and 672 m in MW-03, MW-09 and MW-20, respectively, and continues to the bottom of the wells.

Prehnite: The mineral was observed only in MW-03 at 1394 and 1544-1548 m. The mineral forms at temperatures above 240°C and exhibits small spherical clusters of crystals, pale green to whitish in colour. It can be identified in thin section through its bow tie structure as well as its high interference colour and high relief.

Epidote: It has yellow to green pleochroism and forms small elongated prismatic crystals with high relief. In MW-03, epidote was first observed at 850 m and occurs sporadically to 1936 m. It was note in MW-09 at 1586 m and disappears at 1606 m while for MW 20, the first occurrence was noted at 1000 m and sporadically occurs to 2448 m. No well-formed crystals of epidote with prismatic shape were found in this wells. Epidote has a strong pleochroism of green, yellow and brown in thin section. The occurrence of epidote indicates temperatures above 230°C (e.g. Kristmannsdóttir, 1979) which shows the importance of this mineral when deciding for production casing depth. The mineral will be discussed in Section 3.4.

Wollastonite: It forms at a temperature of about 270°C; the mineral is mostly associated with epidote and garnet, though in the study wells, it appears to occur with epidote and actinolite. Wollastonite was first identified in cuttings at 1450 and 792 m in MW-09 and MW-20 respectively due to its fibrous structure. The minerals show weak birefringence and has a fairly high relief in thin section. It is rare in MW-03, and appears first at 1462 m.

Actinolite: It is a high temperature mineral and classified in the amphibole mineral group. The mineral forms as greenish radiating, acicular crystals/massive to granular aggregates in the groundmass. It was observed through binocular microscope. Frequently, it appears to grow on pyroxene, it replaces the margin of pyroxene. In well MW-09, actinolite was noted at 1554 m, in well MW-20 it appeared at 1222 m, while it was encountered at 2054 m in well MW-03. Actinolite signifies temperatures of above 280°C (Franzson, 2011).

Calcite: In these wells calcite is an abundant secondary mineral, first appearing from 74, 16 and 14 m in MW-03, MW-09 and MW-20, respectively. The mineral was noted all the way to the bottom of the wells. Calcite was identified in drill cuttings by using hydrochloric acid. In thin sections, calcite crystals show clear rhombohedral cleavage and high interference colour. Calcite can form by different ways such as due to boiling, dilution and condensation of carbon dioxide in a geothermal system. Simmons and Christenson (1994), pointed out that calcite can form during the heating of cooler peripheral fluids. The paragenesis of calcite will be discussed further in section 3.4.

Pyrite: The mineral is abundant in all wells, rarely form yellowish cubic crystals and is found below 404 m in MW-03, 372 m in MW-09 and below 68 m in MW-20. Pyrite fills veins/vugs at some depths, in geothermal system, the mineral can indicate the presence permeability.

Chalcopyrite: Appears brassy/golden yellow in colour and occurs in association with pyrite. Chalcopyrite was noted at 484 and 2066 m in well MW 03, bellow 820 m in well MW-09 while in well MW-20 it was first observed at 750 m and continues sporadically to 2096 m.

Albite: In the three wells albite occurs as an alteration product of plagioclase. Under petrographic microscope, albite was noted at 978, 1044, 1210 and 2098 m in MW-03, 1862, 1942 and 2052 m in MW-09 and 1000 and 1832 m in MW-20. It replaces plagioclase and tends to destroy the typical plagioclase twinning habit. This mineral indicates temperature above 180°C.

Fluorite: It forms a typical cubic, and to a lesser extent the octahedral, as well as combinations of the two and other rarer isometric habits. The mineral was noted at 1586 m and occur irregularly to 1704 m in MW-03 and is noted at 1600 m in MW-09 while fluorite mineral was not observed in MW-20.

Clay minerals: They form by hydrous alteration of primary silicate phases such as glass, plagioclase, pyroxene, olivine and pyroxene. The clay minerals are water-rich phyllosilicates. Temperature, pH and fluid composition control the composition, structure and morphology of clay minerals. Clay crystals occur in flake-like or dense aggregates of varying types and they are finely crystalline or meta-colloidal

(Ahmed, 2008). Clay minerals were identified by XRD analysis, petrographic analysis and binocular microscope, but XRD analysis was effective especially in wells MW-09 and MW-20. The minerals were classified into different types at different depths, using temperature, clay minerals were analysed and show clay mineral zonations as described below and in section 3.3.4

Smectite: This mineral occurred at 386 m and from 688-1714 m in well MW-09. The mineral displayed high peak values of 12.2-13.6 Å in untreated and 12.9-14 Å in glycolated samples and 10 Å when heated (Lopeyok, 2013). Smectite occurred from 496 m in well MW-20 and continue sporadically to the bottom of the well. The peak values of the untreated samples displayed values were 12.787-15.178 Å, while for glycolated samples showed 13.101-16.745 Å and the heated sample value were 10.136-10.92 Å (Tables 3 and 4). The appearance of smectite illustrates a temperature of approximately 200°C. In MW-03, smectite was observed petrographically at 372 and 726 m and appears brownish in colour and having low birefringence, mostly filling vesicles, but also as an alteration product of primary minerals.

Illite: The mineral was observed in all wells and indicates temperatures of above 220°C. In well MW-03, illite occurs from 1870 m to the bottom of the well. Untreated, glycolated and heated samples displayed peak values between 10.26-10.329 Å. It occurs at 400 m, and from 1444 m to the bottom in well MW-09. It shows peaks between 10.2-10.3 Å in untreated, glycolated and heated samples (Lopeyok, 2013). This mineral occurred from 898 m to the bottom of well MW-20 with peak values between 10.0 and 10.3Å for untreated, glycolated and heated samples (Tables 3 and 4).

TABLE 3: Results of XRD analysis of clay minerals for well MW-03

Depth (m)	δ(001)A	δ(001)H	δ(001)G	δ(002)	Mineral	Remarks
94	-	-	-	-	-	No clay
258	-	-	-	-	-	No clay
378	-	-	-	-	-	No clay
456	-	-	-	-	-	No clay
536	-	-	-	-	-	No clay
756	-	-	-	-	-	No clay
846	-	-	-	-	-	No clay
954	-	-	-	-	-	No clay
988	-	-	-	-	-	No clay
1032	-	-	-	-	-	No clay
1168	-	-	-	-	-	No clay
1214	-	-	-	-	-	No clay
1308	-	-	-	-	-	No clay
1396	-	-	-	-	-	No clay
1462	-	-	-	-	-	No clay
1528	-	-	-	-	-	No clay
1586	-	-	-	-	-	No clay
1730	-	-	-	-	-	No clay
1870	10.319 8.652	10.319	10.329	-	Illite, Amphiboles	Illite
1940	10.319	10.319	10.329	-	Illite	Illite
2078	10.226	10.226	10.226	-	Illite	Illite

Chlorite: The mineral appears green and non pleochroic in plane polarized light and displays anomalous brown interference colours under crossed polars. In the drill cuttings, chlorite appears green. The mineral was first noted at 740 m in well MW-03 and 932 m from well MW-20. Chlorite was not found in the well MW-09. In XRD analysis, chlorite was identified only in well MW-20 from 1588 m to bottom with peak values at 13.191-14.931Å (Table 4) According to Kristmannsdóttir (1978), chlorite indicates temperatures of above 230°C as it has a crystallization temperature of over 230°C.

TABLE 4: Results of XRD analysis of clay minerals for well MW-20

Depth (m)	δ(001) A	δ(001) H	δ(001) G	δ(002)	Minerals	Type of clay minerals
388	-	-	-	-	-	No clay
414	8.58	-	-	-	Amphibole	No clay
528	8.720	-	-	-	Amphibole	No clay
662	8.613 6.576	-	-	-	Amphibole, feldspar	No clay
748	12.806 8.653 6.576	10.92	13.110		Smectite, Amphibole, feldspar	Smectite
898	12.787 8.653	10.182	13.101		Smectite, Illite, Amphibole	Smectite, Illite
954	13.009	10.136	13.509		Smectite, Illite	Smectite, Illite
998	13.062	10.136	13.589		Smectite, Illite	Smectite, Minor Illite
1026	15.178	10.136	16.745		Smectite, Illite	Smectite, Minor Illite
1074	-	-	-	-	-	No clay
1170	13.447 8.653	10.226	12.894		Smectite, Illite and Amphibole	Smectite, Traces of Illite
1220	-	-	-	-	-	No clay
1370	10.318	10.318	10.318	-	Illite	Illite
1412	10.318	10.318	10.318	-	Illite	Illite
1588	13.386 10.247 8.653	-	13.386 10.247	-	Chlorite, Illite and Amphibole	Chlorite, Illite
1644	13.191 10.099 6.425 8.653	13.191 10.099	13.191 10.099	-	Chlorite, Illite,feldspar and amphibole	Chlorite, Illite
1756	13.191 10.099 6.425 8.576	13.191 10.099	13.191 10.099		Chlorite, Illite, feldspar and Amphibole	Chlorite, Illite
1834	13.208 10.188 8.576 6.425	13.208 10.188	13.208 10.188		Chlorite, Illite, Amphibole, feldspar	Chlorite, Illite
1952	13.501 10.256 8.639 6.425	13.501 10.256	13.501 10.256	-	Chlorite, Illite, Amphibole, feldspar	Chlorite, Illite
2092	13.333 10.206 8.639	13.333 10.206	13.333 10.206		Chlorite, Illite and Amphibole	Chlorite, Illite
2146	13.333 10.275 8.639	13.333 10.275	13.333 10.275	-	Chlorite, Illite and Amphibole	Chlorite, Illite
2258	13.333 10.275 8.639	13.333 10.275	13.333 10.275	-	Chlorite, Illite, Amphibole	Chlorite, Illite
2310	14.931 10.275 8.639	14.931 10.275	14.931 10.275		Chlorite, Illite, Amphiboles	Chlorite and Illite
2450	-	-	-	-	-	No clay

3.3.3 Vein and vesicle fillings

Micro-fractures that are filled up by fluid or with the deposition of secondary minerals are termed as veins, on the other hand vesicles are pore spaces in rocks. These structures are very important since they act as a source of permeability. Alteration minerals that are deposited in vein and vesicles may provide important information on deposition sequences and temperatures as hydrothermal alteration minerals form at different temperatures. Gebrehiwot (2010) explained that porosity and permeability are two important primary factors that control the movement and storage of fluids in rocks and create space for deposition of minerals either in veins or vesicles. Binocular microscope and petrographic analysis were used to study alteration minerals in these structures, though some vesicles have no alteration minerals deposited. Vesicles and veins in the study wells were encountered at different depths however, veins are not prominent. In three wells MW-03, MW-09 and MW-20, veins and vesicles are filled by zeolites, chalcedony, calcite, pyrite, quartz, prehnite, clay minerals and wollastonite (Figure 20).
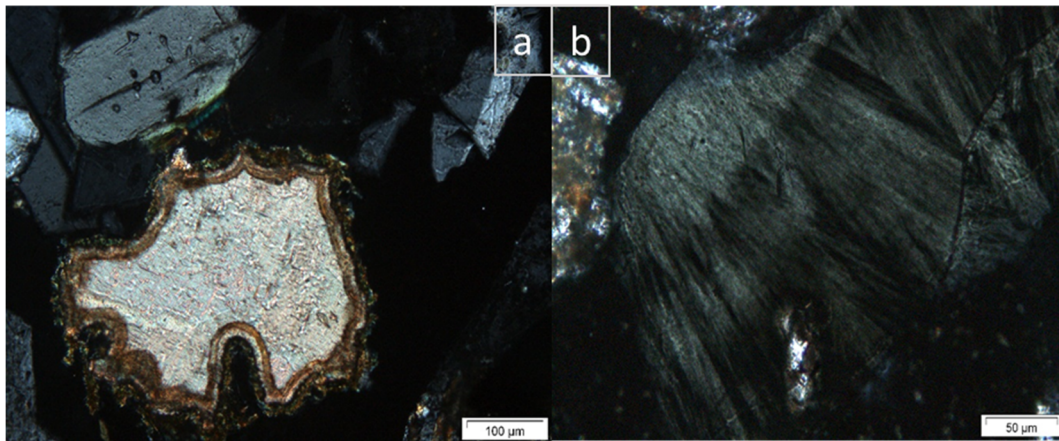
FIGURE 20: a) Calcite deposition at 978 in MW-03; b) Quartz, pyrite and wollastonite deposition at 1832 m, MW-20; both pictures are taken with crossed polars in a petrographic microscope

3.3.4 Alteration mineral zonations

Different methods such as binocular, petrographic and XRD analysis, were used in the study wells to create the alteration mineral zones. The key principles to define the zonations based on the alteration mineral temperatures and its abundance in wells. In Menengai geothermal environment the temperatures are estimated as shown in Table 5.

Low-temperature zeolites and amorphous silica form below 120°C, chalcedony below 180°C, quartz above 180°C, albite above 180°C, epidote above 240°C and garnet and amphibole above 280°C (eg. Kristmannsdóttir, 1979; Saemundsson and Gunnlaugsson, 2002; Franzson, 1998; Mbia, 2014).

TABLE 5: Some temperature dependent minerals in the Menengai geothermal field and their temperature implications (from Mbia, 2014)

Minerals	Min. Temp.(°C)	Max. Temp.(°C)
Zeolite	40	120
Chalcedony	-	<180
Smectite	30	<200
Calcite	50-100	280-300
Quartz	180	>300
Albite	180	>300
Adularia	180	>300
Illite	220	>300
Epidote	230	>300
Chlorite	230	>300
Wollastonite	270	>300
Actinolite	280	>300

Clay minerals smectite crystallizes below 200°C and chlorite above 230°C (Kristmannsdóttir, 1977). Figure 21, 22 and 23 show the alteration zones in wells MW-03, MW-09 and MW-20 respectively. The

boundary between one zone and another was defined by considering the first appearance of the successive dominant alteration mineral.

In MW-03, six alteration zones were identified (Figure 21)
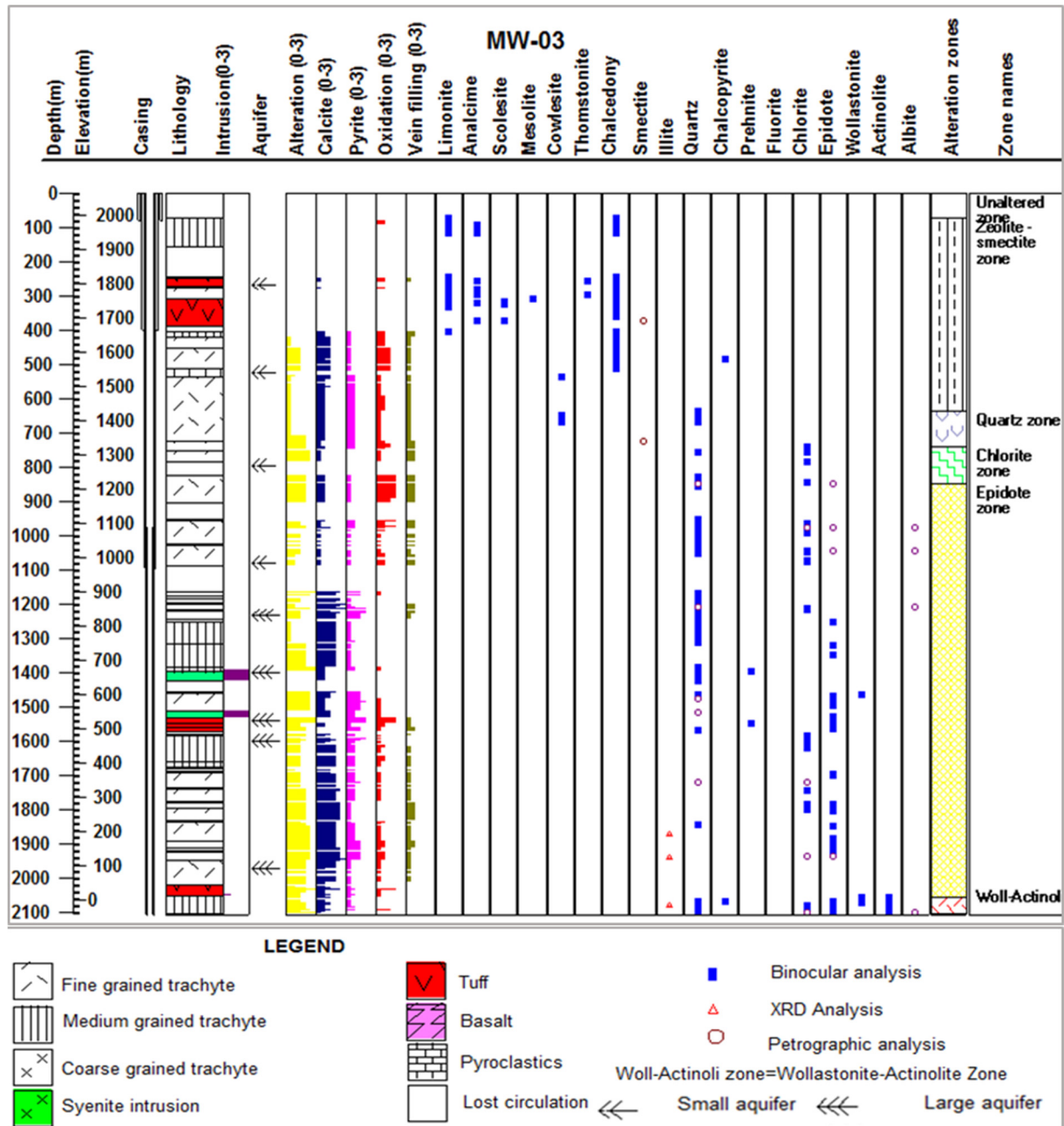
FIGURE 21: Lithology, aquifers, distribution of hydrothermal
alteration minerals and alteration zones of well MW-03

Unaltered zone (0-74 m): The zone is dominated by loss of circulation and about 2 m of relatively fresh trachyte.

Zeolite-Smectite zone (74-638 m): The occurrence of zeolite (analcime) at 74 m by binocular microscope analysis and appearance of smectite at 372 m mark this zone. Below 74 m, mesolite, cowlesite and thomsonite occur in the zone. Also, there is a presence of chalcedony in this zone. The minerals indicate temperatures of 40-180°C.

Quartz (638-740 m): First appearance of quartz marks the upper boundary of this zone, the mineral was noted at 638 m in the cuttings. Quartz indicates temperatures of above 180°C.

Chlorite Zone (740-850 m): Chlorite was first observed at 740 m in the cuttings. Quartz is also present in this zone. This zone indicates temperature above 230°C.

Epidote Zone (850-2054): This zone is characterized by epidote that occurs first at 850 m in well, the mineral was identified first in petrographic microscopy. This zone also contains other alteration minerals; chlorite, albite, quartz, prehnite and illite. Wollastonite first occurred locally at 1462 m. The zone signifies temperature above 240°C. Production casing was set in this zone at 1096 m.

Wollastonite-Actinolite zone (≥2054 m): Actinolite occurs from 2054 m to the bottom, the minerals characterize this zone with wollastonite, illite, quartz, prehnite, chlorite, epidote, fluorite and albite. The mineral assemblage of the zone indicates temperatures of above 280°C. The temperature logs in this zone show progressive heating, especially to bottom of the well (Figure 28, a and d).

Six alteration zones were recognized in MW-09 as shown in Figure 22, also some of the zones were described by Lopeyok (2013).

Unaltered zone (0-122 m): The zone is characterised by low alteration and rocks are generally fresh with little oxidation due to interaction with cold groundwater.

Zeolite-Smectite zone (122-712 m): The zone is characterized by the first appearance of zeolites and chalcedony, also the presence of smectite at 386 m. These minerals were noted under binocular and petrographic microscopes but smectite was analysed further using XRD analysis. This zone signifies temperatures below 180°C.

Quartz zone (712-1450 m): The first appearance of Quartz signifies this zone, first was observed at 712 m and continue to bottom of the well. Smectite and chalcopyrite were also observed in this zone. The zone represents temperatures of above 180°C. In this zone, production casing was set out at 858 m.

Illite zone (1450-1538): Illite is among high temperature clay minerals, it makes this zone and continue to the bottom of the well. The zone indicates temperature of 220°C.

Epidote zone (1538-1554 m): Epidote occurs only in these depths. It occurs first at 1538 m, the mineral characterizes the zone and its presence indicates temperature above 240°C.

Wollastonite-Actinolite zone (1554-2060 m): This zone indicates high temperature, it is characterized by the first appearance of actinolite and the presence of wollastonite. This mineralogical assemblage indicates temperatures above 280°C.

Six alteration zones were recognized in MW-09 as shown in Figure 22, also some of the zones were described by Lopeyok (2013).

Unaltered zone (0-122 m): The zone is characterised by low alteration and rocks are generally fresh with little oxidation due to interaction with cold groundwater.

Zeolite-Smectite zone (122-712 m): The zone is characterized by the first appearance of zeolites and chalcedony, also the presence of smectite at 386 m. These minerals were noted under binocular and petrographic microscopes but smectite was analysed further using XRD analysis. This zone signifies temperatures below 180°C.

Quartz zone (712-1450 m): The first appearance of Quartz signifies this zone, first was observed at 712 m and continue to bottom of the well. Smectite and chalcopyrite were also observed in this zone. The zone represent temperatures of above 180°C. In this zone, production casing was set out at 858 m.
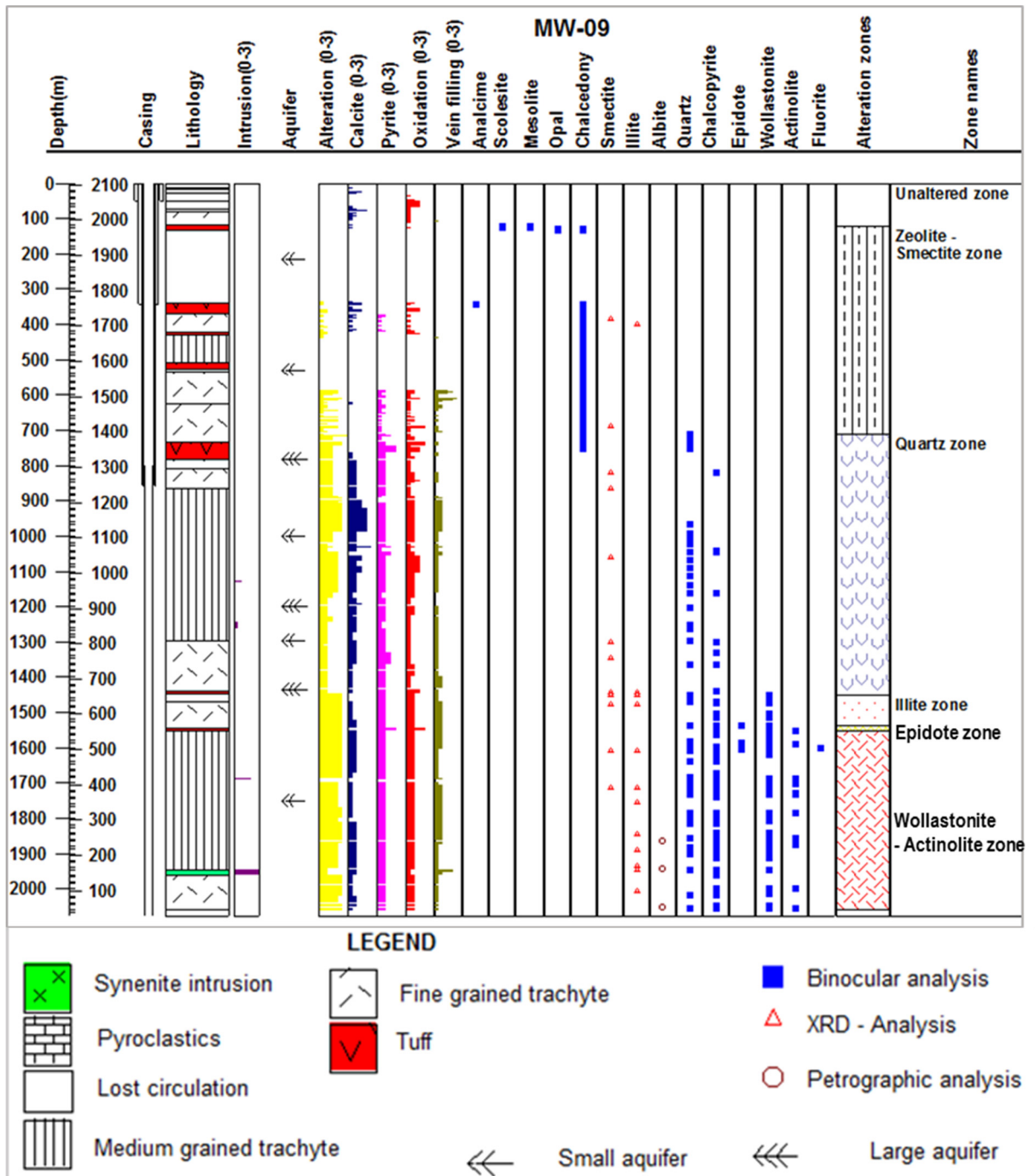
FIGURE 22: Lithology, aquifers, distribution of hydrothermal
alteration minerals and alteration zones of well MW-09

Illite zone (1450-1538): Illite is among high temperature clay minerals, it makes this zone and continue to the bottom of the well. The zone indicates temperature of 220°C.

Epidote zone (1538-1554 m): Epidote occurs only in these depths. It occurs first at 1538 m, the mineral characterizes the zone and its presence indicates temperature above 240°C.

Wollastonite-Actinolite zone (1554-2060 m): This zone indicates high temperature, it is characterized by the first appearance of actinolite and the presence of wollastonite. This mineralogical assemblage indicates temperatures above 280°C.

In well MW-20, Seven alteration zones were identified (Figure. 23).
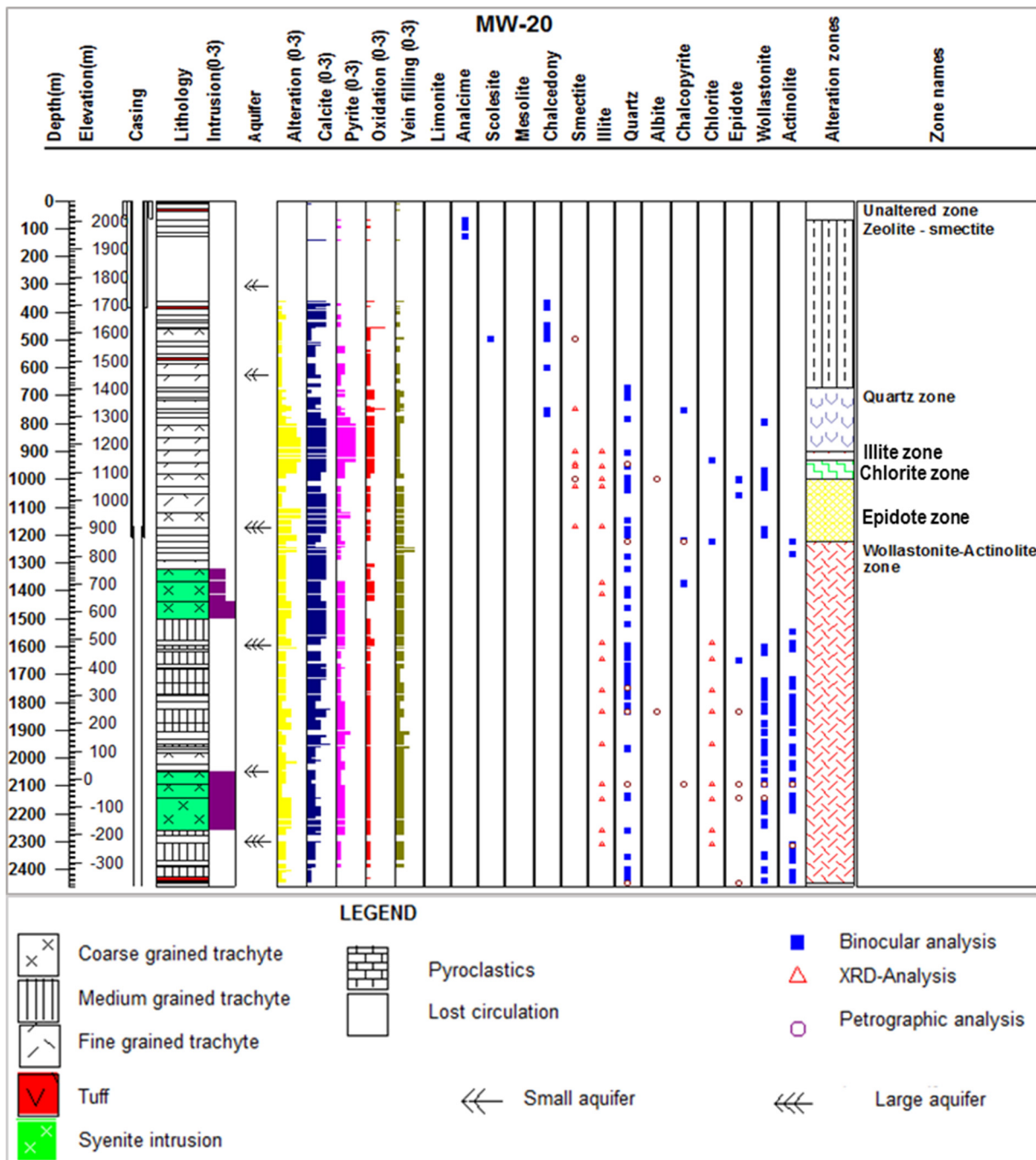
Figure 23: Lithology, aquifers, distribution of hydrothermal
alteration minerals and alteration zones of well MW-20

Unaltered zone (0-70 m): The zone contains relatively fresh rocks showing little oxidation due to interaction with cold groundwater and it is composed of tuffs and trachytes.

Zeolite-Smectite (70-672 m): This is characterized by the first appearance of zeolite particularly analcime, and the presence of smectite, that was observed at 496 m by petrographic analysis. In this zone, chalcedony also is abundant. This mineralogical assemblage implies temperatures below 180°C.

Quartz zone (672-898 m): Quartz first appears at 672 m and marks the upper zonal boundary. Some minerals are also present such as smectite and chalcopyrite. This zone indicates temperatures above 180°C.

Illite zone (898-932 m): Illite first occurs at 898 m and proceed to the bottom of the well, this high temperature clay mineral indicates temperature of above 200°C. In this zone quartz, smectite and albite are also present.

Chlorite zone (932-1000 m): This zone is signified by the first appearance of chlorite at 932 m which was observed in XRD analysis. Its upper boundary indicates temperature of 230°C.

Epidote zone (1000-1222 m): Epidote first appears at 1000 m and marks this zone. Production casing was carried out at 1211 m in this zone. The zone indicates temperature of above 240°C.

Wollastonite-Actinolite zone (1222-2450 m): The zone involves high temperature minerals and is marked by actinolite that first occurs at 1222 m. Wollastonite and illite are also present. Within this zone quartz, chlorite, epidote and chalcopyrite are found, whereby epidote and chalcopyrite are rare occurring. Presence of actinolite in this zone indicates temperature above 280°C.

Hydrothermal alteration zones in the study wells indicates some differences. Wells MW-03 differs from the two wells MW-09 and MW-20, especially on the fourth zone. This zone in MW-09 and MW-20 is characterized by illite while in MW-03, illite is noted at the bottom of the well. Chlorite zone was noted only in MW-03 and MW-20 but not in MW-09. Epidote and chlorite seem to be much more abundant in well MW-03 than in MW- 09 and MW-20. The two wells exhibit significant actinolite and wollastonite at shallower depth as compared to MW-03. These differences are also shown by resistivity cross section (Figure 24) along these wells indicating low resistivity in deeper part in MW-03 compared to MW-09 and MW-20 (GDC, 2014b). The study wells share six alteration zones with neighbouring wells MW-04 and MW-06 except chlorite zone (Figure 25).
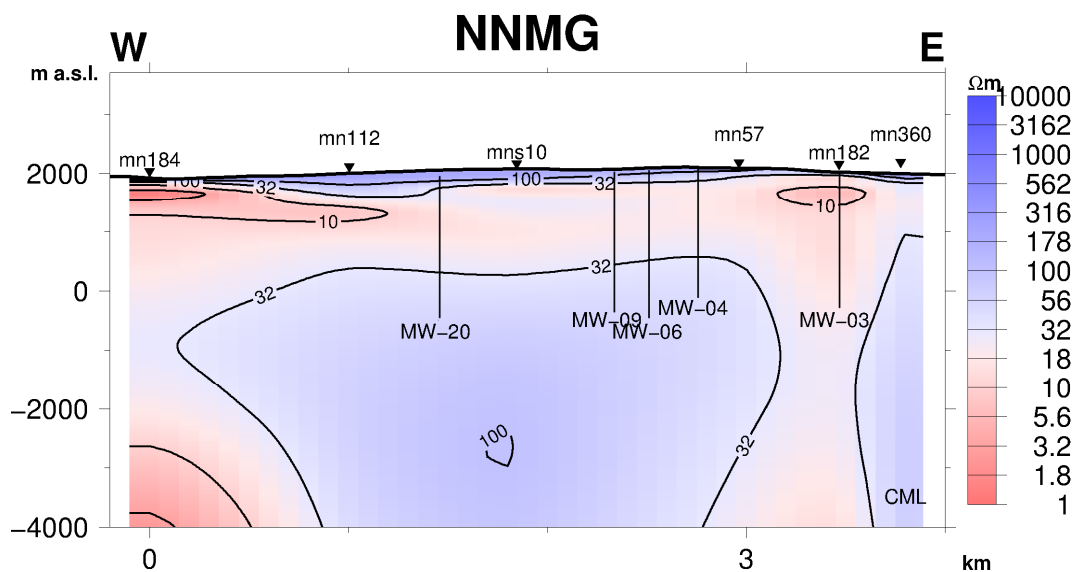
FIGURE 24: Cross section W-E of the study wells and neighbouring wells MW-04 and MW-06 showing low resistivity at deeper part of MW-03 (from GDC, 2014b).

3.3.5 Sequence of mineral deposition

Alteration minerals are formed as replacement minerals, or by deposition. By careful study of depositional sequences of alteration minerals in veins and vesicles, the thermal history and relative time scale of alteration minerals within a geothermal system can be explored (e.g. Mbia, 2010). Mineral deposition sequences are controlled by numerous factors such as temperature, fluid composition, rock type, the interaction of hydrothermal fluids and the host rock, porosity, permeability and the duration of the interactions (Browne, 1978).
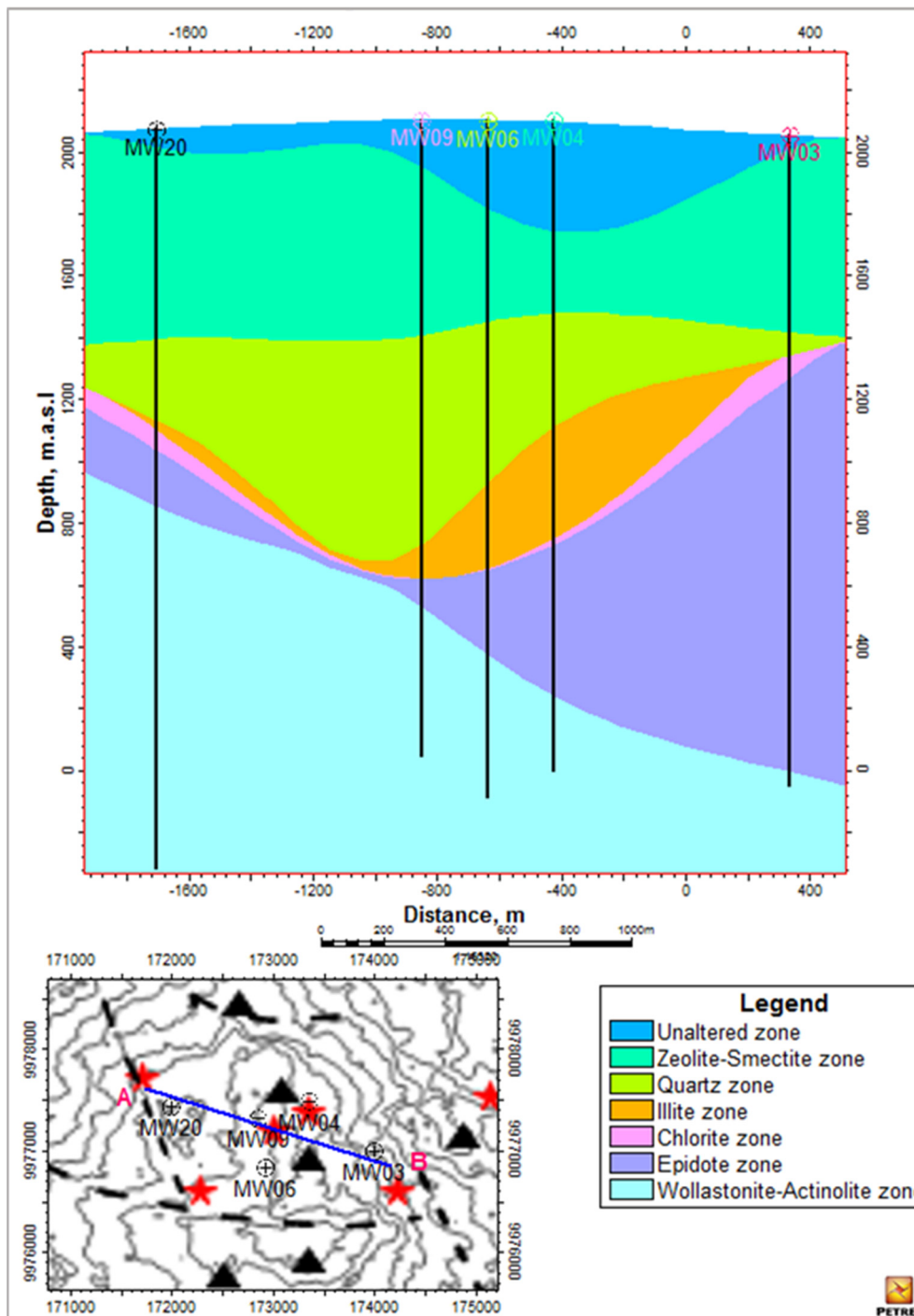
Figure 25: Cross section A to B showing alteration zones in the study wells (MW-03, MW-09 and MW-20) and neighbouring wells (MW-04 and MW-06)

By the aid of binocular and petrographic microscope, the secondary hydrothermal mineralization and the mineral deposition sequences in wells MW-03, MW-09 and MW-20 were identified and the results presented in Tables 18, 19 and 20. The older minerals deposit first, followed by the younger minerals. Most of the observed mineral sequences noted in these wells were deposited in vesicles and less in veins. The dominant deposited minerals in sequence were calcite, quartz, and chlorite, as indicated in the Tables 6-8 below and Figure 26.

TABLE 6: Minerals deposition sequence of well MW-03

Depth(m)	Early	→	Later	Alteration	Type of rock
978	Calcite	Clay minerals	Calcite	Moderately altered	Fine grained trachyte
1210	Calcite	Clay minerals	Quartz	Slightly altered	Fine grained trachyte
1720	Quartz		Calcite	Moderately altered	Fine grained trachyte

TABLE 7: Mineral depositional sequence of well MW-09

Depth(m)	Early	→	Later	Alteration	Type of rock
1420	Clay minerals		Calcite	Slightly altered	Fine grained trachyte

TABLE 8: Mineral depositional sequence of well MW-20

Depth(m)	Early	→	Later	Alteration	Type of rock
436	Smectite		Zeolite	Slightly altered	Medium grained trachyte
1176	Chlorite	Calcite	Quartz	Slightly altered	Fine grained trachyte

At a depth of 978 m in MW-03, calcite precipitated and was followed by clay minerals and then calcite again, which might suggest that the reservoir was heating up then cooling down (Table 6). Calcite seems to be present in all the sequences, which may imply cooling especially at the end of high temperature alteration minerals. However, calcite may also indicate permeability of the formation. At 1210 m calcite forms first, followed by clay minerals then quartz deposited later, which may suggest deposition from low temperature to high temperature. At 1720 m calcite is formed first in the sequence of quartz and calcite and followed by quartz.

Table 7 shows that in MW-09 clay minerals formed first and followed by calcite, these minerals exhibit the same range of temperatures, they may indicate permeability in the formation.

In MW-20 at 1176 m, chlorite appears to form first, followed by quartz. Calcite came later in the sequence. The sample is near the boundary of fine grained trachyte and medium grained trachyte (Table 8).

3.4 Paragenesis of calcite and epidote

3.4.1 Calcite

Calcite is an abundant secondary mineral in all the study wells. The mineral stability depends on boiling, dilution and condensation of carbon dioxide in a geothermal system and can form from shallow steam
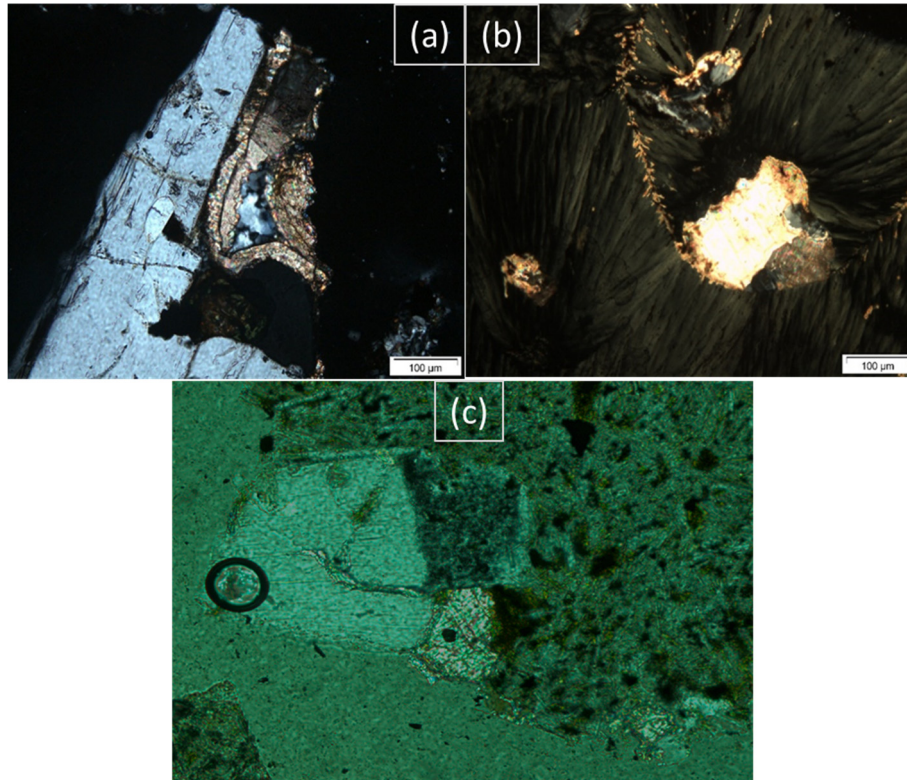
FIGURE 26: a) Calcite with quartz at 1210 m, MW-03 b) quartz with calcite and chlorite at 1176 m, MW-20 c) Calcite with clay minerals at 1420 m, MW-09. Photomicrographs a and b were taken by crossed polars, whereas c was taken by 1 polariser

heated groundwater and deep geothermal water. The methods used to identify the mineral were binocular microscope and petrographic analysis while hydrochloric acid was used to determine the presence of calcite in the drill cuttings as represented in a plot of lithology against calcite (the minerals was assigned value from 1-3) in Figure 28. The clear rhombohedral cleavage and high interference colour of the mineral and change of relief with rotation made it easy being identified in thin section. Calcite is common and extensive mineral occurring filling veins and vesicles in the studied wells. Variable shapes of euhedral, subhedral and anhedral calcite are observed in the wells. In the wells MW-03, MW-09 and MW-20 calcite occurs in three main ways (Figure 27);

1) *Replacement of rock forming minerals, especially feldspar and/ pyroxene.*
Interaction between the deep fluids and feldspar or pyroxene result in replacement of alteration minerals such as calcite, clay minerals and other minerals as shown in the equation below;

$$\text{Feldspar} + CO_2 + H_2O = \text{Calcite} + \text{clay minerals} + \text{Ca aluminosilicate} + Na^+$$
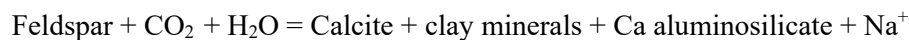
This occurs when the temperature is above 170°C. Calcite is also observed to form as a product of alteration of interstitial glass. Volcanic glass is also replaced by calcite under similar process of hydrolysis.

2) *Boiling of the reservoir fluids which leads to loss of CO₂ and calcite precipitates in veins or open spaces and creates bladed calcite as illustrated in the equation below:*

$$Ca^{2+} + 2HCO_3^- = CaCO_3 + CO_2 + H_2O$$

3) *Calcite precipitating in veins or fractures when hotter fluids mix with circulating ground water.*
This process may produce platy calcite if the crystallization is rapid. The platy calcite can be distinguished based on the crystal shape that is dominated by basal pinacoid form as described by Simmons and Christenson (1993). In the studied wells no well-formed platy calcite was observed.

37
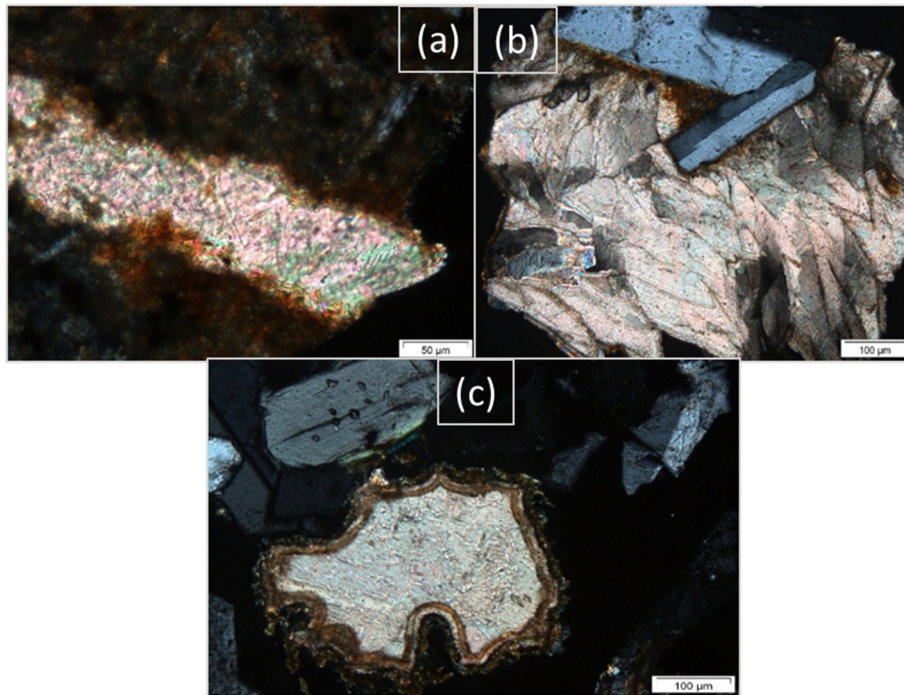
FIGURE 27: a) Calcite filling a fracture in MW-20 b) Calcite filling an open space in MW-03 c) Calcite filling a vesicle in MW-03. All photomicrographs were taken with crossed polars

The frequency of calcite precipitating in open spaces is high above 1210 m compared to calcite that is formed due to alteration of feldspar, pyroxene and glass. In MW-20, calcite filling open spaces are prominent at 1000 m and above while below 1000 m calcite is more product of alteration of primary phases like glass, pyroxene and feldspar.

Excess deposition of calcite in open spaces such as veins, fractures, vesicles and vugs may lead to decrease in permeability. However, it can be of great importance if the filling of open spaces is occurs above the geothermal system forming a cap rock in such a way that the inflow of cold water in the production zone is blocked or reduced.

3.4.2 Epidote

Epidote has yellow to green colour, high relief and it forms small elongated prismatic crystals and exhibit strong pleochroism of green, yellow and brown in thin section depending on the iron content of the mineral. It has 2nd order interference colours that helps distinguishing the mineral (Figure 29). In the geothermal system, epidote exhibits a wide range of octahedral substitution of Al^{3+} for Fe^{3+}, with irregular zoning as described by Bird and Spieler (2004). The mineral occurs in various geological environments. Its chemical formula is $Ca_2Fe_xAl_{3-x} Si_3O_{12} (OH)$. Arnórsson et al. (1990) pointed out that temperature, O_2 and CO_2 fugacities, bulk rock and fluid composition control the variations in epidote composition.

Epidote in active geothermal system is formed by reactions of hot fluids and host rocks of various bulk compositions. The mineral precipitates in veins and cavities, but also by replacement of silicates, iron oxides and carbonates. Bird and Spieler (2004) have noted that the paragenesis is simple but others shows multiple stages of epidote formation and dissolution. Epidote in active geothermal systems is common and an abundant phase, which is stable over a temperature range of 230-300°C in volcanic rocks (e.g. Browne, 1978, Kristmannsdóttir, 1979). The occurrence of epidote reflects the relationship with temperatures, permeability and fluid composition in the geothermal system.

In the study wells MW-03, MW-09 and MW-20 epidote is a rare alteration mineral. In well MW-03 epidote is occurring at 850 m and occurs sporadically to 1936 m. The first appearance of epidote in MW-09 was at 1586 m only to disappear below 1606 m. In well MW-20 epidote was first observed at a
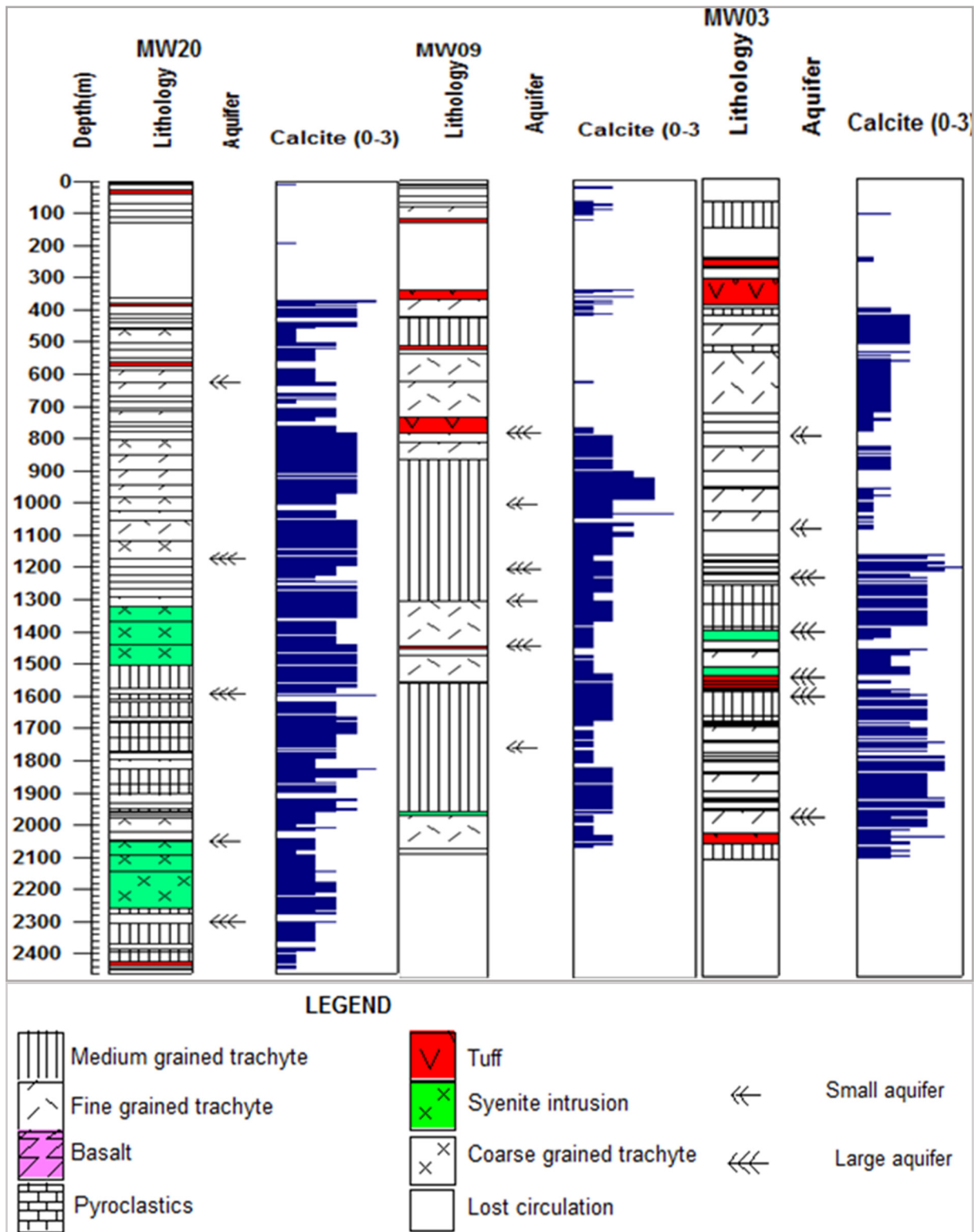
FIGURE 28: Variation of calcite in wells MW-20, MW-09 and MW-03

depth of 1000 m and it occurs infrequently to the depth of 2448 m. As noted earlier no well-formed crystals of epidote with prismatic shape was encountered in these wells.

There is a possibility that low permeability in the rocks may contribute to relatively low abundance of epidote in the studied wells. The rocks have not reached equilibrium with hydrothermal fluids to form an abundance of secondary minerals, including epidote. The rocks with reasonable permeability enhance hydrothermal alteration processes. The rock composition can also be a limiting factor. Low
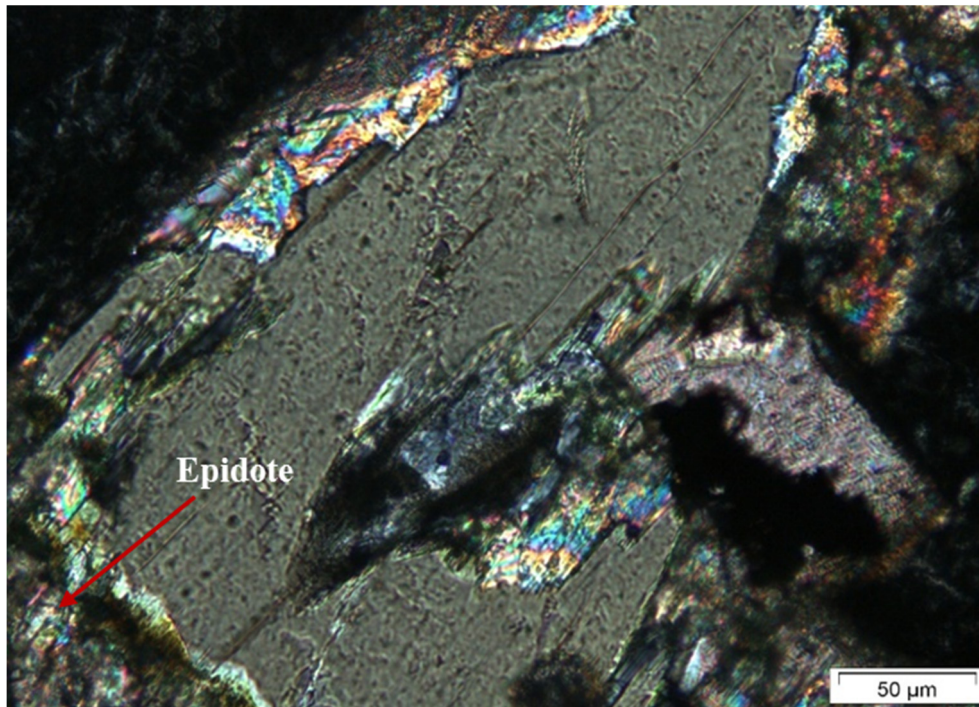
FIGURE 29: Pyroxene altering to epidote at 1832 m depth in well MW-20;
photomicrograph is taken with crossed polars

concentration of iron and high concentration of CO_2 could also be a cause for rare occurrence of epidote in the Menengai wells.

3.5 Formation and alteration mineral temperatures

Formation and alteration mineral temperatures were plotted with boiling point temperature curve in Figure 30a and b for MW-03 and MW-20, respectively. In MW-03, at depths below 500 m, formation and alteration temperatures show the same trend but at the bottom, the well is heating up and the sharp rise in temperature at the bottom shows that the well is conductive. For well MW-20, formation temperature is higher than alteration temperatures which may indicate heating up of the well.

Well MW-09 in Figure 30c, fluid inclusion geothermometry was reported by Lopeyok 2014, fifteen fluid inclusions of calcite crystals gave homogenisation temperature values from 220-260ºC with an average of 245°C. He noted that the fluid inclusion temperatures plot within the temperature range from 210-245°C.

Fluid inclusion temperatures plotted on the boiling temperature curve suggesting that calcite precipitated under boiling conditions. In this well, formation temperature seems to be higher than the alteration mineral temperatures above 1280 m depth, which indicates that the well is heating up. Measured temperatures used in MW-09 may be slightly lower than those found in the present natural system. Formation temperatures in MW-03, MW-09 and MW-20 together with neighbouring wells MW-04 and MW-06 in Figure 31a increases in the change of alteration minerals, from low to high alteration zone. At 1000 m a.s.l., formation temperature contours show well MW-03 with low temperature of about 170°C compared to MW-09 and MW-20 and neighbouring wells MW-04 and MW-06 (Figure 31), this depth in wells exhibits high temperature alteration minerals. The behaviour of well MW-03 indicates inflow of cold water towards the well and cool with time.
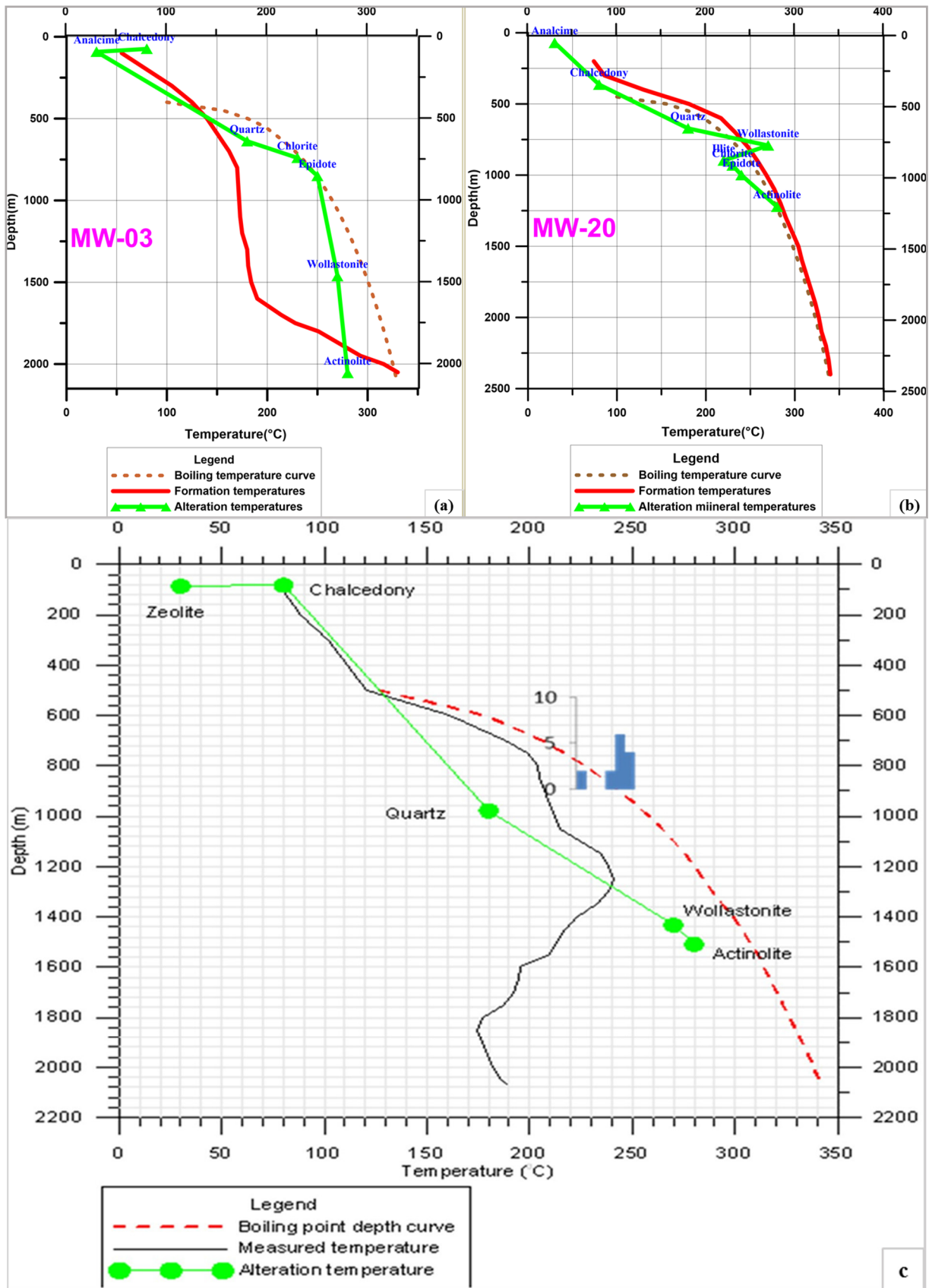
FIGURE 30: Formation, alteration mineral temperatures and boiling point depth curve,
a) MW-03; b) MW-20; and c) MW-09

41
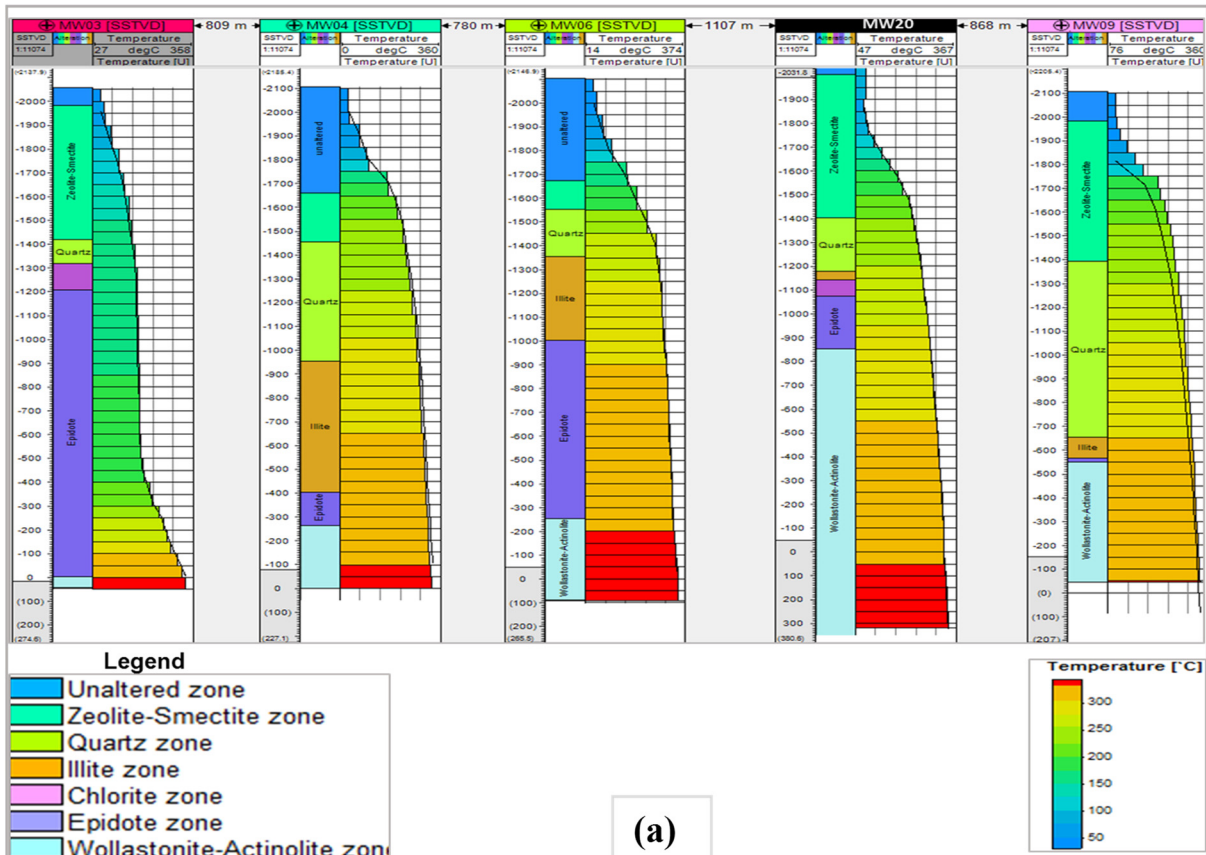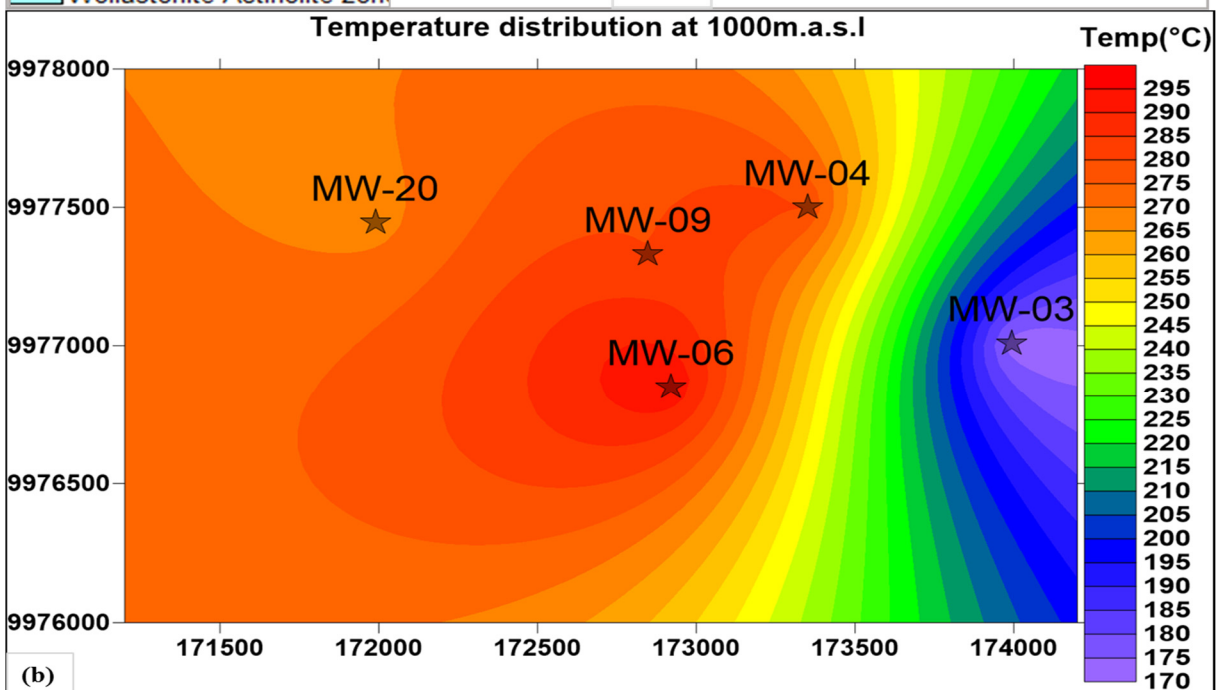
FIGURE 31: a) Formation temperatures with alteration zones; and
b) formation temperature contours at 1000 m a.s.l. in MW-03, MW-20
and MW-09 and neighbouring wells MW-04 and MW-06

3.6 Whole-rock geochemistry

3.6.1 Rock classification

A total of 28 samples from wells MW-03, MW-09 and MW-20 were analysed for whole – rock major and trace element concentrations. Major elements are Si, Al, Fe, Mn, Mg, Ca, Na, K, Ti and P while trace elements are Rb, Ba, La, Sr, Zr, Y, Zn, Cu, Co, Sc, V, Cr and Ni. The results are shown in Tables 9, 10, and 11. The uncertainty for standards is; Si and Mg is ~1%,

Ti <2%, Al, Fe, Ca, Na, K from 4-6%, Mn and P<8% whereas, trace elements from 4-8%. The results are used to classify the rock types especially volcanic rocks based on the total alkalis ($Na_2O + K_2O$) and silica contents (TAS diagram, from Le Bas et al., 1986 and Macdonald and Katsura, 1964). Generally, for mafic alkaline rocks, such besides bulk rock composition, the mineralogical and textural criteria are also needed for proper classification (Le Maitre et al., 2002).

TABLE 9: Whole rock chemical analysis for well MW-03

MW-03										
Depth(m)	250	470	690	870	1230	1366	1588	1654	1912	2070
Major elements (wt %)										
SiO2	66.26	62.84	61.32	62.75	60.82	62.05	64.53	62.15	64.13	62.54
Al2O3	10.94	15.10	16.78	16.34	16.71	16.97	13.60	18.48	14.65	16.54
FeO	9.32	6.55	5.70	5.00	6.80	6.27	8.46	4.56	7.06	5.15
MnO	0.34	0.25	0.22	0.20	0.25	0.27	0.37	0.18	0.27	0.21
MgO	0.31	0.47	0.66	0.79	0.50	0.34	0.26	0.29	0.29	0.47
CaO	1.03	1.51	1.93	2.14	2.49	1.29	1.09	1.73	1.08	1.56
Na2O	6.50	7.18	6.33	6.46	6.11	6.35	5.90	5.65	6.79	7.13
K2O	4.25	5.09	5.81	5.25	5.24	5.54	4.81	5.76	4.77	5.40
TiO2	0.69	0.75	0.89	0.66	0.82	0.73	0.72	0.85	0.67	0.72
P2O5	0.08	0.10	0.21	0.22	0.16	0.12	0.07	0.20	0.09	0.13
Trace elements(ppm)										
Ba	49.17	212.71	751.96	1264.09	211.95	42.60	90.71	798.01	106.50	702.43
Co	5.51	5.85	7.07	6.10	7.17	5.02	5.72	6.49	5.16	5.85
Cr	3.06	9.13	3.88	22.40	41.62	34.97	5.03	3.23	18.20	14.31
Cu	15.34	11.93	14.63	23.29	18.91	14.00	12.34	13.33	17.81	11.23
La	375.34	191.21	78.16	57.07	87.98	227.10	102.63	89.72	216.36	85.98
Ni	4.03	0.00	1.11	36.57	2.23	17.49	0.00	0.00	7.11	0.00
Rb	167.57	91.34	56.04	144.76	84.12	80.48	59.84	77.32	188.01	137.20
Sc	2.65	5.65	9.20	8.82	8.49	4.14	7.12	5.74	3.59	5.35
Sr	30.69	35.21	50.94	131.40	36.07	19.58	5.92	69.55	22.74	59.83
V	19.04	10.72	13.56	14.55	6.63	7.61	1.19	4.53	10.62	7.37
Y	239.04	108.05	43.74	37.32	44.86	134.93	43.54	52.67	152.93	50.24
Zn	331.86	172.69	159.71	87.51	117.91	223.61	129.87	96.38	177.94	116.40
Zr	1686.45	839.36	280.44	218.81	281.42	942.82	332.72	305.81	972.72	351.45

The results of major element analyses are plotted on a TAS diagram (Figures 32 and 33). The rocks plot in the trachyte field above the Macdonald and Katsura (1964) division line showing that the rocks are alkaline in composition. All selected samples plot in the fields of Menengai, Eburru and Longonot trachytes, indicated by M, Et and L in Figure 32. The trachytic analyses of Menengai, Eburru and Longonot are from surface samples reported by MacDonald and Scaillet, (2006). The variation and composition of major and trace elements in MW-03, MW-09 and MW-20 shows nearly the same chemical trends and concentrations in Figure 35 (a-p). Figure 33 shows the comparison between the nearest wells MW-04, MW-06 and MW-07 by Mbia (2014) and the results of this study. Wells MW-02, MW-04, MW-06 and MW-07 show chemical variations from basalt to trachyte and rhyolite in composition, but in this study all analysed samples show trachytic composition. In addition, all the rocks analysed in study wells are metaluminous based on the higher concentration of Al_2O_3 compared to amount of $Na_2O + K_2O$ in the rocks (Table 9, 10 and 11), while MW-02, MW-04, MW-06 and MW-07

TABLE 10: Whole rock chemical analysis for well MW-09

MW-09								
Depth(m)	118	402	882	1452	1544	1560	1800	2048
Major elements (wt %)								
SiO_2	64.58	65.00	60.86	64.17	62.32	63.21	65.62	64.30
Al_2O_3	12.55	12.96	16.38	14.39	15.51	15.00	12.44	14.50
FeO	9.07	8.48	6.14	7.36	6.15	7.23	8.19	7.15
MnO	0.38	0.34	0.21	0.29	0.23	0.28	0.32	0.29
MgO	0.13	0.23	0.81	0.23	0.47	0.24	0.15	0.32
CaO	1.04	1.11	2.38	1.04	1.71	1.11	0.91	1.23
Na_2O	6.73	6.19	6.29	6.82	6.43	6.95	6.59	6.25
K_2O	4.53	4.67	5.35	4.81	5.66	5.02	4.85	5.02
TiO_2	0.75	0.74	1.09	0.63	1.12	0.69	0.65	0.68
P_2O_5	0.06	0.05	0.28	0.07	0.22	0.08	0.04	0.09
Trace elements(ppm)								
Ba	14.37	37.18	1598.91	58.80	806.45	134.72	57.29	110.68
Co	4.37	4.63	9.38	23.61	9.43	4.90	3.77	5.29
Cr	0.00	4.72	13.66	12.29	8.65	0.79	3.73	49.97
Cu	11.58	11.19	13.20	22.36	39.70	12.90	8.37	20.86
La	228.99	262.42	57.12	220.27	84.80	225.92	294.72	130.77
Ni	0.00	0.00	6.37	4.55	54.28	0.00	0.00	31.77
Rb	137.66	155.64	106.16	152.79	130.49	116.54	264.04	122.66
Sc	3.51	3.41	10.50	3.95	7.06	3.69	3.05	4.55
Sr	3.56	44.98	62.74	7.66	78.93	14.51	6.91	28.94
V	3.85	18.68	10.38	6.06	9.72	7.77	7.76	10.09
Y	150.19	166.26	29.85	111.85	60.92	133.25	191.02	117.05
Zn	261.82	254.09	115.74	160.31	113.81	181.74	258.20	187.84
Zr	989.59	1251.55	164.45	1036.16	417.40	1053.52	1375.41	875.19

TABLE 11: Whole rock chemical analysis for well MW-20

MW-20										
Depth(m)	376	506	760	988	1142	1300	1570	1790	2262	2398
Major elements (wt %)										
SiO2	64.60	63.57	62.56	63.44	62.73	62.28	63.38	64.99	64.34	62.60
Al2O3	10.38	13.83	16.43	15.89	15.43	15.77	14.57	12.41	13.60	14.03
FeO	8.18	7.83	5.28	4.87	6.56	6.52	7.98	8.88	8.47	8.60
MnO	0.33	0.35	0.23	0.20	0.26	0.25	0.34	0.36	0.31	0.35
MgO	0.32	0.25	0.60	0.48	0.37	0.35	0.22	0.15	0.13	0.17
CaO	5.68	1.46	1.81	1.84	1.51	1.47	1.18	1.05	1.05	1.13
Na2O	5.59	6.82	6.49	6.25	6.63	6.70	6.09	7.04	6.71	7.23
K2O	4.00	4.88	5.55	5.79	5.38	5.60	5.31	4.15	4.50	5.04
TiO2	0.66	0.74	0.70	0.88	0.85	0.81	0.71	0.74	0.64	0.62
P2O5	0.04	0.09	0.17	0.19	0.15	0.14	0.04	0.06	0.04	0.03
Trace elements(ppm)										
Ba	111.54	67.54	1057.95	1063.67	319.97	141.69	20.29	15.95	24.04	18.29
Co	4.32	5.39	5.38	6.40	13.25	6.05	4.39	4.48	4.11	3.86
Cr	7.58	33.51	101.16	5.66	2.75	1.64	2.28	5.96	5.68	3.47
Cu	34.26	11.59	19.24	17.61	20.92	38.98	14.80	20.04	48.87	24.09
La	164.25	225.13	44.74	52.10	125.24	105.86	212.83	204.14	230.49	236.17
Ni	42.53	0.00	15.29	15.56	14.96	59.69	0.00	0.81	59.95	17.78
Rb	142.49	222.22	130.45	177.36	116.20	164.58	167.36	221.64	183.76	179.76
Sc	2.83	5.04	8.55	8.39	6.67	7.13	3.88	4.09	2.64	3.06
Sr	61.04	8.12	77.38	56.94	22.15	7.47	5.62	3.71	5.85	4.54
V	8.61	5.28	9.85	8.37	3.53	1.04	5.07	3.66	5.82	5.11
Y	149.67	128.04	32.66	36.43	73.98	63.71	130.18	130.47	151.62	150.84
Zn	241.69	218.32	104.67	87.46	137.47	140.02	198.87	237.32	215.52	213.64
Zr	1086.79	951.14	211.58	214.53	483.41	393.45	972.36	940.39	1131.32	1121.47
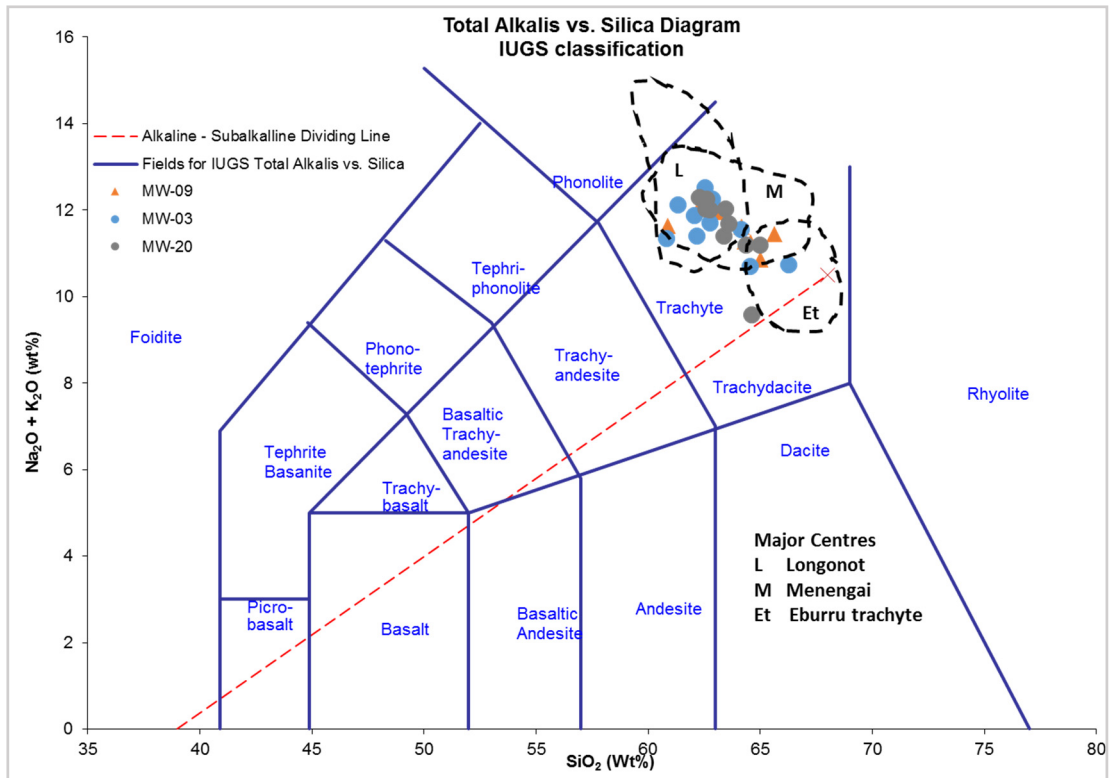
Figure 32: Total alkali – silica plot showing the composition range of Menengai subsurface rocks from well MW-03, MW-09 and MW-20 and surface composition of Menengai and the neighbouring volcanic centres (Eburru and Longonot) denoted by L, M and Et from Macdonald and Scaillet (2006)
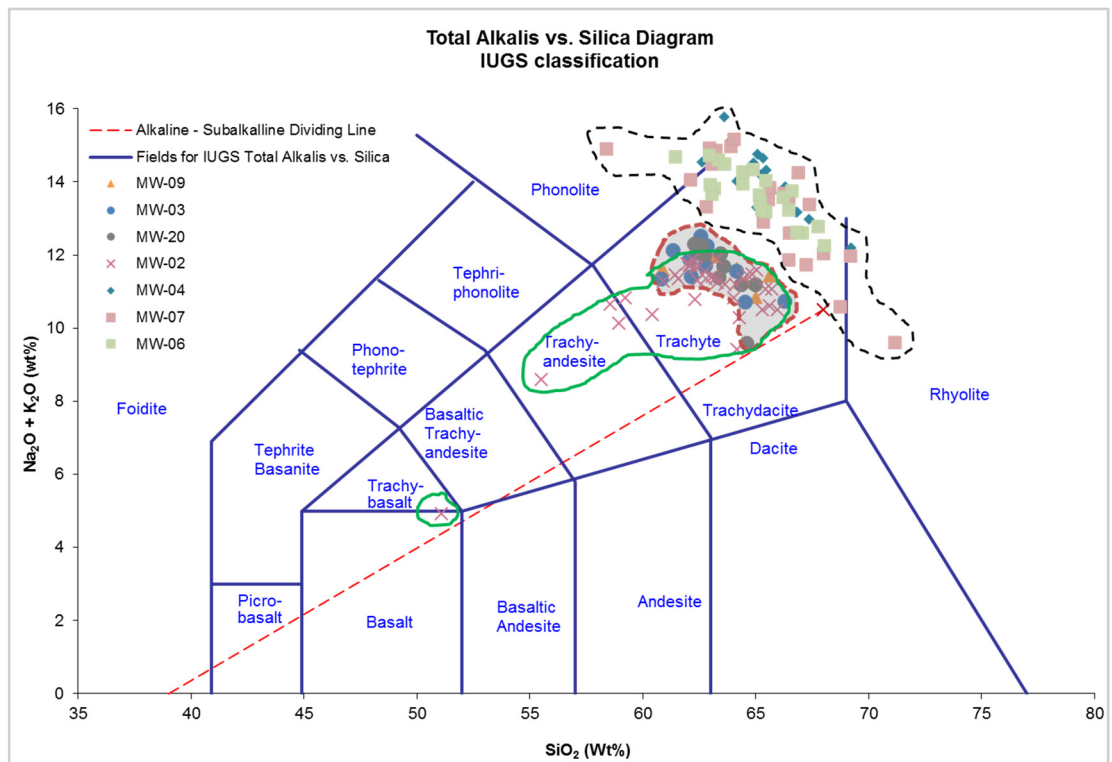
FIGURE 33: Total alkali – silica plot showing the composition range of Menengai subsurface rocks from well MW-03, MW-09 and MW-20 (red dotted polygon) and other wells (MW-02, MW-04, MW-06 and MW-07 dark dotted polygon and circled green solid line (additional data from Mbia, 2014)
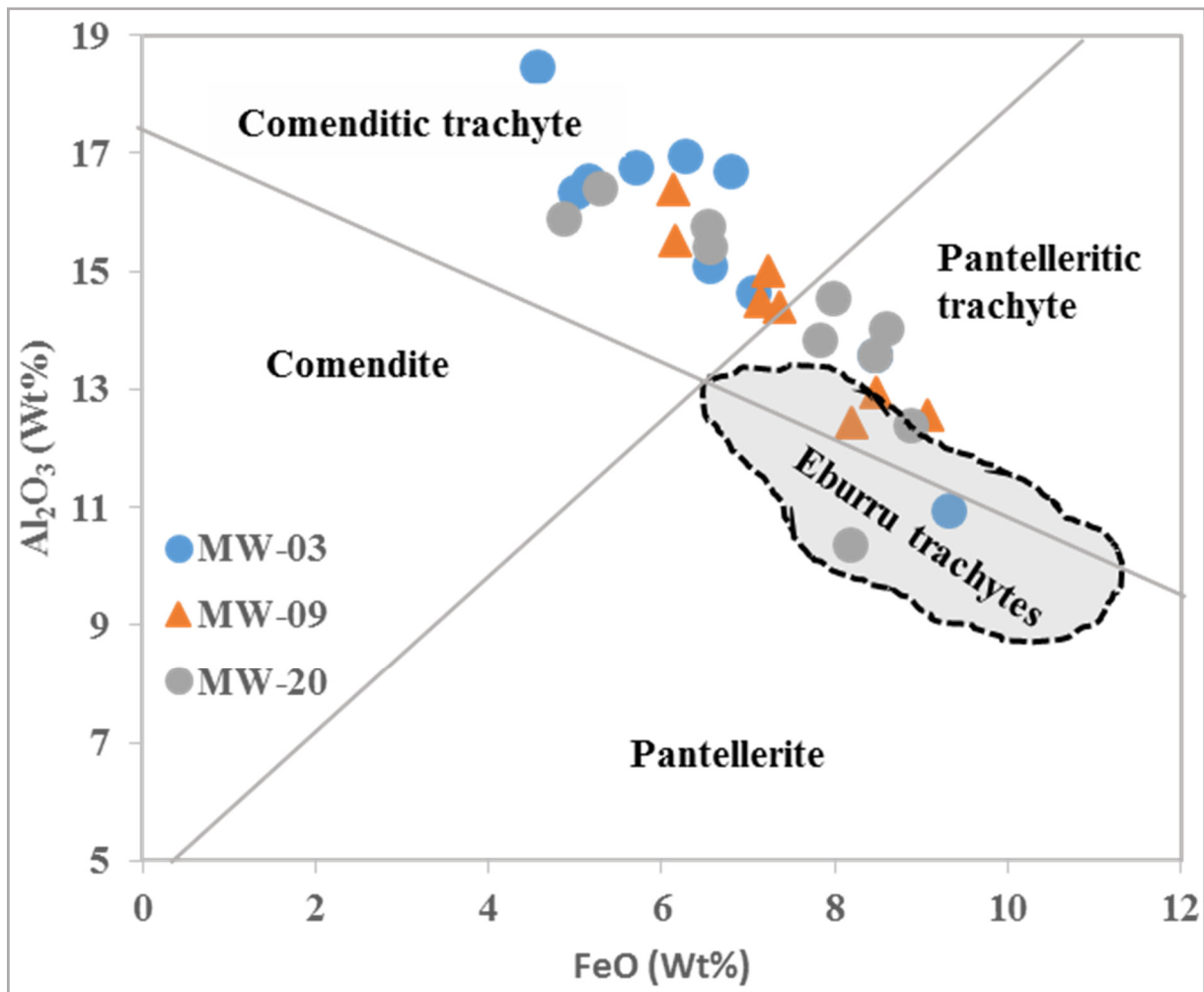
FIGURE 34: The plot of Al_2O_3 as a function of FeO classifying the Menengai subsurface rocks
and Eburru volcanic centre (Modified from Macdonald, 1974)

are more peralkaline as observed by Mbia (2014). When classifying volcanic rocks based on Al_2O_3
content and concentration of FeO (Macdonald, 1974), most of the samples plot in the fields of
pantelleritic trachyte, comenditic trachyte, while the two samples plot in the pantellerite field (Figure
34). Some samples show the same chemical trend as surface samples of Menengai pantelleritic trachyte.

3.6.2 Magma differentiation processes

In Figure 35, the major oxides such as TiO_2, MgO, CaO, Al_2O_3, P_2O_5 and K_2O show negative correlation
with SiO_2. This negative correlation reflects the fractional crystallization of ferromagnesian minerals,
feldspar and apatite. FeO and MnO seem to increase with SiO_2, in the study wells, however, FeO tends
to decrease with SiO_2 in the neighbouring wells as described by Mbia (2014). The same negative
correlation of FeO with SiO_2 was reported by Musonye, (2015) in wells from Olkaria. While many
oxides correlate negatively with SiO_2, Na_2O is scattered and remain nearly constant. Na is a mobile
element and is easily leached from the rock provided there is fluid-rock interaction. In figure 35(h), the
high CaO at one depth is caused by the abundance of calcite at 376 m depth in MW-20. Figure 35 (j-r)
shows distribution of selected trace elements such as Zn, Y, La, Zr, Rb, Co, Cr, Ba and Sr versus SiO_2.
The first five elements show a positive correlation with SiO_2 which may indicate that they are enriched
in melt during fractional crystallization, but the last two elements, Ba and Sr, shows a slight negative
correlation with SiO_2 which implies the possibility of these elements being partitioning into feldspar
during crystallization. This negative correlation is best seen in well MW-09, but is less obvious in the
other two. Largely, the decrease in major elements (Figure 35), Ba, Sr, Co, V, Cr and Ni is corresponding
to the fractionation of the observed mineral assemblage of feldspar, pyroxene, olivine, apatite, and iron–
titanium oxide in the rocks.
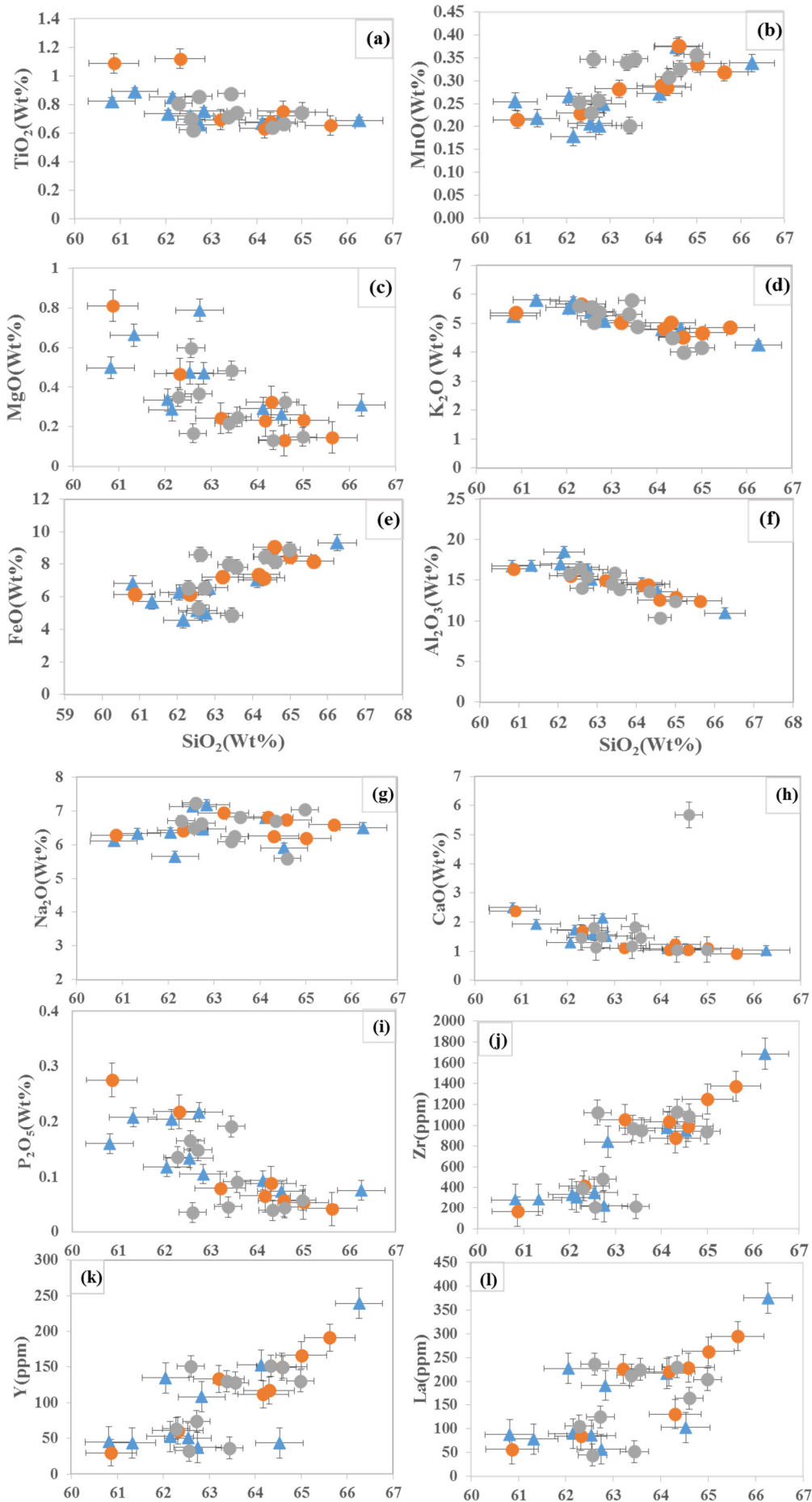
Figure 35: Major oxides plotted as function of SiO₂ and selected trace elements
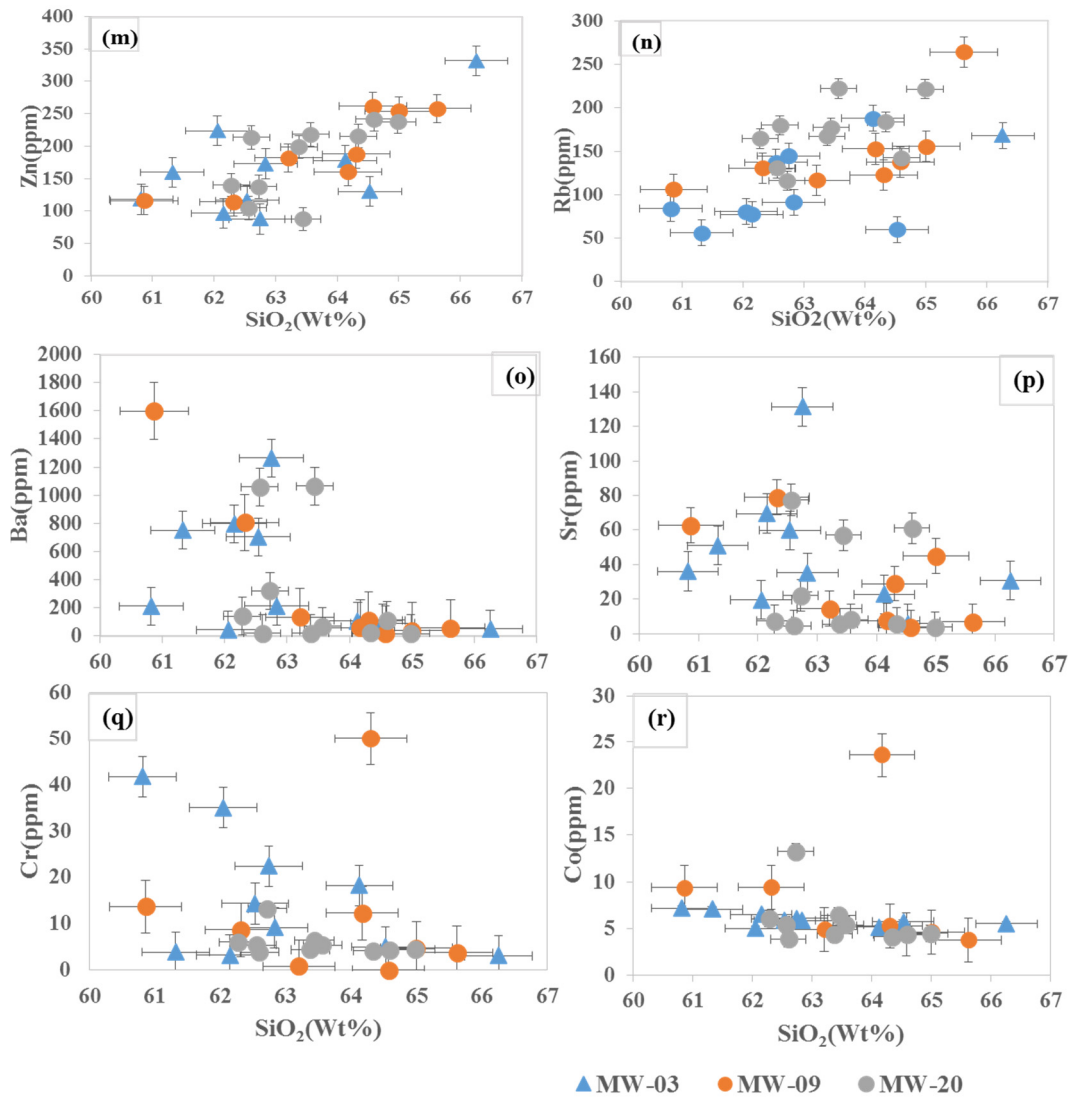
Figure 35 cont.: Major oxides plotted as function of SiO$_2$ and selected trace elements
(a-r) in wells MW-03, MW-09 and MW-20

3.6.3 Effects of hydrothermal alteration on rock chemistry

As explained earlier hydrothermal alteration is the response of the rock being subjected to thermal environments in the presence of hot fluids. This leads to changes of the rock in mineralogical and textural context. From whole rock geochemistry point of view, selected trace elements (Figure 36a-f) and major oxides (Figure 35a-i) are examined to point out the effects of hydrothermal alteration on rock chemistry. Selected trace elements were plotted as a function of Zr, which is considered as least mobile.

In Figure 36a-f, plots of Rb, La, Sr, Ba, Y and Cr versus Zr indicate that hydrothermal processes has insignificant effect on trace elements such as Rb, La and Y. La and Y show a clear positive correlation with Zr, whereas Rb shows a slightly positive one. Sr, on the other hand shows a more significant scatter. In well MW-09, Sr and Zr are negatively correlated, but this correlation is less obvious in the other wells. At low Zr contents Sr in all rocks vary between 63 and 131 ppm. Similarly, to Sr, Ba is most variable at low Zr contents. During hydrothermal processes Ba and Sr can be leached from the rock due to its fluid mobile nature, and can be deposited elsewhere. These elements can also be weakly enriched in feldspar particularly in plagioclase.

48
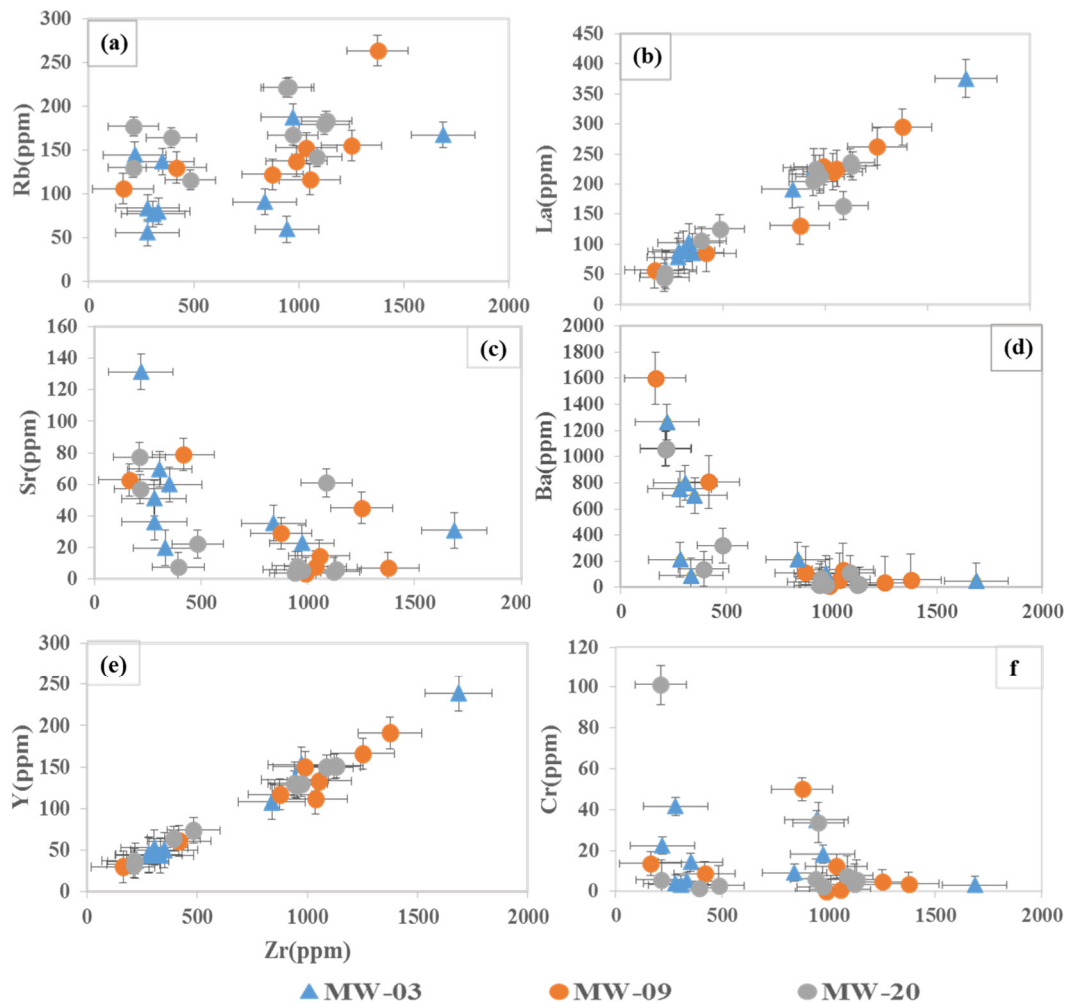
FIGURE 36: Plots (a-f) showing relationship between Zr concentrations and
other trace elements during hydrothermal processes

3.6.4 Geochemical evolution of Menengai

Data from well MW-03, MW-09 and MW-20 are used to describe the geochemical evolution of Menengai also compared to previous subsurface (Mbia, 2014) and surface geochemical data (Macdonald et al., 2006, 1994). As described earlier most of the major oxides show the same trend, decreasing with the increase of SiO_2 suggesting crystal fractionation of ferromagnesian minerals, feldspar and apatite. Trace elements from well MW-03, MW-09 and MW-20 show the same trends. Data show significant variation of Ba (14-1600 ppm) and Zr (218-1700 ppm) in the study wells, and these variations are comparable to the variations noted by Mbia, (2014) in wells MW-04, MW-06 and MW-07. The variation of Ba (14-1600 ppm), Zr (218-1700 ppm), Sr (3-132 ppm), La (45-375 ppm) and Y (30-239 ppm) are used in this study as the main geochemical tools to revealing the evolution of Menengai.

In Figure 37, trace element concentrations are normalized to continental crust on spider diagram to understand better their behaviour in the volcanic rocks of Menengai wells. In most samples, Ba and Sr show clear negative anomalies, which suggests that the elements are partitioned in sanidine and plagioclase during crystal fractionation. Generally the concentration of Ba and Sr seem to be low in the top part of the wells (top volcanic unit) while that of La, and Y are high (Figure 38, a, c and e). Then Ba and Sr increase in the next volcanic unit and Zr (Figure 37), La and Y tend to decrease. La, Y, Zr increases while Ba, Sr decrease again in MW-09 and MW-03 at ~1400-1600 m depth and the data show more scatter in all three wells below approximately 1600 m. Thus the variation of these trace elements distinguish four episodes which may represent the evolutionary stages of Menengai caldera. Compatible trace elements are depleted relative to continental crust compositions in all wells at all depths due to
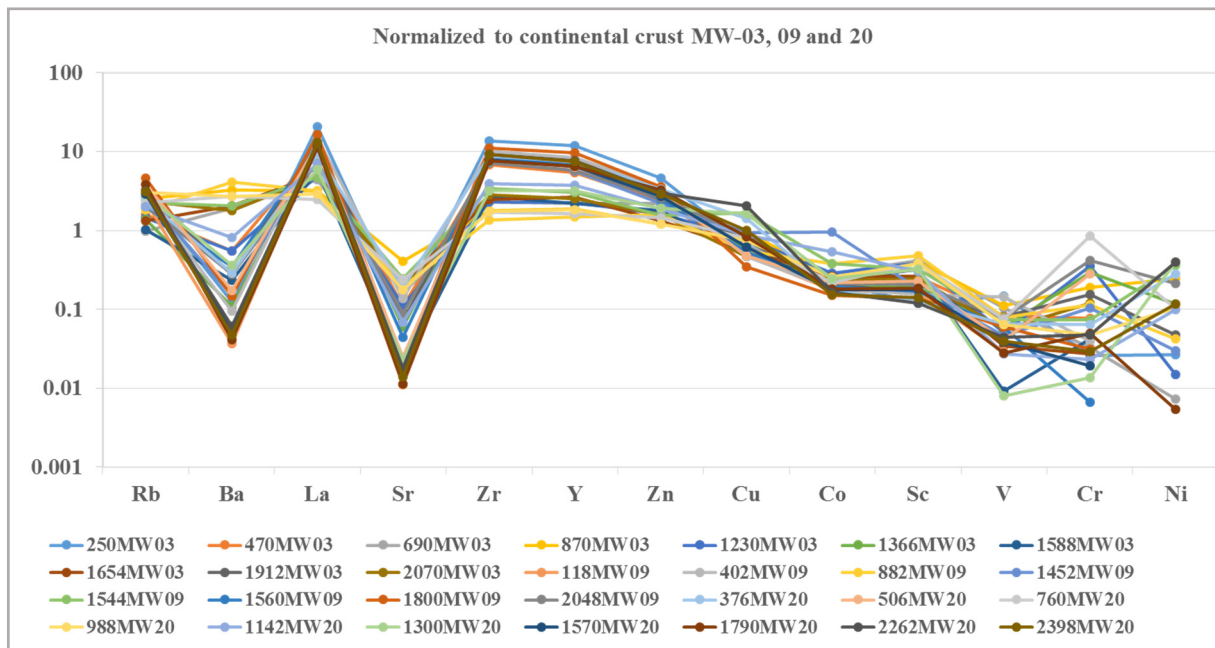
FIGURE 37: Variation of trace elements in volcanic rocks of Menengai wells in wells
MW-03, MW-09 and MW-20 on a spider diagram (normalized to
continental crust of Rudnick and Fountain, 1995)

crystal fractionation. For example the Ni, Co, Cr, Sc and V depletion trends could be the consequence of crystal fractionation of olivine, pyroxene, and titanomagnetite (Fe-Ti oxides) in a magma chamber.

Some of the Menengai caldera activity is separated by tuff marker horizons as observed by Mibei (2012), Mbia (2014), but the caldera is dominated by trachytes (fine - coarse grained trachytes). The trace elements distribution in the spider diagrams (Figure 37) and variations of Ba, Sr, Y and La in wells MW-03, MW-09 and MW-20 (Figure 38, a-f) reveals three distinct chemical compositions in the four episodes which can represent caldera formation (post-, syn-, upper-pre caldera and lower pre-caldera) (Figure 38, a-d) with depth. The shallowest formations in all wells show distinct strong negative anomalies of both Ba and Sr and significant enrichment in La, Zr and Y (Figure 38 a, b). This pattern might be typical for the post- and syn-caldera formations described by Leat (1983). He has shown that the first and second ignimbrite trachyte formations are enriched in Zr (1356-271ppm and 804-383ppm) and depleted in Ba (6-17ppm and 6-21ppm). Syn-caldera and post caldera lava show highly systematic chemical variations such as 1118 to 836ppm of Zr. Post- and syn-caldera formations cannot be distinguished based only on chemical compositions only. Among pre-caldera formations there is a larger compositional variability (Figure 39. c, d). Some of the rock compositions show low Ba and smaller negative Sr-anomalies than the syn- and post-caldera formations and these rocks also have relatively low La, Zr and Y contents. Most commonly these formations are found between 700 and 1000 m depth. Other pre-caldera compositions have intermediate trace element contents between the syn-post-caldera formations and the Ba- and Sr-rich rocks. These formations are most commonly found below 1500 m depth.
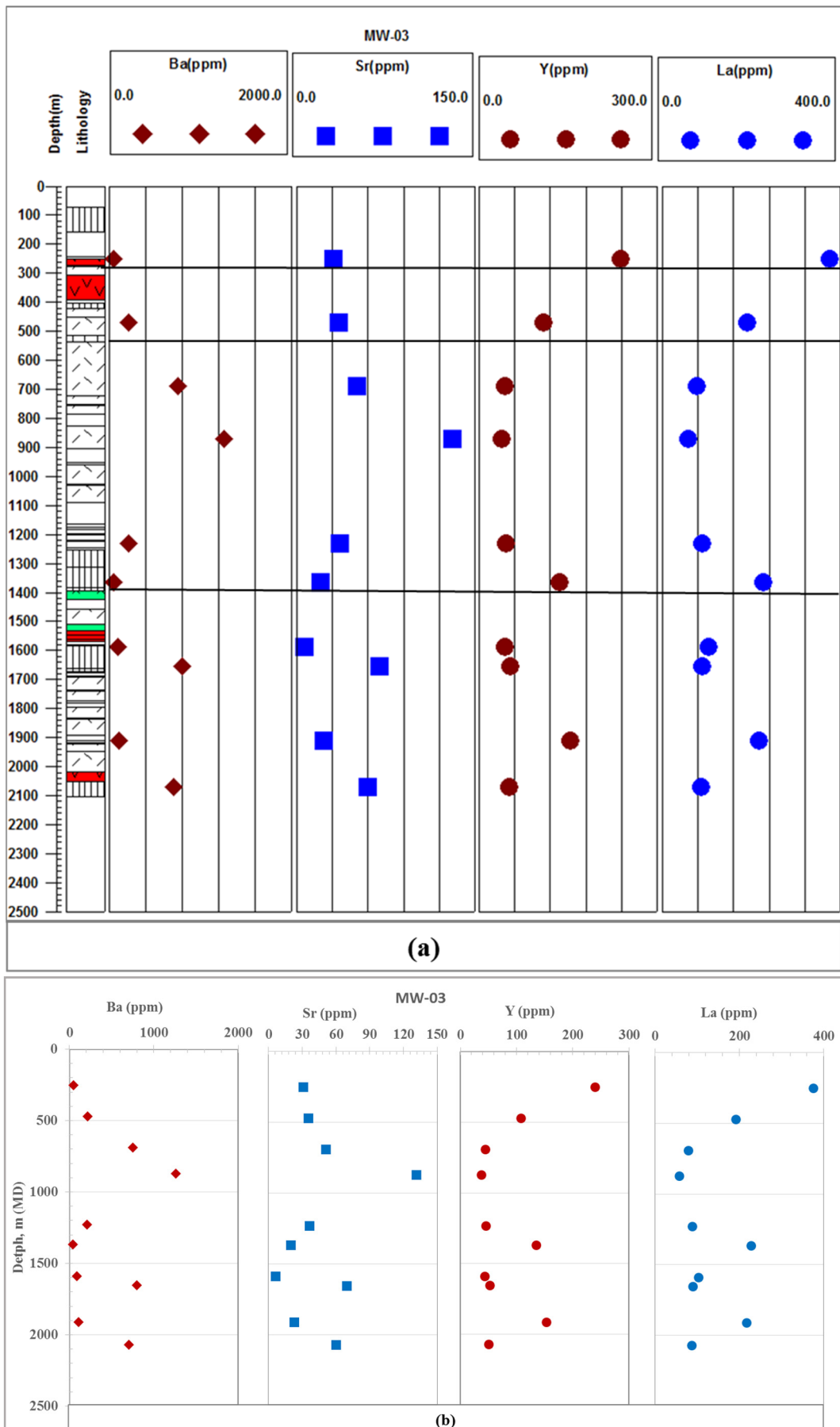
FIGURE 38A: Variation of trace elements (Ba, Sr, Y and La) in volcanic rocks of Menengai well MW-03 (a and b); dark lines in a, c and e demarcate the same trends of trace elements concentration

51
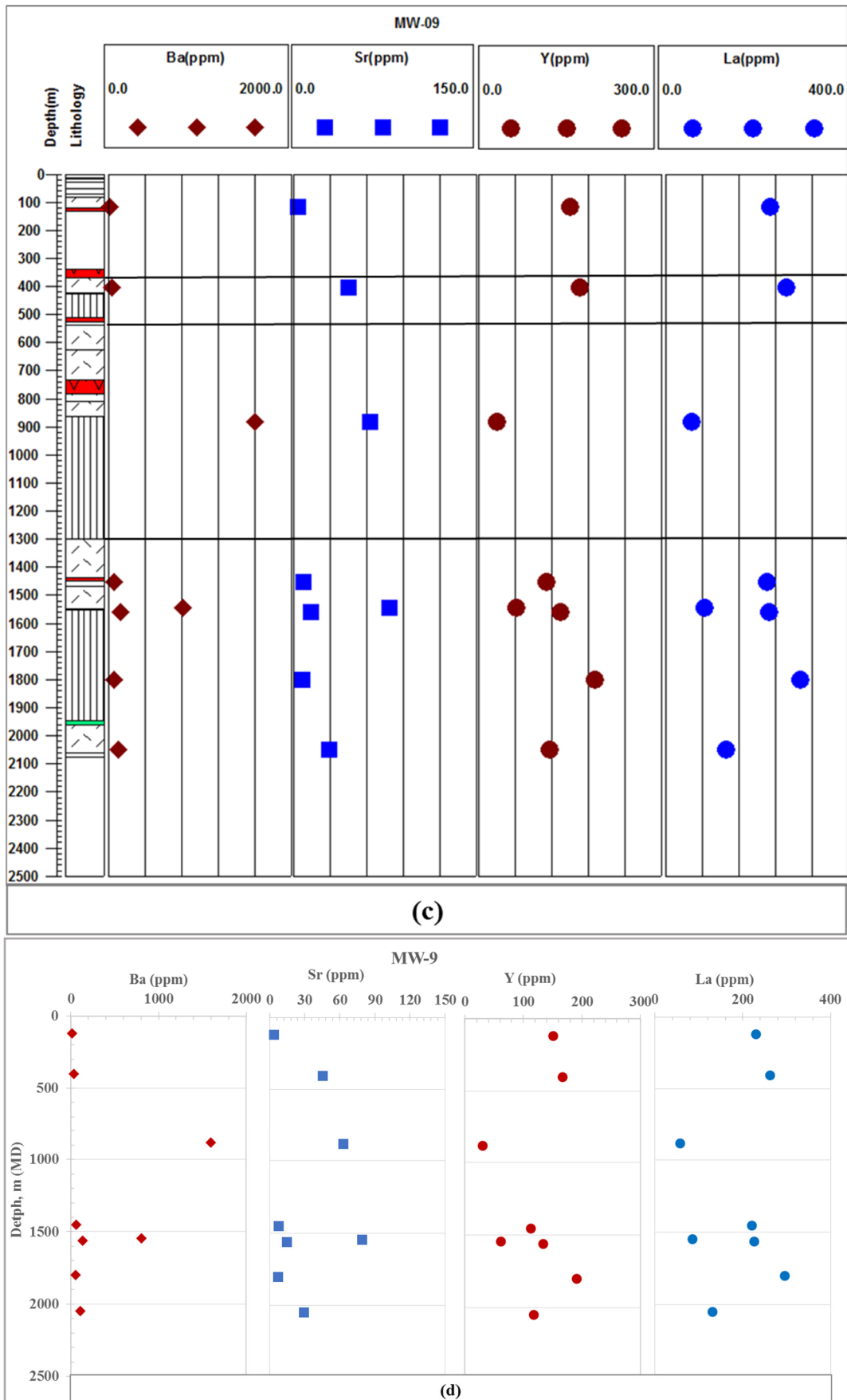
FIGURE 38B: Variation of trace elements (Ba, Sr, Y and La) in volcanic rocks of Menengai well MW- 09 (c and d); dark lines in a, c and e demarcate the same trends of trace elements concentration
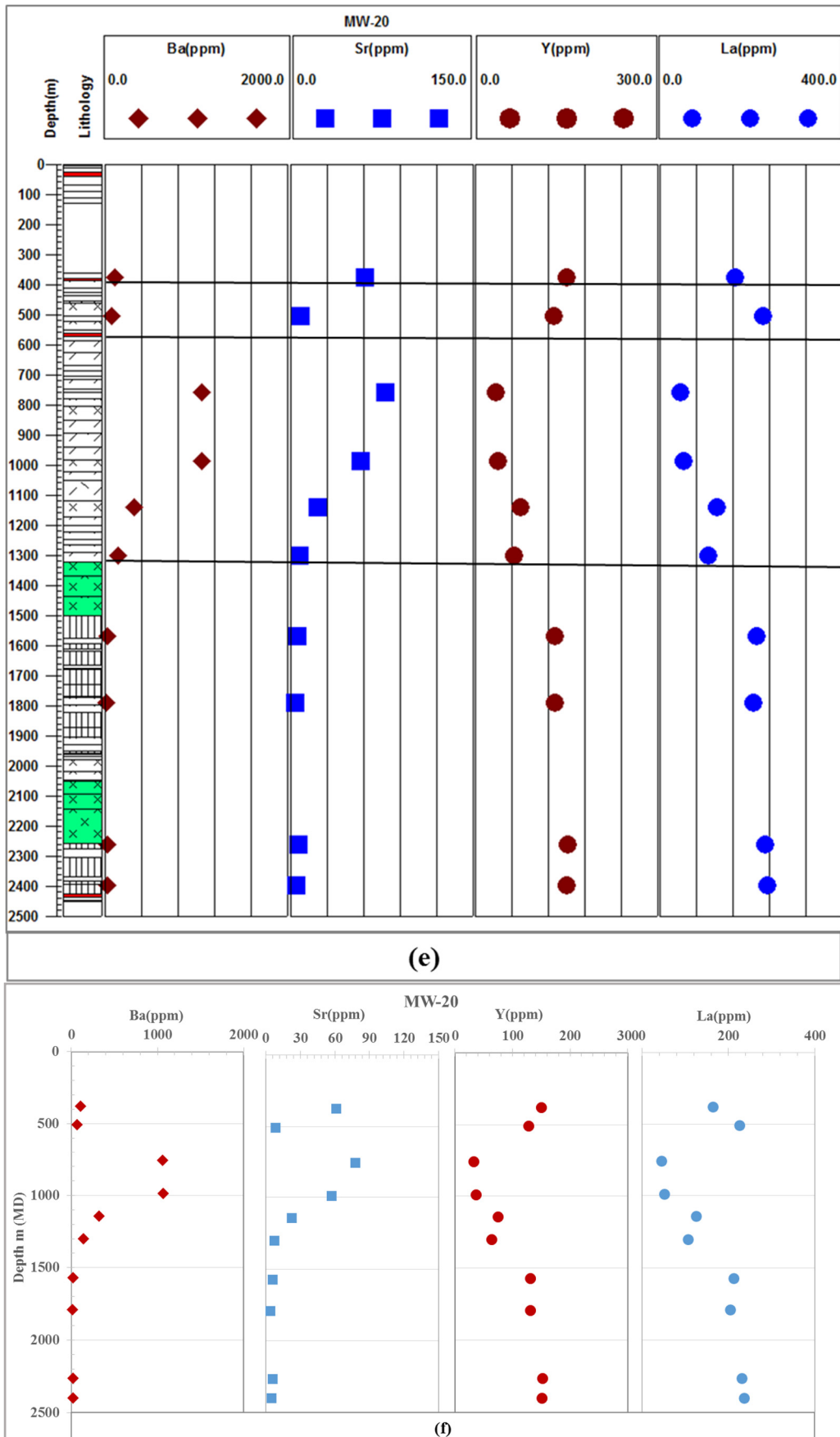
FIGURE 38C: Variation of trace elements (Ba, Sr, Y and La) in volcanic rocks of Menengai
well MW-20 (e and f); dark lines in a, c and e demarcate the same trends
of trace elements concentration
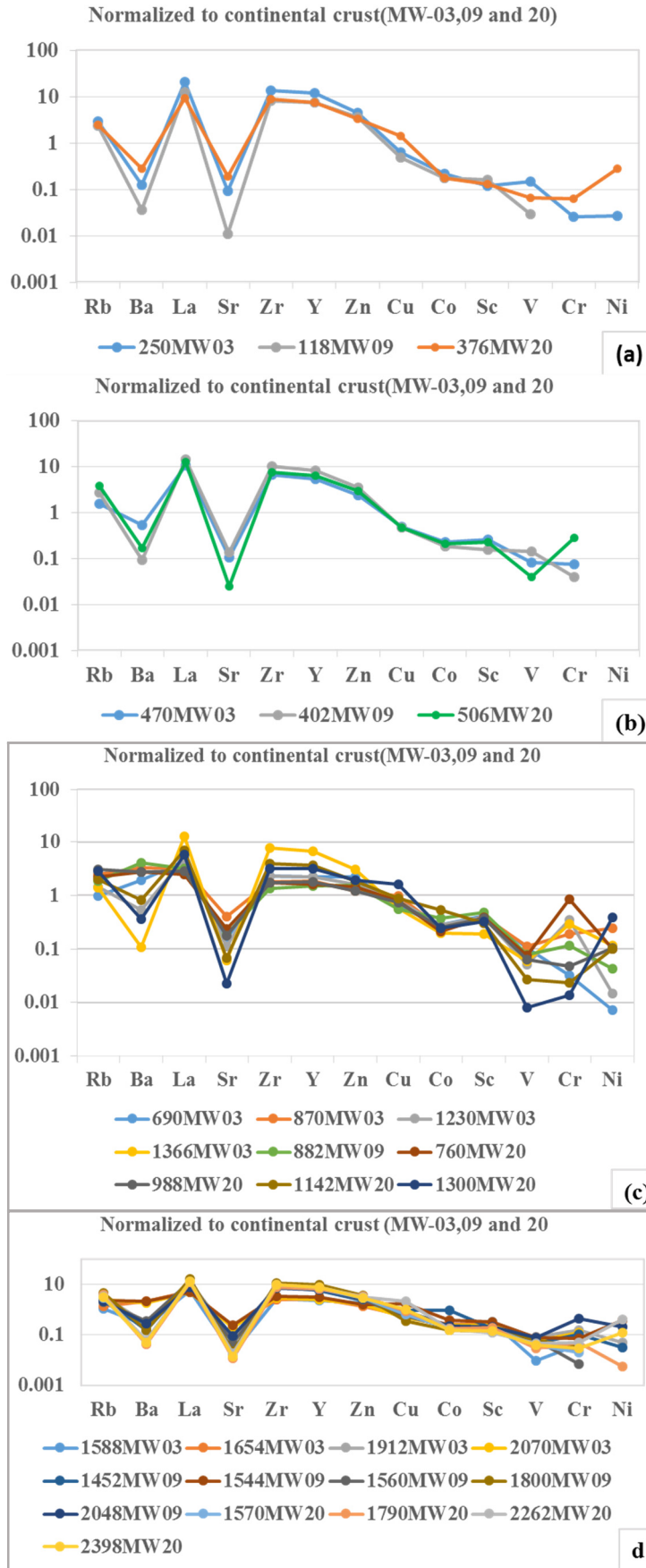
FIGURE 39: Variations of trace elements in MW-03, MW-09 and MW-20
showing a) Post caldera, b) Syn-caldera, c) Upper Pre-caldera and
d) lower Pre-caldera (normalized to continental
crust of Rudnick and Fountain, 1995)

54

4. DISCUSSION

4.1 Geology

The Menengai caldera is dominated by Quaternary volcanics. The subsurface geology shows various rock types; trachyte, pyroclastics, trachy-basalt, phonotephrite, trachyte andesite, tuff, phonolite, rhyolite, and basalt. Syenite intrusives are also present (e.g. Omondi, 2011, Mibei, 2012, Kipchumba, 2013, Lopeyok 2013, Kahiga, 2014, Mbia, 2014 and Mutua, 2015). In this study five formations were observed in wells MW-03, MW-09 and MW-20 which are trachyte, pyroclastics, tuffs, basalt and syenite intrusives: Trachyte are dominating by more than 90% of the stratigraphy in the wells. The trachytes are classified according to their grain sizes; fine to coarse grained trachytes as observed in binocular and petrographic microscope. The same scheme of classifying trachytes by their grain sizes have been used in the other wells in Menengai field. Trachytes were noted at different depths. The rock matrix mostly is composed of feldspar, especially sanidine. Pyroxene with aegirine-augitic composition seem to be common in the matrix at some depths. The trachytes are dominated by sanidine, pyroxene (dominantly aegirine - augite), amphiboles (riebickite), volcanic glass, less olivine and Fe-Ti oxides as primary minerals, though feldspar being dominant.

The rocks exhibit different colours, grain sizes and texture which indicates different volcanic eruptions during the pre- syn- and post-caldera, however the difference in grain sizes could be caused by same eruption but different parts of the magma chamber which cooled at different rate. The alteration minerals in trachytes are zeolites, calcite, pyrite, clay minerals, epidote, wollastonite and actinolite. The rocks are alternating commonly with tuff and less commonly with other pyroclastics and syenite. The presence of the abundance trachytes in the field suggests the source being of more trachytic composition. Leat (1983) described the lavas during pre-caldera stage as mainly of trachytic composition and containing over 95% of sanidine crystallites with small amounts of riebeckite/arfvedsonite that was also observed in the study wells.

Basalt is found only in MW-03, it is almost holocrystalline composed of plagioclase, aegirine augite, and Fe-Ti oxides. The rock is vesicular where vesicles are filled by calcite and clay minerals along with epidote.

All wells penetrate through intrusions, mostly plutonic equivalent to trachyte. These are medium to coarse grained and appear the outer boundary oxidized and this may be caused by loss of heat to the country rock. The intrusives were noted at different depths below 1300 m in the wells. These intrusions may create fractures which could become a source of permeability in the area, in the study wells some of the aquifers are associated with intrusion margins.

Pyroclastics in the study wells are unconsolidated and altered, mixed with volcanic glass and trachytic fragments, especially in well MW-20. In well MW-20 pyroclastics were noted at 456-462 m while 514-536 m and 0-2 m in MW-03 and MW-09 respectively. In neighbouring wells pyroclastics occur at different depths and end at 1578 m and 960 m in MW-04 and MW-06 (Mbia, 2014) respectively. Pyroclastics are believed to form during the caldera collapse (syn-caldera) (Leat, 1984). The unit contains pyrite, calcite, and clay minerals as secondary minerals.

Tuff occurs at 250-272 m and appear irregularly to 2058 m depth in well MW-03 for MW-09 the rock is noted at 118-132 m depth and appear regularly to 1552 m. In MW-20, the rock is at 4-6 m and 380-386 m and occurs regularly down to 1502 m. This rock is common also in neighbouring wells MW-04 and MW-06 as observed by Mbia, 2014. In MW-03, at 250-272 m and 308-390 m vesicles are filled with silica and the same is observed in MW-09. However, some vesicles are filled by zeolite. These rocks contain zeolites, calcite, pyrite, and clay minerals as secondary minerals. According to Leat (1983 and 1991) ash flow tuffs represent the syn-caldera activity and these tuffs were both preceded by pumice falls and are separated by sediment beds up to 4 m thick. Depth between 250-386 m tuff occur in all wells and shows little displacement which can be caused by some faults related to Molo TVA and Solai TVA. The same tuff unit was reported by Mibei (2012) in MW-04 and MW-06 and Kahiga (2014) in MW-13, they referred it as tuff marker horizon of syn-caldera in age.

The feed zones/aquifers in wells are found at different depths. Temperature logs, circulation losses, hydrothermal alteration, variation in penetration rate, lithological boundaries and margins of intrusions revealed the inferred aquifers in the wells. Feed zones/aquifers were observed at 268, 526, 790, 1080, 1234, 1398, 1540 1600 and 1972 m in MW-03, most of them hosted by trachytes. Aquifer 3 and 4 at 790 and 1080 m respectively noted from slight increase in temperatures and some losses of circulation. At 1234 m, large aquifer observed which may associate with hot fluids, the feed zone is hosted in fine grained trachyte formation and medium altered. At the boundary between medium grained trachyte and syenite intrusion at 1398 m, a small feed zone is located seen as a decrease in temperature and rate of penetration, and the same happens to an aquifer at 1540 m. This behaviour might be contributed by the loss of heat in the host rocks. The eighth feed zone is large, located in moderately altered medium grained trachytes at 1600 m. The aquifer is seen by temperature increase, and an increase in rate of penetration from 8 to 15 m/hr. Also there is deposition of calcite, which is good sign of permeability. The last observed aquifer in MW-03 is at 1972 m, it is a small aquifer in fine grained trachyte, shown by increase in temperature with less calcite and pyrite deposition (Figure 17).

In MW-09, eight aquifers were found of which four are small and three large (Figure 18). The small aquifers are located at 1000, 1298, and 1750 m while large aquifers were noted at 782, 1200 and 1436 m. The four aquifers show positive changes in temperatures which implies hot permeable zone, while the aquifer at 1750 m indicated by decrease in temperature, also less calcite and pyrite are deposited. This may signify inflow of cold water in the well. At 782 m the feed zone is at a lithological boundary between tuff and trachyte. Small aquifer at 1000 m is hosted by less altered medium grained trachyte, there is slight increase in temperature logs and rate of penetration. The aquifer located at 1200 m shows increase in temperature and rate of penetration and is hosted in less altered medium grained trachyte.

The small aquifer at 1298 m is associated with lithological boundary between fine grained trachyte and medium grained trachyte. A larger aquifer at 1436 m shows moderate increase in rate of penetration and positive increase in temperature logs and there was a loss of circulation. The aquifer is hosted by fine grained trachyte that seems to be less altered. The sixth aquifer in well MW-09 is at 1750 m characterised by moderately altered rock, decrease in temperature and slight increase in rate of penetration and is hosted by tuff.

In MW-20, six aquifers were observed, one small aquifer at 626 m in less altered fine grained trachyte is characterised by temperature increase and slight increase in rate of penetration at this depth. Another at 306 m noted from loss of circulation and slight increase in temperature. Two larger feed zones are located at 1174 and 1594 m, the former is at the boundary of coarse grained trachyte and fine grained trachyte whereas the other is associated with lithological boundary of fine grained trachyte and medium grained trachyte. Both aquifers were identified through rate of penetration that tend to increase at this depths and temperature shows slightly decrease to the bottom. All the aquifers are categorised by deposition of calcite and less pyrite which indicate that at these depths the rocks are permeable. The fourth aquifer is recognized at 2050 m whereby temperature logs show a negative change and increase in the rate of penetration from 2.07 to 13.33 m/hr. However, the aquifer is small in terms of magnitude (Figure 19)). The aquifer occurs at the boundary of syenite intrusion and coarse grained trachyte, the two formations are less altered with little calcite and pyrite deposition. The last aquifer located at 2300 m is characterized by loss of circulation and slight increase in temperature logs. The aquifers 2, 3, 4 and 5 are found in Wollastonite-Actinolite zone.

4.2 Hydrothermal alteration

Reyes (1990) described that hydrothermal minerals can also be used to predict the scaling and corrosion tendencies of fluids, measure permeability, possible cold water influx and as a guide to the hydrology. In the wells some aquifers are characterized by deposition of calcite and pyrite which may indicate permeability.

The alteration can be used to uncover the history and the future of the geothermal system. In MW-03, MW-09 and MW-20, the main primary minerals observed are volcanic glass, less olivine, alkali

feldspars, plagioclase, pyroxene, amphiboles and Fe-Ti oxides. These minerals are common in Menengai rocks, however, sanidine as alkali feldspar is dominant. These primary minerals alter to different alteration minerals as shown in Table 2 and Figures 21, 22 and 23.

By the aid of binocular, petrographic microscope and XRD analysis, the secondary minerals are distributed in the study wells starting with low temperature alteration minerals such as zeolites, chalcedony and smectite to high temperature minerals including chlorite, illite quartz, epidote, wollastonite and actinolite. Some of the alteration minerals in the wells are filling the microfractures (vein and vesicles) in the rocks (Figure 20) and provide vital information on deposition sequence and temperature, since hydrothermal alteration minerals are regarded as geothermometers (Table 8). The observed vesicles and veins are filled by zeolites, chalcedony, calcite, pyrite, quartz, prehnite, clay minerals and wollastonite.

Calcite is the dominant secondary alteration mineral in the study wells and neighbouring wells. Calcite as abundant alteration mineral in the wells, it seems to form in three ways; 1) replacing of rock forming minerals such feldspar, pyroxene and volcanic glass, 2) boiling of the reservoir fluid that cause to the loss of CO_2 and calcite precipitates in veins or open spaces, 3) also calcite precipitates in veins or fractures when the hotter fluid mixes with circulating ground water. The deposition of calcite in veins and open spaces may decrease the permeability but it is good for geothermal system if deposition/precipitation of calcite happens above the geothermal system that can block or reduce the inflow of cold water.

The presence of significant CO_2 could be among the reasons to why epidote is rare in Menengai wells. In the study wells there are no well-developed epidote crystals. In the wells the mineral was noted at 850, 1586 and 1000 m in MW-03, MW-09 and MW-20, respectively. In MW-03 epidote sometimes is significant compared to the other two wells. In other geothermal field epidote is considered as indicator mineral for production casing. For example, in the Iceland geothermal fields and Olkaria geothermal field in Kenya epidote is mostly used in deciding the production casing, as its first appearance in the rock indicates temperatures above 240°C. In addition to high concentration of CO_2, possibly low permeability in the rocks limit the formation of epidote in Menengai geothermal field and the rocks and thermal fluids might compose less iron which is very important for the epidote to form.

The secondary minerals divide the wells into zones with low to high temperature hydrothermal alteration minerals. Seven zones were defined in the well, four zones are common to all wells but differ at depths at which the zones are located. The five zones are Unaltered zone, Zeolite-smectite zone, Quartz zone, Epidote zone and Wollastonite-actinolite zone. The other two zones, Illite zone and Chlorite zone both are seen in MW-20, while the two wells MW-03 and MW-09 exhibits Chlorite zone and Illite zone respectively. Wells MW-09 and MW-20 show significant actinolite and wollastonite at the shallower depth as compared to MW-03 this is also indicated by temperature logs which show increase of temperature at the bottom of the well. These differences in alteration zones are also revealed by resistivity cross section along the wells showing low resistivity at deeper for MW-03 compared to MW-09 and MW-20 (e.g. GDC, 2014).

Unaltered zone found at 0-74, 0-122 and 0-70 m in wells MW-03, MW-09 and MW-20 respectively. Zeolite-smectite zone in all wells defined at 74-638, 122-712 and 70-672 m in MW-03, MW-09 and MW-20 respectively. Quartz zone found from 638-740, 712-1450, and 672-898 m in MW-03, MW-09 and MW-20 respectively. Illite zone was defined in MW-09 and MW-20 from 1450-1538 and 898-932 m. Chlorite zone found from 740-850 and 932-1000 m in MW-03 and MW-20 respectively. Epidote zone was found from 850-2054, 1538-1554 and 1000-1222 m in wells MW-03, MW-09 and MW-20 respectively. Chlorite and epidote in this zone may signify temperature above 230°C (e.g. Kristmannsdóttir, 1979). The final zone is wollastonite-Actinolite which is characterized by high temperature minerals, was found from greater than 2054, 1554 and 1222 m in MW-03, MW-09 and MW-20, the presence of high temperature alteration minerals such as wollastonite and actinolite in the zone indicates temperatures above 280°C (Franzson, 2011).

Based on alteration mineral temperatures and formation temperatures in well MW-03, the formation temperatures seem to be low compared to alteration mineral temperatures, although formation temperature is showing an increase at the bottom part of the well indicating system heating up to above 300°C. Formation temperatures in well MW-20 are high compared to alteration mineral temperature. Formation temperatures continue to increase to the bottom of the well which indicate heating up of the geothermal system.

For well MW-09, fluid inclusions analyses were done by Lopeyok (2013). He analysed about fourteen (14) fluid inclusions in calcite crystals from 1000-1100 m and gave homogenization temperature (Th) ranging from 220-260°C with average of 245°C. The fluid inclusion temperatures plots on boiling temperature curve which ends up describing boiling conditions, but generally the formation temperatures in this well appear to be high compared to alteration mineral temperatures, which indicates heating up of the geothermal system from 550-1400 m with maximum temperature of about 240.8°C. MW-

FIGURE 40: Conceptual model in relation to alteration mineral zones and formation temperatures in MW-03, MW-04, MW-06, MW-09 and MW-20

09 the measured temperatures were taken after 18 days of heating which does not reveal true formation temperatures. However, formation and alteration mineral temperatures need to be complemented by fluid inclusion temperatures to reveal whether the geothermal system is heating, cooling or in equilibrium. In this study inclusions study was not possible as the crystals mostly calcite ended up breaking during polishing.

Based on the findings it shows that there is a local inflow around well MW-03 (Figure 40) which is probably connected to the inferred fault trending NNW-SSE and leading to low temperature zone above 1700 m with temperature below 200°C. This is evidenced by the thinning out of the Wollastonite-Actinolite zone towards MW-03. However, all wells show a good up-flow and they were drilled at the centre of the caldera, probably at the triple junction of Mola TVA and Solai TVA.

4.3 Whole-rock geochemistry

Classification of rocks based on Al_2O_3 content and concentration of FeO (Macdonald, 1974), most of the samples are comenditic trachyte, followed by pantelleritic trachyte and few pantellerite (Figure 34) but the neighbouring wells MW-04, MW-06 and MW-07 seem to cluster between pantellerites and comendite (Mbia, 2014). The differences could be mainly caused by fractional crystallization. The analysed rocks are metaluminous based on higher concentration of Al_2O_3 as compared to the total concentration of Na_2O+K_2O. This behaviour differs from the neighbouring wells MW-02, MW-04, MW-06 and MW-07 which are peralkaline as reported by Mbia (2014). The rocks contain more Al than

K and Na. On TAS diagram the rocks are showing trachytic composition while samples from MW-02, MW-04, MW-06 and MW-07 varies from basalt to trachytic composition. The samples from the study wells plots in the field of surface Menengai, Eburru and Longonot trachyte, indicating the possibility of originating from the same source.

The negative correlations between major oxides versus SiO_2; TiO_2, MgO, CaO, Al_2O_3, P_2O_5 and K_2O indicates the crystal fractionation of ferromagnesian minerals, feldspars and apatite controlled the observed compositional variation. Abundance of calcite at 376 m depth in well MW-20 is reflected by high content of CaO compared to other depths. FeO, MnO and Na_2O behave differently, FeO and MnO increase with increasing SiO_2 while Na_2O show scattering nature and remain relatively constant. Data from neighbouring wells and that of Olkaria suggests that FeO correlates negatively with SiO_2 (eg. Mbia, 2014, Musonye, 2015). The reason of the different behaviour of FeO and MnO in the study wells could be the result of zoned magma chamber from which the lavas were evolved with time by enrichment in FeO and MnO and depletion of TiO_2, MgO, CaO, Al_2O_3, P_2O_5 and K_2O (eg. Leat, 1983).

The concentration of trace elements such as Zn, Y, La, Zr and Rb increases with increase in SiO_2 (Figure 35, j-r), which reveals that these trace elements become enriched in the remaining melt during fractional crystallization. Other trace elements like Ba and Sr decrease, which show that they partitioned into feldspars during crystal fractionation. In volcanic rocks containing feldspars, Sr is strongly portioned into plagioclase while Ba into alkali feldspar (Mahood and Hildreth, 1983). Zr is among the classic incompatible elements but can substitute Ti in accessory phases such as sphene and rutile (Hardarson, 1993), however, results show enrichment in the melt. The negative correlation is more pronounced in MW-09 compared to the other two wells. The reason for depletion of Co, V, Cr and Ni suggests crystal fractionation of the mineral assemblages encountered in rocks such as pyroxene, olivine, and iron-titanium oxide.

The effect of hydrothermal alteration on the rock chemistry is insignificant as demonstrated by Rb, La, Sr, Ba, Y and Cr when plotted against Zr. Rb, La and Y show positive correlation with Zr which is thought to be immobile. Rb might be slightly affected the hydrothermal process. In MW-09, Sr correlates negatively with Zr and less clear in MW-03 and MW-20, Ba behave like Sr but most variable at low Zr concentration. Ba and Sr are mobile in fluid phase, so they may be leached from the rock and deposited elsewhere. They can also be weakly enriched in sanidine or plagioclase feldspar. Chromium (Cr) show slight negative correlation with Zr, possibly substituting Fe and Mg in fractionating pyroxene.

Furthermore, trace elements on a normalized spider diagrams show high depletion trends of Ba and Sr compared to others, whereas La, Y and Zr illustrate enrichment relative to continental crust compositions in all wells (Figure 37). As pointed out above Ba and Sr are partitioned into sanidine or plagioclase feldspar during fractionation while enriched La, Y and Zr enriched in the melt. Ba, Sr, La and Y concentrations in the rocks when plotted with depth in the study wells. Ba and Sr are low at shallower depths while La and Y are high. Then elements Ba and Sr tend to increase while decrease in the next units. At~1400-1600 m depth Zr (Figure 34), La and Y increases again in MW-09, MW-03 and MW-20. The two wells show data scattering below approximately 1600 m which might be attributed to alteration. The variation of trace elements in the wells depict four episodes that may be linked to the Menengai caldera formation that is post, syn, and upper and lower pre-caldera which was also explained by Leat (1983), Mibei (2012) and Mbia (2014).

5. CONCLUSIONS

- The rocks in the Menengai caldera is dominated by trachytes. In the study wells, trachytes, pyroclastics, tuffs, basalt and intrusives (syenite) were observed.

- Geochemical evolution of the Menengai rocks is controlled mainly by fractional crystallization, however the trends of some trace elements in the wells indicate the possibility of more than one process being involved.

- Most of the rocks analysed in MW-03, MW-09, and MW-20 are metaluminous based on Al_2O_3 and $Na_2O + K_2O$ contents in the rocks. The total concentration of $Na_2O + K_2O$ is less than concentration of Al_2O_3.

- Four episodes or horizons in the Menengai caldera were revealed which may be linked to post-, syn-, upper- and lower pre-caldera formation.

- Seven alteration zones were identified in the study wells; Unaltered, Zeolite-Smectite, Quartz, Illite, Chlorite, Epidote and Wollastonite-Actinolite zones. Five zones are common in all wells. Illite zone is found in MW-09 and MW-20 while Chlorite zone is found in MW-03 and MW-20.

- The hydrothermal alteration in Menengai is controlled by temperature, rock chemistry and structures, though the hydrothermal processes have relatively small effects on rock composition.

- There could be inferred fault near MW-03 trending NNW-SSE, which leads to low temperature zone above1700 m, and the fault may be related to Molo-TVA, probably with other structures related to Solai TVA.

- Seven aquifers were encountered in MW-03, six in MW-09 and five in MW-20. The permeability seems to be linked to lithological boundaries, fractures and faults in trachytes and permeable formations, like tuffs.

- Calcite in the wells form in three ways; replacing rock forming minerals such as feldspar, pyroxene and volcanic glass (more prominent below 1000 m), boiling of the reservoir fluid that causes to the loss of CO_2 and calcite precipitates in veins or open spaces. Calcite also precipitates in veins or fractures when hotter fluids mix with circulating ground water.

- Epidote formation might be hindered by high CO_2 concentration, probably low permeability and low content of iron in the rocks, which are important in epidote formation.

- Deposition sequences, alteration mineral and formation temperatures suggest the wells are heating up. MW-03 appears progressively heating from approximately 1800 m.

6. RECOMMENDATIONS

Further petrochemical studies in other Menengai wells are recommended to understand more geochemical evolution of the rocks in Menengai.

Detailed studies of chemical fluid composition in Menengai geothermal wells is recommended to provide more insights about factors that precludes the formation of some hydrothermal alteration minerals such as epidote. This also will help to put forward the alteration mineral zonation baseline for Menengai geothermal system.

Detailed fluid inclusions analysis study in the abundant calcite alteration minerals is recommended in MW-03, MW-09, MW-20 and other wells to complement on the history of the Menengai geothermal system. The analysis includes homogenization temperature measurements, textural analysis, and determination of chemical composition by freezing stage experiments and spectroscopic methods.

REFERENCES

Ahmed Youssouf, M., 2008: Borehole geology and hydrothermal mineralization of well HN-08, Hellisheidi geothermal field, SW-Iceland. Report 8 in: *Geothermal training in Iceland 2008*. UNUGTP, Iceland, 1-29.

Arnórsson, S., Björnsson, S., Muna, Z. W., and Ojiambo, S. B., 1990. The use of gas chemistry to evaluate boiling processes and initial steam fractions in geothermal reservoirs with an example from the Olkaria field, Kenya. *Geothermics 19,* 1307- 1325.

Baker, B.H., Mitchel, J.G., and Williams, L.A.J., 1988: Stratigraphy, geochronology and volcanotectonic evolution of the Kedong-Naivasha Kinangop region, Gregory Rift Valley, Kenya. *Geological Society of London, 145,* 107-116.

Baker, B.H., Mohr, P.A., and Williams, L.A.J., 1972: Geology of the Eastern Rift System of Africa. *Geol. Soc. of America, Special Paper,* 136, 67 pp.

Bird D. K., and Spieler A. R.: Epidote in geothermal systems, *Reviews in Mineralogy and Geochemistry,* 56, (2004), 235-300.

Browne, P.R.L., 1978: Hydrothermal alteration in active geothermal fields. *Annual Reviews of Earth and Planetary Science, 6,* 229-250.

Ebinger, C.J. (2005). "Continental break-up: The East African perspective." *Astro. Geophys.* 46: 216–21.

Fernandes, R.M., Ambrosius, B.A.C., Noomen, R., Bastos, L., Combrinck., Miranda, J.M. and Spakman, W., 2004: Angular velocities of Nubia and Somalia from continuous GPS data: Implications on present-day relative kinematics. *Earth Planet. Sci. Lett*., 222, 197-208.

Franzson, H., 1998: Reservoir geology of the Nesjavellir high-temperature field in SW-Iceland. *Proceedings of the 19th Annual PNOC-EDC Geothermal Conference, Manila,* 13-20.

Franzson, H., 2011: Borehole geology. UNU-GTP, Iceland, *unpublished lecture notes.*

GDC., 2010: Menengai geothermal prospect; an investigation for its geothermal potential. Geothermal Development Company (GDC), Geothermal resource assessment project, *unpubl*. report.

GDC., 2013: Structural characteristics of Menengai Caldera, central Kenya Rift; Preliminary assessment of the structural characteristics of Menengai Caldera and regions farther north. Geothermal Development Company (GDC), Geothermal exploration and structural assessment, *Unpubl*. Report

GDC., 2014a: Borehole geology of well MW-20 from Menengai Geothermal Field. Geothermal Development Company (GDC). *Unpubl*.report

GDC., 2014b: Geo-scientific data integration for Menengai geothermal field. Geothermal Development Company (GDC). *Unpubl*.report

Gebrehiwot M., K., 2010: *Subsurface geology, hydrothermal alteration and geothermal model of Northern Skardsmýrarfjall, Hellisheidi geothermal field, SW Iceland.* University of Iceland, MSc thesis, UNU-GTP, Iceland, report 5, 65 pp

Geotermica Italiana Srl., 1987: Geothermal reconnaissance survey in the Menengai- Bogoria area of the Kenya Rift Valley. *UN (DTCD)/GOK*.

Hardarson, B.S., 1993: Alkalic Rocks in Iceland with special Reference to the snaefellsjokull volcanic system. *Unpubl*. Ph.D. thesis, Univ. of Edinburgh.

Hetzel, R., and Strecker, M.R., 1994: Late Mozambique Belt structures in western Kenya and their influence on the evolution of the Cenozoic Kenya Rift. *J. Structural Geology,* 16-2, 189- 201.

Jones, W.B., 1985: Discussion on geological evolution of trachytic caldera and volcanology of Menengai volcano, Rift Valley, Kenya. Journ. *Geop\l. Soc. Lon,* vol 142, 711pp.

Kahiga, E.W., 2014: Borehole geology and hydrothermal alteration mineralogy of well MW-13, Menengai geothermal field, Kenya. Report 16 in: *Geothermal training in Iceland 2014*. UNU-GTP, Iceland, 34 pp.

Kanda, I., 2013: Geochemical exploration of geothermal prospects: a case study of Menegai, Kenya. Proceedings, Short Course VIII on Surface Exploration for Geothermal Resources, UNU-GTP, Lake Naivasha, Kenya.

Kipchumba, L.J., 2013: Borehole geology and hydrothermal alteration of wells MW-08 and MW-11, Menengai geothermal field, Kenya. Report 10 in: *Geothermal training in Iceland 2013.* UNU-GTP, Iceland, 143-176.

Koestono, H., 2007: Borehole geology and hydrothermal alteration of well HE-24, Hellisheidi geothermal field, SW-Iceland. Report 10 in: *Geothermal Training in Iceland, 2007*. UNU-GTP, Iceland 199-224.

Kristmannsdóttir, H., 1977: Types of clay minerals in altered basaltic rocks, Reykjanes, Iceland. *Jökull,* 26 (in Icelandic with English summary), 3-39.

Kristmannsdóttir, H., 1979: Alteration of basaltic rocks by hydrothermal-activity at 100-300°C. *Developments in Sedimentology*, 27, 359-367.

Lagat, J., 2011: Geothermal surface exploration approach: Case study of Menengai geothermal field, *Proceedings Kenya Geothermal Conference*, Kenyatta International Conference Centre, Nairobi, November 21-21, (2011).

Leat, P.T., 1983: The structural and geochemical evolution of Menengai caldera volcano, Kenya Rift Valley. *PhD thesis,* University of Lancaster U.K.

Leat, P.T., 1984: Geological evolution of the trachytic caldera volcano Menengai, Kenya Rift Valley. *J. Geol. Soc*. London, 141, 1057-1069.

Leat, P.T., 1991: Volcanological development of the Nakuru area of the Kenya rift valley. J of African Earth sciences, 13, 3/4, 483-498.

Le Bas, M.J., Lemaitre, R.W., Streckeisen, A. and Zanettin, B. (1986). A Chemical Classification of Volcanic-Rocks Based on the Total Alkali Silica Diagram. *Journal of Petrology 27(3):* 745-750.

Le Maitre (editor), R. W., Streckeisen, A., Zanettin, B., Le Bas, M. J., Bonin, B., Bateman, P., Bellieni, G., Dudek, A., Efremova, S., Keller, J., Lamere, J., Sabine, P. A., Schmid, R., Sorensen, H., and Woolley, A. R., 2002: Igneous Rocks: A Classification and Glossary of Terms, Recommendations of the International Union of Geological Sciences, Subcommission of the Systematics of Igneous Rocks. *Cambridge University Press*, 2002.

Lopeyok, T.P., 2013: Borehole geology and hydrothermal alteration of wells MW-09 and MW-12, Menengai geothermal field, Kenya. Report 15 in: *Geothermal training in Iceland 2013*. UNU-GTP, Iceland, 289-324.

Macdonald, G.A. and Katsura, T., 1964: Chemical composition of Hawaiian lavas: *J. Petrol.,* 5: 82-132.

Macdonald, R., 1974: Nomenclature and Petrochemistry of the peralkaline oversaturated extrusive rocks. *Bulletin Volc.* 38, 498- 516.

Macdonald, R., 2002: Magmatism of the Kenya Rift Valley: a review. Trans. Royal Society of Edinburgh: Earth sciences, 93, 239-253.

Macdonald, R., Baginski, B., Leat, P.T., White, J.C and Dzierzanowski., 2011: Mineral stability in peralkaline silicic rocks: Information from trachytes of the Menengai volcano, Kenya. *Lithos,* 125, 553-568.

Macdonald, R., Navarro, J.M., Upton, B.G. J., and Davies, G.R., 1994: Strong compositional zonation in peralkaline magma: Menengai, Kenya Rift Valley. *J. Volc Geotherm Res*, 60: 301-325.

Macdonald, R., and Scaillet, B., 2006: The central Kenya peralkaline province: insights into the evolution of peralkaline salic magmas. *Lithos,* 91, 59-73.

Mahood, G.A., and Hildreth, W.,1983: Large partition coefficients for trace elements in high-silica rhyolite. *Geochem. Cosmochim. Acta* 47, 11-30.

Mbia, P.K., 2010: Borehole geology and hydrothermal alterations of well HE-39, Hellisheidi in SW Iceland. Report 19 in: *Geothermal training in Iceland 2010.* UNU-GTP, Iceland, 337-360.

Mbia, P., 2014: *Sub-surface geology, petrology and hydrothermal alteration of Menengai geothermal field, Kenya*. University of Iceland, MSc thesis, UNU-GTP, Iceland, report 1, 99 pp.

McCall, G.J.H., 1957a: The Menengai caldera, Kenya Colony. 20th Int. *Geol. Congress*, section 1, 55-69.

McCall, G.J.H., 1957b: Geology and groundwater conditions in the Nakuru Area. M.o.W., Hydraulic Branch, Nairobi, *tech.* report 3.

McCall, G.J.H., 1964: Froth flows in Kenya. Geol. Runsch., 54, 1148-1195.

McCall, G.J.H., 1967: Geology of the Nakuru - Thomson's Fall - Lake Hannington area. Geolog. Surv. Kenya, Rep., 78.

Mibei, G.K., 2012: Geology and hydrothermal alteration of Menengai geothermal field-Case study of Wells MW-04 and MW-05. Report 21 in: Geothermal training in Iceland 2012. UNU-GTP, Iceland, 437-466.

Mibei, G., and Lagat, J.: Structural Controls in Menengai Geothermal Field, *Proceedings Kenya Geothermal Conference*, Kenyatta International Conference Centre, Nairobi, November 21-21, (2011).

Mungania, J., 2004: Geological studies of Menengai geothermal prospects. KenGen Ltd., internal report, 18pp.

Mungania J., Lagat J., Mariita N.O., Wambugu J. M., Ofwona C.O., Kubo B. M., Kilele D. K., Mudachi V.S,.Wanje C. K., Menengai prospect: Investigations for its geothermal potential, 2004 . The Government of Kenya and Kenya Electricity Generating Company Limited, internal report. pp 7.

Musonye, X, S., 2015: sub-surface petrochemistry, stratigraphy and hydrothermal alteration of the domes area, olkaria geothermal field, Kenya. University of Iceland, MSc thesis, UNU-GTP, Iceland, report 3, 118 pp.

Mutua, F.M., 2015: Borehole geology and hydrothermal alteration mineralogy of well MW-19A, Menengai geothermal field, Kenya. Report 25.

Ofwona, C.O., 2002: *A reservoir study of Olkaria East geothermal system, Kenya. University of Iceland,* M.Sc. thesis, UNU Geothermal Training Programme, Iceland, Report 2, 74 pp.

Omenda, P.A., 1997: The geochemistry evolution of quaternary volcanism in the south-central portion of the Kenya rift. University of Texas, El Paso, *Ph.D. thesis*, 218 pp.

Omenda, P. A., 2007: Status of Geothermal Exploration in Kenya and Future Plans for its Development, Proceedings, Short Course II on Surface Exploration for Geothermal Resources, *UNU-GTP*, Lake Naivasha, Kenya.

Omondi, C., 2011: Borehole geology and hydrothermal of wells MW-01 and MW-02, Menengai geothermal field, Central Kenya Rift valley. Report 30 in: *Geothermal training in Iceland 2011.* UNUGTP, Iceland, 737-774.

Reyes, A.G., 1990: Petrology of Philippine geothermal systems and the application of alteration mineralogy to their assessment. *J. Volc. Geoth. Res., 43,* 279-309.

Reyes, A.G., 2000: Petrology and mineral alteration in hydrothermal systems: from diagenesis to volcanic catastrophes. UNU-GTP, Iceland, report 18-1998, 77 pp.

RockWare Inc., 2007: *LogPlot program.* Rockware Inc.

Rogers, N., Macdonald, R., Fitton, J. G., George, R., Smith, M., Barreiro, B., 2000: Two mantle plumes beneath the East African rift system: Sr, Nd and Pb isotope evidence from Kenya Rift basalts. Earth and Planetary Science Letters, 176, 387-400.

Rudnick, R.L. and Fountain, D.M. (1995). Nature and composition of the continental crust -- a lower crustal perspective. *Reviews in Geophysics 33:* 267-309.

Saemundsson, K., and Gunnlaugsson, E., 2002: *Icelandic rocks and minerals.* Edda and Media Publishing, Reykjavík, Iceland, 233 pp.

Simiyu, S.M and Keller, G.R., 1997: An integrated analysis of lithospheric structure across the East African plateau based on gravimetry anomalies and recent seismic studies. *Tectonophysics 278,* 291–313.

Simiyu S.M., 1998: Seismic and gravity interpretation of the shallow crustal structure along the KRISP 94 line G in the vicinity of the Kenya Rift Valley. *J. African Earth Sciences, 27*, 367-381.

Simmons, S. F. and Christenson, B. W. (1993). Towards a Unified Theory on Calcite Formation in Boiling Geothermal Systems. *Proc.15th New Zealand Geothermal Workshop,* pp. 145-148.

Simmons, S.F., and Christenson, B.W., 1994, Origins of calcite in a boiling geothermal system: *American Journal of Science, v. 294*, p. 361–400.

Smith, M., and Mosley, P., 1993: Crustal heterogeneity and basement influence on the development of the Kenya Rift, East Africa. *Tectonics*, 12, 591-606.

Yoshio, W., Eiichiro, M. and Kozo, S., 2011: *X-ray diffraction crystallography*. Springer, NY, Heidelberg, Dordrecht, 67-80.

APPENDIX I: Detailed descriptions of lithology, alteration minerals of well MW-03 as observed under binocular and petrographic microscope analysis

0 – 72 m: No returns

72 – 156 m: Trachyte: Dark grey, medium grained rock and porphyritic with pyroxene and feldspar. The rock unit looks less oxidized though seems to be fresh and quartz is noted as part of primary minerals. Some tuff fragments with green colouration observed at 84-90 m and some tuff vesiculated and filled by chalcedony/silica material. Light green to brownish grey, red and green colouration on tuff fragments noted at 94-118 m. No returns from 120-154 m. Alteration minerals are limonite, chalcedony, calcite and clay minerals.

156 – 244 m: No returns.

244 – 250 m Trachyte: Fine to medium grained rock, light grey to light green, mixed with tuffs and clays are present. The tuffs exhibit with some vesicles filled with silica. Pyroxene and feldspar were observed as primary minerals. No cutting at 248 m. The alteration minerals, Limonite, zeolites, chalcedony, calcite and clay minerals.

250 – 272 m Tuffs: Light greenish grey to brownish, mixed with few fine grained trachyte cuttings. Vesiculated tuffs are filled by silica and limonite, this was noted at 252 m and 258 m. No cuttings from 274-278 m. Alteration minerals are Limonite, chalcedony and calcite.

272 – 278 m: No cuttings.

278 – 302 m Trachyte: Dark grey to brownish grey, oxidized rock, fine grained and phyric with feldspar. At 282-284 m and 302-308 m cutting are missing. In this rock unit, limonite, chalcedony, zeolites, calcite and clay minerals were encountered as secondary minerals.

308 – 390 m Tuff: Dark grey to brownish grey, volcanic ashes mixed with trachyte cuttings fine grained and altered. The rock shows pilotaxitic texture and the microphenecrysts of feldspar are randomly oriented. Silica/chalcedony seems to fill the vesicles. The rock is oxidized, it shows green colouration from 332-338 m with few lining noted at 378 and 386 m. Cuttings from 312 m, 320 m, 328-330 m, 348-356 m and 384 m are missing. Alteration minerals observed in this unit are limonite, zeolite (analcime, scolesite, mesolite), chalcedony, pyrite, calcite and clay minerals.

390 – 404 m: No cuttings.

404 – 422 m Trachyte: Light grey, medium to coarse grained lava, porphyritic with feldspar and pyroxine as phenocrysts, less oxidized and altered. The rock is showing some greenish colour. Cuttings at 422 m are missing. Limonite, chalcedony, calcite and pyrite are the alteration mineral encountered.

422 – 452 m Trachyte: Dark grey with brownish grey and light green. Porphyritic with feldspar and mafic minerals. Fractured rock/surface and altered, calcite noted on the fractured surface. Secondary minerals are calcite, pyrite and chalcedony.

452 – 514 m Trachyte: Light grey to brownish grey, fine grained rock, mafic minerals in feldspar groundmass. Though feldspar is dominant and rock is oxidized and moderately altered. Some vugs on the cuttings observed at 458 m and 462 m and green colouration from 482 – 488 m due to clay minerals were noted. Cuttings at 478 m and 504 m are missing. In this unit the observed alteration minerals are chalcedony, pyrite, chalcopyrite and clay minerals.

514 – 526 m Tuff/Pyroclastic: Light grey and some greenish colour to some cuttings. Pyrite, clays and calcite were noted as secondary minerals. No cuttings at 518 m, 522-524 m and 528-534 m.

536 – 724 m: Trachyte: Light grey to brownish grey, fine grained feldspar porphyritic lava. Calcite crystals noted in this unit and the rock is slightly altered and oxidized. Some losses at 546 m, 556 m, 566 and 582-592 m. From 536-592 m there is more shining feldspar. Feldspar displays the carlsbad and albite twinning at 596 m. Depths from 626-630 m, the cuttings are greenish and darkish grey mixed with tuff cuttings. Alteration minerals are calcite, pyrite, cowlesite, quartz and clay minerals.

724 – 752 m Trachyte: Brownish grey to whitish, fine grained lava. It is a porphyritic feldspar rock. The rock is oxidized and relatively fresh. Pyrite present in the groundmass and fill some vesicles present in the rock. Calcite, pyrite and clay minerals were noted as secondary minerals.

752 – 754 m: No returns.

754 – 786 m Trachyte: Grey to whitish, fine grained lava and feldspar appear to be the main phenocrysts. The rock is altered and oxidized, green colouration noted at 784 m. Epidote was noted at 778 and 786 m. The alteration minerals are calcite, clay minerals, quartz and epidote.

786 – 826 m: No returns.

826 – 904 Trachyte: Whitish grey in colour. Fine grained rock with feldspar dominating and shows glittering surface also mafic minerals were encountered mainly pyroxene and olivine. The rock is slightly altered and oxidized. At 850 m pyroxene is altering to epidote. There is loss of circulation at 858 m. Alteration minerals identified are calcite, quartz, clay minerals, chlorite and epidote.

904 – 952 m: No returns.

952 – 954 Trachyte: Light grey, fine grained lava with bleached surface and feldspar seemed to be prominent in this rock. Dark minerals probably Fe-oxidized minerals and pyroxene were observed. The following secondary minerals were noted Calcite, clay minerals and quartz.

954 – 958 m: No returns.

958 – 1026 m Trachyte: Brownish grey to whitish, porphyritic rock with feldspars phenocrysts and mafic minerals noted in laths of feldspars. Feldspar altering to calcite at 978 m, at the depth calcite replaces glass materials. The rock is more or less holocrystalline. Some Losses from 982-986 m, 988-992 m, 994-998 m, 1012 m, 1016 m and 1020-1024 m. Alteration minerals are calcite, oxides, pyrite, quartz, chlorite, epidote and albite.

1026 – 1030 m: No returns.

1030 – 1088 m Trachyte: Whitish grey, fine grained feldspar porphyritic, slightly oxidized. The rock compose mainly of feldspar, pyroxene, olivine, amphibole as its primary minerals. Feldspar is altering calcite and shows albite twinning. Less vesicles in the rock and occupied by pyrite and glass material. Losses from 1032-1042 m, 1050 m, 1054 m and 1058 m. Calcite and pyrite, quartz, chlorite and epidote are the secondary minerals in this unit.

1088 – 1164 m: No returns.

1164 – 1176 m Trachyte: Light grey, slightly bleached. Light green colouration with disseminated pyrite. Pyroxene and feldspar are the main primary minerals and as phenocrysts. Loss at 1174 m. The alteration minerals are calcite, pyrite, clay minerals, quartz, and epidote.

1176 – 1184 m: No returns.

1184 – 1198 m Trachyte: Dark grey in colour, fine grained lava with feldspar exhibiting glittering surface. Epidote observed at 1188 m. Loss at 1190 m. The alteration minerals in this rock are Calcite, pyrite, quartz, and epidote.

1198 – 1200 m: No returns.

1200 – 1218 m Trachyte: The rock is dark grey, porphyritic lava with feldspar (alkali feldspar and plagioclase) and pyroxene as main phenocrysts. The rock is fractured and less vesiculated. Abundance of calcite and vein filled by silica observed in this unit. At 1210 m, calcite replaces interstitial volcanic glass and quartz is deposited in vesicles. Cubic crystals of pyrite noted at 1216 m. Secondary minerals in this unit are Calcite, pyrite, quartz, chlorite and epidote.

1218 – 1222 m: No returns.

1222 – 1244 m Trachyte: Fine grained lava with dark grey colour. The rock is moderately altered and seems to be permeable. Feldspar and mafic minerals were noted as primary minerals. Losses at 1234 m and 1242 m. In this unit pyrite, calcite, epidote and quartz are noted as primary minerals.

1244 – 1252 m: No returns.

1252 – 1314 m Trachyte: Fine to medium grained feldspar phyric lava, with light and dark grey colour. The rock is slightly altered as evidenced by brownish colour in this unit. Missing samples at 1314 m. Secondary minerals in this unit are Calcite, pyrite, and quartz.

1314 – 1382 m Trachyte: Dark grey with light grey, fine to medium grained. Feldspar porphyritic lava, the rock is highly altered while clay minerals and calcite minerals deposited on the surface of the rock as observed in binocular. Epidote noted at 1320 m and 1346 m. Missing cuttings at 1334 m. Alteration minerals are calcite, clay minerals, pyrite, quartz and epidote.

1382 – 1394 m Trachyte: The rock is light grey to greenish in colour. Porphyritic rock with phenocrysts of feldspars and mafic minerals. The rock seems to be highly altered. Missing cuttings at 1388 m. Secondary minerals are calcite, pyrite, quartz and prehnite.

1394 – 1424 m Syenite: Light grey to greenish grey in colour, medium to coarse grained porphyritic texture with feldspars and pyroxene as phenocrysts. Pyroxene mainly augerine-augite embayed in laths of feldspar. The groundmass rich in volcanic glass seem to altering to calcite. The unit is moderately altered to some point. Secondary minerals noted are Calcite, pyrite and quartz.

1424 – 1456 m: Missing samples.

1456 – 1458 m Basalt: Dark grey in colour, vesiculated rock, is moderately to highly altered. The vesicles are filled by calcite and clay minerals. Alteration in this rock are calcite, pyrite and clay minerals.

1458 – 1510 m Trachyte: Dark to light grey, fine grained but with feldspars and dark minerals as phenocrysts. It is moderately to highly altered to greenish clay minerals. Mottled rock from 1500 m to 1510 m with more greenish colour. Microfractures at 1472 m filled by calcite recognized. There is abundance of calcite in this unit. High temperature hydrothermal alteration mineral wollastonite was noted at 1462 m. In this unit secondary minerals are calcite, clay minerals, quartz, epidote and wollastonite.

1510 – 1532 m Syenite: The rock is greenish in colour, fresh but mixed with some fine grained trachytic rock. Less vesiculated, the vesicles are filled by quartz. Pyroxene, feldspar, amphibole and Fe-Ti oxides are primary minerals in this unit but feldspar being dominant. Calcite, quartz, clay minerals and epidote observed as secondary minerals.

1532– 1548 m Tuff: Reddish brown with light green colouration. The rock is altered with a fractured surface and vesiculated, the vesicles are filled by calcite and clay minerals. Pyrite, calcite, clay minerals and epidote noted as main alteration minerals.

1548 – 1558 m Tuff: Light grey with reddish brown, coarse grained fresh rock. Dark mafic minerals are phenocryst in the rock. Some cuttings are altered and some are fresh. Missing cuttings at 1560 m. The alteration minerals are calcite, quartz, pyrite, epidote and clay minerals.

1560 – 1570 m Tuff: Altered vesiculated rock, reddish to brownish grey. The vesicles are filled with calcite and clays. Epidote noted at 1564 m. Secondary minerals observed are epidote, pyrite, calcite and clay minerals.

1570 – 1580 m: Sample missing.

1580 – 1582 m Tuff/Trachyte: Reddish to brownish grey, fine to medium grained lava. Mixture of tuff and cuttings of porphyritic trachyte and the rock is highly altered and some tuffs are vesiculated. Alteration minerals are calcite, pyrite and clay minerals.

1582 – 1660 Trachyte: Light grey to brownish grey medium to coarse grained lava with dark minerals and feldspar as phenocrysts. The rock is bleached and highly altered to reddish brown and greenish grey. Calcite, pyrite, chlorite, fluorite and clay minerals were observed as secondary minerals.

1660 – 1674 m Trachyte: Brownish grey, light blue and greenish to the bottom of this unit. The rock is fine to medium grained lava, porphyritic with feldspar and pyroxene as primary minerals. Disseminated pyrite in the groundmass noted and some quartz vein observed. Alteration minerals are calcite, pyrite, and clay minerals.

1674 – 1678 m: No returns.

1678 – 1688 m Trachyte: Light grey to grey lava that changes to largely greenish lava then to greenish brown at the bottom of this unit. Slightly to highly altered rock. The unit is fine grained and slightly porphyritic exhibits veins filled by quartz, pyrite veins also noted. Calcite, pyrite, quartz, clay minerals, and chlorite are the secondary minerals in this unit.

1688 – 1692 m: No returns.

1692 – 1736 m Trachyte: Light grey with green colouration, fine grained and slightly porphyritic texture noted. Veins of quartz present and disseminated pyrite observed. Alteration minerals observed are pyrite, calcite, clays, fluorite and epidote.

1736 – 1740 m: No returns.

1740 – 1774 Trachyte: Brownish grey and light grey, fine grained lava with feldspar as phenocrysts. The rock is altered to greenish brown at some depths. The unit is fairly altered. Veins filled by silica material and the rock is fractured at 1742 m. Some samples are missing at 1752 m, 1762 m and 1772 m. Secondary minerals are calcite, pyrite, clay minerals and chlorite.

1774 – 1780 m: No returns.

1780 – 1832 m Trachyte: The rock is light grey to brownish grey with mottled surface. It is fine to medium grained feldspar porphyritic lava with greenish brown. Quartz veins noted and the rock is altered. At 1720 m, pervasive calcite alteration noted on alkali feldspar and volcanic glass. No returns from 1794-1796 m while 1788 m is missing. The rock seem to consist of pyrite, calcite, chlorite, clay minerals and epidote as secondary minerals.

1832 – 1836 m: No returns.

1836 – 1890 m Trachyte: The rock is light to dark grey with brownish in colour. Fine to medium grained with dark phenocrysts of mafic minerals. The rock is moderately altered and some cuttings show flow

texture. Clay minerals, quartz, oxides, calcite, pyrite and epidote noted as secondary minerals. Cuttings at 1864 m is missing.

1890 – 1892 m: No returns.

1892 – 1910 m Trachyte: Light grey in colour, fine grained lava. The rock is altered to grey – red colour. Feldspar and mafic minerals appear as phenocrysts in the rock but the former is dominant and part of groundmass. Alteration minerals like calcite, pyrite, Clay minerals and epidote were observed.

1910 – 1918 m Trachyte: Light grey with light greenish in colour. Pyrite intergrown with calcite. Trachytic texture were observed in this rock. Feldspar seem to dominate as primary mineral. Pyrite, calcite, clays and epidote noted as secondary minerals.

1918 – 1922 m: No returns.

1922 – 1946 m Trachyte: Light grey brownish, fine grained rock with light greenish. Alkali feldspars appear to be the main phenocrysts and groundmass in this unit. Pyroxene and amphibole also constitute the primary minerals of this unit. Pyrite, calcite clay minerals and epidote were noted as secondary minerals.

1946 – 1948 m: No returns.

1948- 2018 m Trachyte: Light grey fine grained lava showing greenish colour, the rock is dominated by feldspar and mafic minerals and few feldspar and pyroxene phenocrysts are manifested. Seem to be highly altered with pyrite and greenish minerals deposition. No samples at 1956, 1978, 1990, 1994 and 2006 m. Alteration minerals are Pyrite, calcite, clay minerals and epidote.

2018 – 2052 m Tuff: Green in colour, fine grained rock with tuffaceous in nature and vesiculated, the vesicles are filled with silica. Flow features were noted on some cuttings. The rock unit from 2028 – 2052 m is Light grey to greenish grey fine grained feldspar porphyritic rock. Sample at 2022 m is missing. The secondary minerals are calcite, pyrite and quartz.

2052 – 2102 Trachyte: The rock is whitish/light grey with greenish in colour, fine to medium grained. The rock is dominated by alkali feldspar and plagioclase as primary mineral, also mafic minerals (aegirine – augite and amphibole) are noted in feldspar groundmass. The rock is moderately altered. Less vesiculated and vesicles filled with volcanic glass and some altering to calcite and clay minerals. The unit is mixed with fresh green glass at 2102 m. Cuttings missing at 2062, 2064, 2076, and 2092 m. Alteration minerals are calcite, quartz, chalcopyrite, clay minerals, Albite, epidote, wollastonite and actinolite.

0-2 m Pyroclastics: A mixture of pumice, brownish tuff, trachyte, and obsidian were encountered. Showing reworking mechanically.

2-14 m: Circulation loss.

14-16 m Trachyte: Greyish in colour, fine grained porphyritic trachyte. Secondary mineral is calcite
16-18 m: Circulation loss.

18-28 m Trachyte: Fine grained porphyritic trachyte with few tuff fragments. Grey to dark grey colour. Calcite observed as secondary mineral.

28-50 m Trachyte: Light grey, hypocrystalline trachyte with phenocrysts of pyroxene noted. Calcite was observed as secondary minerals.

50-72 m Trachyte: Light grey to brownish grey, fine grained, porphyritic trachyte. The rock is oxidized compared to the overlying formation. Calcite noted as secondary minerals.

72-82 m Trachyte with tuff lenses: Light grey to greenish grey, fine grained trachyte and few tuff fragments are noted at 78-82 m. The formation is oxidized mostly at 76-78 m. Secondary minerals is calcite in this unit.

82-120 m Trachyte: Light to greenish grey, fine grained trachyte. The formations seem to be a bit fresh. Greenish coating noted and few tuff fragments observed from 88 – 118 m. Calcite was noted as secondary mineral.

118-132 m Tuff: Light grey, fine grained vesicular tuff and slightly oxidized. The vesicles are filled with silica and zeolites (scolesite and mesolite). Secondary minerals are zeolites (scolesite and mesolite), calcite and chalcedony.

132-340 m: Circulation loss.

340-368 m Tuff: Brownish with light green and less vesiculated tuff with the vesicles being filled by silica and zeolites. The formation is slightly oxidized at the top and highly oxidized from 360-368 m. Circulation noted at 354-356 m. Secondary minerals are calcite and chalcedony.

368-422 m Trachyte: Light- brownish - greenish grey fairly fresh, fine grained lava. It is porphyritic with phenocrysts of pyroxenes and feldspars. Pyrite is disseminated in the groundmass. Secondary minerals are calcite, pyrite, zeolite (analcime) and clay minerals.

422-428 m Tuff: Light grey to reddish brown, fine grained rock with vesicles showing a silica lining. It is moderately oxidized. Some fresh and fine grained trachyte fragments were also observed. Secondary minerals are pyrite, calcite and chalcedony.

428-510 m Trachyte: Light grey in colour, fresh to greenish grey fine to medium grained rock, composed of pyroxenes and whitish feldspars as primary minerals. The rock is slightly altered to greenish. Oxidation noted from 480-500 m. Chalcedony observed as secondary mineral.

510-526 m Tuff: Very light grey, fine grained rock that is fairly altered. Reddish brown colours on the rock surface showed evidence of oxidation. Vesiculated rock, the vesicles filled by silica. The rock is tuff however few cuttings of trachyte were also noted at 526 m. Chalcedony observed as secondary mineral in this unit.

526-536 m: Circulation loss.

536-624 m Trachyte: Brownish grey, fine grained lava composed mainly of feldspars and pyroxene phenocrysts. Altered rock with occasionally quartz veins are observed. Fine grained tuff also were observed between 536-552 m. Pyrite is disseminated in the groundmass. Alteration minerals are calcite, pyrite and chalcedony.

624-734 m Trachyte: Light grey, fine grained porphyritic lava with pyroxenes and large feldspar phenocrysts. Pyroxene and feldspars observed as primary minerals. The rock is moderate oxidized and is slightly altered to light greenish clay minerals. Tuff lenses were observed within this unit, especially from 628-684 and 718-730 m. The formation contains some amount of calcite and pyrite. Also quartz noted at 712 m. Losses were encountered at 624-628, 654-660, 684-684, 714-718, and 730-734 m. Secondary minerals are Chalcedony, calcite, pyrite, quartz and clay minerals.

734-782 m Tuff: Reddish brown, fine grained rock with some vesicles filled by calcite and pyrite is disseminated in the groundmass. A few grains of trachyte were observed. Secondary minerals are chalcedony, calcite, pyrite and quartz.

782-810 m Fine grained trachyte: Light grey in colour, very fine grained, feldspar phyric trachyte. Mixer of some cuttings of brownish tuff and trachyte was evident. Losses at 784-790 m and 800-810 m. Pyrite and calcite noted as primary minerals.

810-864 m Fine grained trachyte: Grey to greenish grey, fine grained porphyritic rock with feldspar and pyroxene as phenocrysts. Altered rock with minor veins filled with silica. Pyrite is disseminated in the groundmass and the rock exhibits vesicles filled by calcite. Alteration minerals are pyrite, calcite, chalcopyrite and clay minerals.

864-1298 m Medium grained trachyte: Light grey in colour, fine to medium grained feldspar porphyritic trachyte lava. Sporadically phenocrysts of pyroxene are observed. The groundmass is almost dominated by glassy. The rock exhibits slight alteration and calcite is abundant across the unit. Calcite to some part is filling some vesicles and pyrite is disseminated on the groundmass and filling the veins from 810-854 m. Alteration minerals are calcite, pyrite, chalcopyrite, quartz and clay minerals.

1298-1438 m Trachyte: Light grey to greenish grey, fine grained, porphyritic trachyte. This formation is having more pyrite, chalcopyrite and calcite. Secondary minerals are Pyrite, calcite, quartz, chalcopyrite and clay minerals.

1438-1448 m Tuff: Light grey to light greenish grey in colour, fine grained tuff with the matrix dominated by feldspar especially sanidine. Pyrite, chalcopyrite and Calcite were observed as secondary minerals.

1448-1468 m Trachyte: Brownish to light greenish grey, fine grained trachyte and the rock is highly altered, wollastonite is abundant in this unit. Wollastonite noted from 1450 m which indicates high-temperature environment. Secondary minerals are calcite, quartz, chalcopyrite clay minerals and wollastonite.

1468-1546 m Trachyte: Brownish grey to greenish grey, the rock is fine grained and highly altered trachyte with porphyritic in nature. Plentiful pyrite, chalcopyrite, calcite, clay minerals and wollastonite noted in this unit as secondary minerals.

1546-1552 m Tuff: Reddish brown and greenish, fine grained, tuff with vesicles filled with calcite and pyrite. Pyrite seems to be disseminated in the groundmass. Secondary minerals are pyrite and calcite.

1552-1946 m Trachyte: Light grey to greenish grey in colour, medium grained porphyritic lava with feldspar as phenocrysts showing slight alteration to green and brownish clay minerals. The unit shows adequately of pyrite and disseminated on the surface of the rock fragments and the rock is highly altered. Tuff fragments were observed at 1574-1596 m, 1674, 1712 m, 1718-1720 m, 1778-1782 m, 1840 m, 1884 and 1912 m. The high temperature alteration minerals such actinolite at 1552 m and wollastonite

were noted in the rock formation. Epidote noted at 1586 m and albite was observed at 1862 m. The presence of these minerals especially epidote, wollastonite and actinolite may indicate high-temperature environment. Secondary minerals in this unit are calcite, pyrite, chalcopyrite, quartz, clay minerals, fluorite, albite, wollastonite and actinolite.

1948-1960 m Syenitic intrusion: The rock is whitish with dark greenish a bit, it is fresh dominated by alkali feldspar and it is coarse to medium grained rock. The alteration minerals are pyrite and calcite.

1960-2060 m Trachyte: Light grey to greenish grey in colour, fine grained rock and highly altered trachyte. Some bluish tuff fragments were noted. No cuttings at 1970 m, 2044 m and 2046 m. Alteration minerals in this unit are calcite, pyrite, chalcopyrite, quartz, clay minerals, albite, wollastonite and actinolite.

APPENDIX III: Detailed descriptions of lithology, alteration minerals of well MW-20 as observed under binocular and petrographic microscope analyses

0 – 4 m: No returns.

4 – 6 m Tuff/pyroclastics: Light grey to greenish grey, vesicular tuff, partly filled with silica and some trachyte cuttings present.

6 – 12 m: No returns.

12 – 28 m Trachyte: Light dark greyish lava, fairly fresh and rarely oxidized. Pyrite, calcite and vein filled with silica materials noted. No samples from 14-28 m.

28 – 40 m Tuff/Proclastics: Light grey to greenish grey in colour, fine grained vesicular and vein fillings. Zeolite noted probably analcime, occurs as vesicle fillings associated with calcite.
Alteration minerals are calcite and zeolite (analcime).

40 – 68 m: No returns.

68 – 92 m Trachyte: Brownish grey, fine grained rock with mafic minerals mainly pyroxene and feldspar in the groundmass. Though the formation seems to be fresh and mixed with some tuff cuttings.

92 – 114 m Trachyte: Light grey with brownish grey. Fine grained rock, the groundmass is dominated by mafic minerals and feldspar phenocrysts embayed in groundmass. The rock is slightly altered. The rock has less disseminated pyrite in the groundmass. No samples at 108 m. Pyrite and zeolite noted as alteration mineral.

114 – 130 m Trachyte: Dark grey, fine grained lava dominated by pyroxene rich groundmass and fine grained alkali feldspar and plagioclase crystals and amphibole observed. The rock is less oxidized. Volcanic glass in the groundmass alter to limonite however very minute. Alteration mineral are limonite and zeolite.

130 – 362 m: No returns.

362 – 380 m Trachyte: Brownish grey in colour, fine grained porphyritic lava mixed with tuffs and drilling materials (cement) and some cuttings exhibit blue dots. The formation is fairly fresh. No cuttings (losses) from 366-372 m. The rock micro-veins at 364 m filled with silica. Abundance of calcite from 372-80 m, also pyrite noted in the rock groundmass. Alteration minerals are calcite, pyrite and chalcedony which seem fill few vesicles at 364 m.

380 – 386 m Tuff/Pyroclastics: Light grey to brownish and some greenish, fine grained tuff mixed with little volcanic glass. Slightly altered. Alteration minerals are chalcedony and calcite.

386 – 410 m Trachyte: Light grey, brownish grey and greenish in colour. Fine grained lava and slightly vesicular. Vesicles are filled by clay materials and glass. Upper part of this unit is more green. Tuff intercalation with trachyte noted from 404-412 m, the unit is highly altered at 402 m. No samples at 396 m. Alteration minerals are calcite and chalcedony.

412 – 428 m Trachyte: Light grey to greenish grey, fine grained porphyritic lava slightly oxidized and altered. Minor pyrite disseminated in the rock. Alteration minerals are pyrite and calcite.

428 – 438 m: No returns.

438 – 456 m Trachyte: Light grey in colour. Fine to medium grained porphyritic lava and the rock is fresh. Mafic minerals are more abundant from 450-454 m. Alteration minerals are pyrite, calcite and chalcedony.

456 – 462 m Pyroclastics: Greyish brown, fine to medium grained tuff with alkali feldspar, plagioclase and pyroxenes as primary minerals. Pyrite and calcite noted as secondary minerals in this unit.

462 – 504 m Trachyte: Grey to brownish grey, medium grained lava, slightly altered with strong oxidation at 482–502 m. The formation may signify the presence of permeable zone in this unit. Alkali feldspar and plagioclase dominate the rock groundmass together with volcanic glass. Pyroxene especially aegirine– augite embayed in feldspar groundmass. Glass and feldspar seem altering to smectite and zeolite (scolesite). Alteration minerals are zeolite (scolesite), smectite, chalcedony and calcite.

504 – 524 m Trachyte: Grey in colour, coarse grained lava that appears fresh. Mafic minerals in alkali feldspar rich groundmass were observed. Some minor losses of circulation at 508, 518 and 520 m. Little calcite present in this unit and stand as secondary mineral.

524 – 550 m Trachyte: Dark to brownish grey, medium grained lava. It is oxidized, fractured surface and mafic minerals are observed. The unit is mixed with altered tuff and drilling materials at 548 m. No samples at 538, 546 and 550 m. Alteration minerals are pyrite and calcite.

550 – 562 m Trachyte: The rock is grey in colour. It is fresh fine grained porphyritic trachyte with alkali feldspar and plagioclase being dominant phenocrysts and as primary minerals. Little alteration seen in this unit. Alteration mineral is calcite.

562 – 574 m Tuff: Light grey to brownish grey. The rock is oxidized and slightly altered. Fine grained lava containing alkali feldspar and plagioclase phenocrysts. Bluish colour noted in this unit which indicates the presence of clay minerals.

574 – 586 m Trachyte: It is grey in colour, fine grained lava, specs of mafic minerals were noted. Porphyritic trachyte with feldspar phenocrysts were identified. Calcite and pyrite noted at bottom of this unit, which are secondary minerals.

586 – 626 m Trachyte: Light grey, and it is fine grained crystalline lava. The mafic minerals occurs as randomly oriented acicular phases in the rock groundmass. Chalcedony deposited at 600 m. Pyrite, calcite and chalcedony are the alteration minerals.

626 – 658 m Trachyte: Light grey to brownish grey, fine to medium grained lava and less altered with mafic minerals noted. The rock is oxidized. At 634 m the rock is porphyritic with alkali feldspar and plagioclase phenocrysts and from 632-628 m the unit contains less porphyritic minerals. Titanomagnetite also noted due to light greyish colour in reflected light. In this formation, some tuff fragments noted from 640-658 m. Alteration minerals are calcite and pyrite.

658 – 670 m Tuff: Light grey to greenish grey, fine grained vesicular rock. Vesicular and vesicles are filled with clay minerals due to oxidation, veins are filled by calcite. Cuttings at 668 m are missing. Alteration minerals are calcite and calcite.

670 – 686 m Trachyte: Light grey to brownish grey lava. The rock is slightly vesicular, vesicles are filled by clay minerals and tuff fragments noted. Slightly altered to greenish grey, porphyritic lava at 672 m. Bluish colour in some cuttings were observed. Alkali feldspar, plagioclase and pyroxene are the main primary minerals in this formation. Titanomagnetite also is present. Secondary quartz observed at 642 m with its undulating boundaries in thin section. Alteration minerals are calcite, pyrite and quartz.

686 – 706 m Tuff: Brownish grey, fine grained tuff. Some tuff exhibits vesicles filled with clay minerals. Pyroxene as phenocrysts were noted clearly at 702 m. Alteration minerals are calcite and quartz.

706 – 714 m Trachyte: Greyish in colour, altered porphyritic lava. Radiating assemblages of greenish clay minerals and prismatic mafic minerals were observed. Calcite, pyrite, quartz as secondary minerals observed in this unit.

714 – 748 m Trachyte: Light grey, the rock is dominated by alkali feldspar and plagioclase as primary minerals. The rock is slightly altered. Minor loss of circulation noted at 724 m. Alteration minerals are calcite, pyrite and smectite.

748 – 760 m Trachyte: The rock is moderately oxidized, light grey to brownish grey in colour. Green colouration at 760 m due to oxidation. Less veins filled with silica. Golden yellow colour indicated chalcopyrite occurrence at 750 m. Chalcedony, calcite, smectite, chalcopyrite as secondary minerals were observed.

760 – 780 m Trachyte: Grey to greenish grey, fine grained lava. Feldspar is the main primary mineral in this formation and display trachytic texture. Also Fe-Ti Oxides present in the laths of feldspar, they are dark in plane polarized light and closed polars. Some of the cuttings are vesicular in which the vesicles are filled by silica and clay minerals. This unit has disseminated pyrite, chalcedony, clay minerals, and calcite noted as secondary minerals.

780 – 804 m Trachyte: Light grey to brownish grey, porphyritic lava with vesicles filled by clay minerals and glass. The unit is mixed with tuff cuttings and is slightly altered to greenish. Fibrous aggregates wollastonite as high temperature alteration mineral noted at 792 and 798 m that indicate temperature above 270°C. Alteration minerals are calcite, pyrite, quartz and wollastonite.

804 – 850 m Trachyte: Grey in colour, porphyritic lava with some greenish colour which suggests the presence of clay minerals. A lot of sanidine feldspar and plagioclase as primary minerals encountered, while calcite and pyrite are abundant as secondary minerals. Cuttings at 814 and 838 m are missing. Alteration minerals are calcite and pyrite.

850 – 896 m Trachyte: Light grey, the rock is moderately altered to greenish. No samples at 890 m. Alteration minerals are calcite and pyrite.

896 – 942 m Trachyte: Grey in colour, porphyritic lava with pyrite, calcite and quartz as secondary minerals. Chlorite as secondary mineral also noted at 932 m. Minor circulation losses at 912 and 926 m. Alteration minerals are calcite, pyrite, clay minerals (smectite and illite), quartz and chlorite.

942 – 982 m Trachyte: Light grey to brownish grey, fine grained alkali feldspar and plagioclase rich lava, moderately altered. Pyroxene, olivine and Fe-Ti Oxides also present in this formation. The lava exhibits abundant calcite. High temperature alteration mineral; wollastonite are also observed as secondary minerals at 968 and 972 m. Presence of indicates temperature above 270°C. Alteration minerals are calcite, pyrite, clay minerals, quartz and wollastonite.

982 – 1024 m Trachyte: Light grey, porphyritic lava that seems to be less altered having abundant calcite as secondary mineral. The formation begins to show abundance in phenocrysts at 1012 m. Alkali feldspar (sanidine) and pyroxene growing together in the groundmass, though feldspar is the main primary mineral. Sanidine feldspar seem to alter to albite that appear cloudy and whitish. In this unit crystallized acicular mineral; wollastonite form as secondary mineral. Calcite, pyrite, clay minerals, quartz, albite and wollastonite are secondary minerals in this formation.

1024 – 1052 m Trachyte: Grey to greenish grey, fine grained lava. Containing minor disseminated pyrite and abundant calcite as secondary minerals. The rock is moderately altered. No samples at 1052 m. Alteration minerals are calcite, pyrite, clay minerals, quartz and wollastonite.

1052 – 1118 m Trachyte: Grey brownish, porphyritic lava and less altered. The unit has abundant calcite and minor pyrite as secondary minerals and clay minerals were observed from 1088-1104 m and at 1106 m. In this unit epidote colouration was encountered particularly at 1058 m. Secondary minerals are calcite, pyrite, clay minerals and epidote.

1118 – 1146 m Trachyte: Light to dark grey in colour, fine to medium grained porphyritic lava with alkali feldspar as phenocrysts. The rock is highly altered with abundant calcite and minor disseminated pyrite in the rock matrix. No cuttings at 1128 and 1146 m. Alteration minerals are calcite and pyrite.

1146 – 1174 m Trachyte: Light to dark grey/brownish, fine to medium porphyritic rock, slightly altered with abundant calcite and minor pyrite noted. Quartz as secondary mineral appears to fill vugs in this unit. Bluish fragments noted at 1170 m. No cuttings at 1168 m. Alteration minerals are calcite, pyrite, clay minerals and quartz.

1174 – 1200 m Trachyte: Light grey in colour. Fine grained porphyritic lava with phenocrysts of feldspars and pyroxene, the rock seems slightly altered. Olivine, glass and Fe-Ti Oxides are among of primary minerals in this formation. Spectacles of poorly crystalline and bluish rock fragments are seen mixed with the cuttings. Pervasive calcite alteration observed in the rock. No samples at 1200 m. Alteration minerals are calcite, pyrite, quartz and wollastonite.

1200 – 1222 m Trachyte: Light grey with brownish grey in colour. Fine grained porphyritic lava with feldspar as phenocrysts. The rock seems highly altered. In this unit pyrite, calcite, chalcopyrite, quartz, wollastonite and actinolite are noted as secondary minerals.

1222 – 1246 m Trachyte: Light grey, fine grained porphyritic lava with a bit subhedral large phenocrysts of feldspars and few pyroxene phenocrysts. Feldspar and pyroxene are part of groundmass. Glass and Fe-Ti-Oxide noted in this formation. Specs of whitish feldspar rich rock fragments are seen mixed with the cuttings. The unit exhibits less alteration. Alteration minerals are calcite, pyrite, quartz, chlorite, chalcopyrite and actinolite.

1246 – 1264 m Trachyte: The rock is light grey to whitish in colour. Fine grained lava with phenocrysts of feldspar. The cuttings are moderately altered to greenish colour that indicates the presence of clay minerals. Also black crystals are noted in the matrix. Some samples are missing from 1252-1256 m. Alteration minerals mainly are calcite and pyrite.

1264 – 1292 m Trachyte: Light grey to whitish, fine grained porphyritic lava mixed with drilling materials. The rock altered to greenish clay minerals and calcite as secondary minerals. No samples at 1272 and 1274 m. Alteration minerals are pyrite, calcite, quartz and actinolite.

1292 – 1322 m Trachyte: Light grey to white, fine grained and porphyritic lava with phenocrysts of feldspar (alkali feldspar and plagioclase). The rock is slightly altered to greenish clay minerals. The unit exhibits oxidation from 1306-1318 m. The rock has less veins filled with silica. No cuttings at 1322 m. Alteration minerals are calcite, clay minerals and quartz.

1322 – 1368 m Tuff/Trachyte/Syenite: Light to dark grey, brownish grey, porphyritic lava and mottled with feldspar phenocrysts. The unit is mixed with trachyte and tuff cuttings, some cuttings appear with light bluish colour. Quartz seem being deposited. The nature of the rock indicates presence of the dyke (syenite intrusion). Alteration minerals are calcite, pyrite and quartz.

1368 – 1438 m Tuff/Trachyte/Syenite: Light grey to brownish grey, slightly altered feldspar porphyritic lava. The unit progressively changes to a poorly porphyritic and more altered to lower part of this unit. Alteration lead to brownish grey colour. The unit is mixed with tuff and trachyte while tuff shows lineation. Alteration minerals are calcite, pyrite, chalcopyrite and quartz.

1438 – 1502 m Tuff/Trachyte/Syenite: Light grey with brown shade aphyric lava exhibiting moderate alteration and fractured surface. Feldspar and pyroxene phenocrysts in feldspar groundmass. Glass and Fe-Ti Oxide noted as the former show are clear in plane polarized light and dark in closed polar while latter being dark in both. Also bluish tuff cuttings are noted in this unit. Glass alter to calcite. Well formed pyrite as secondary mineral at 1492 m. Alteration minerals are calcite, pyrite, chalcopyrite and quartz.

1502 – 1576 m Trachyte: Light grey, mottled with mafic minerals, poorly porphyritic, very slightly altered lava. Tuff fragments also noted in this unit. The rock is fractured at 1576 m that shows changes of lithology where the lava is brownish grey with red colouration caused by oxidation. Whitish grey from 1548 to 1560 m were observed and green colouration from 1560 to 1576 m. Alteration minerals are calcite, pyrite, quartz and actinolite.

1576 – 1594 m Trachyte: Light grey, fine grained lava. The rock is slightly altered. Presence of green colour in this unit may indicate the presence of clay minerals or epidote colouration. The rock has less calcite and pyrite as secondary minerals. Alteration minerals are calcite, pyrite, illite, chlorite and actinolite.

1594 – 1610 m Trachyte: Light grey/brownish grey with greenish colouration. Fine to medium grained porphyritic lava showing mixed with intrusive/dyke cuttings. Fracturing nature noted at 1602 m and intergrowth of wollastonite and quartz encountered at 1608 m. Less vesicles and veins filled by calcite and glass. Light bluish colour observed from 1594 to 1600 m. Alteration minerals are calcite, pyrite, quartz, wollastonite and actinolite.

1610 – 1618 m: No returns.

1618 – 1664 m Trachyte: Light grey, medium grained lava porphyritic with shiny prismatic crystals that are fibrous and radiating in some instances. Feldspar, pyroxene and amphibole are present as primary minerals. The rock shows trachytic texture as evidenced by laths of alkali feldspar. At some depths tuff fragments appear to be blue and green particularly 1644-1648 m. Minor pyrite is disseminated and calcite observed. Alteration minerals are calcite, pyrite, quartz, illite, chlorite and wollastonite.

1664 – 1676 m Trachyte: Light grey/brownish/greenish grey, fine grained lava with disseminated pyrite in ground matrix. More greenish noted at 1676 m and some minor losses at 1658 – 1662 m. Secondary minerals in this unit are pyrite, calcite and quartz.

1676 – 1680 m Trachyte: Light greyish green in colour. It is a porphyritic lava, dominated by feldspar as phenocrysts and groundmass. The rock is less altered. Pyrite seem dispersed in the rock. Secondary mineral in this unit are pyrite, calcite and quartz.

1680 – 1730 Trachyte: Light grey in colour, medium to coarse grained lava with shiny dark minerals (pyroxene), and the rock is slightly altered. More prismatic shape of mafic minerals noted from 1704 m to the bottom of this unit. Needle like structure radiating that indicates the presence of wollastonite. Alteration minerals are calcite, pyrite, quartz, wollastonite and actinolite.

1730 – 1770 Trachyte: Light greyish green in colour. Fine grained lava with shiny dark prismatic crystals and also vitreous radiating, fibrous prismatic crystals encountered in this unit. At 1748 m interfingering between feldspar and pyroxene is noted. Both are primary minerals in this formation. Glass and Fe-Ti Oxides are also present, glass altered to quartz. The present vesicles are filled with glass and pyrite. The rock is moderately altered. No samples at 1762 and 1766 m. Alteration minerals are calcite, pyrite, quartz, clay minerals, wollastonite and actinolite.

1770 – 1774 m No returns.

1774 – 1796 m Trachyte: Whitish grey, porphyritic lava, medium to coarse grained with shiny dark prismatic crystals radiating. Minor pyrite is disseminated in the groundmass. Alteration minerals are pyrite, calcite, quartz, wollastonite and actinolite.

1796 – 1824 m Trachyte: Whitish to brownish grey with greenish grey, porphyritic lava that is medium to coarse grained with dark prismatic minerals clearly shown. The unit has less calcite and minor disseminated pyrite. Also wollastonite and actinolite observed. The rock is less oxidized and vesicles are minute. Alteration minerals are calcite, pyrite, quartz, wollastonite and actinolite.

1824 – 1874 m Trachyte: The rock is light grey and bluish grey with greenish in colour. Fine to medium grained lava and moderately altered. The rock is dominated by alkali feldspar and plagioclase in composition. Glittery dark radiating prismatic crystals which are mafic minerals especially pyroxene (aegirine – augite), olivine and amphiboles are also evident as primary minerals. Quartz veining noted and disseminated pyrite present. The lower part of this unit from 1854 to1874 m changes to whitish grey course grained and fractured. No sample at 1876 m. Alteration minerals are pyrite, calcite, quartz, albite, epidote, clay minerals, wollastonite and actinolite.

1874 – 1904 m Trachyte: Light grey to greenish grey in colour. Medium grained, moderately altered lava that is fractured and vitreous fibrous radiating prismatic crystals are also evident with disseminated pyrite as secondary mineral. Alkali feldspar is the main primary minerals. The unit is mixed with tuff fragments. No cuttings at 1904 m. Alteration minerals are calcite, pyrite, wollastonite and actinolite.

1904 – 1930 m Trachyte: Whitish grey with some greenish colouration. Coarse grained porphyritic lava, fractured with disseminated pyrite. Alteration minerals are pyrite, calcite, wollastonite and actinolite.

1930 – 1950 m Trachyte: Light greyish green, coarse grained, moderately altered lava with feldspar and pyroxene as its primary minerals. Disseminated pyrite also observed in this formation. Alteration minerals are calcite, pyrite and wollastonite.

1950 – 1958 m Trachyte: Greenish grey and some whitish grey, medium to coarse grained lava. There is mixing of cuttings the fresh one and the altered one exhibiting clay minerals. No samples at 1958. Alteration minerals are calcite, pyrite, clay minerals and wollastonite.

1958 – 1960 m Trachyte: Whitish grey coarse grained lava. Primary minerals include mafic mainly pyroxenes in a feldspar groundmass. The formation appears fresh but calcite occurs as secondary minerals. Alteration minerals are calcite, pyrite, wollastonite and actinolite.

1960 – 1968 m Trachyte: Light grey fine grained lava mixed with tuff fragments. The formation is altered at this depth range with Actinolite at 1960-1968 m. The formation appears dotted and shows evidence of water rock interactions. Clays, quartz and few pyrite as secondary minerals are noted. Secondary minerals are calcite, pyrite, quartz, wollastonite and actinolite.

1968 – 1980 m Syenite: Whitish grey coarse grained lava with mafic minerals which are prismatic in shape embayed in a feldspar ground mass. This unit has calcite, clay minerals, quartz, wollastonite and actinolite as secondary minerals.

1980 – 2020 m Trachyte: Light grey with brownish grey and some greenish to some cuttings. Coarse grained lava with few tuff fragments in this unit. Pyroxene and feldspar are present as primary minerals. The rock is altered to pyrite, calcite, wollastonite and actinolite as secondary minerals. The presence of these alteration minerals may indicate permeable zone of high temperature.

2020 – 2046 m Trachyte: Whitish grey to brownish grey, coarse grained lava. The unit appear mixed with intrusive cuttings, the unit indicates feed zone but small based on the altered texture of the formation as demonstrated by minor clay minerals present. The formation is altered with visible wollastonite and actinolite, less calcite and pyrite. Alteration minerals are pyrite, calcite, wollastonite and actinolite.

2046 – 2092 m Intrusive: Whitish grey, coarse grained lava. The formation seems to be fresh. Dark mafic minerals were noted in a feldspar groundmass showing prismatic shape. It is porphyritic lava with white large grains of feldspars observed in the cuttings from 2054 to 2092 m. Calcite, pyrite, wollastonite, actinolite and quartz noted as secondary minerals.

2092 – 2142 m Intrusive: Whitish grey, coarse grained dominated by green colouration probably due to presence of clay minerals. The rock is porphyritic with white grain of feldspar, pyroxene embayed in feldspar groundmass. Glass, amphiboles and Fe-Ti oxides also noted in this unit. The rock exhibits some

vesicles that are filled with glass and calcite. The alteration minerals are calcite, pyrite, quartz, chalcopyrite, wollastonite and actinolite.

2142 – 2258 m Intrusive: Whitish grey, Light grey to slight greenish grey coarse grained lava and some depths are showing fine grained mixed with medium and coarse grained. The formation is an altered intrusive with a mottled texture. Total loss from 2218 to 2230 m, Minor losses from 2238 to 2244 m while samples at 2256 m are missing. The hydrothermal minerals present includes; quartz, pyrite, clay minerals, wollastonite, epidote and actinolite.

2258 – 2276 m Trachyte: Light grey to pale greenish grey, medium grained, porphyritic and altered lava. Clay minerals, quartz, calcite and pyrite are secondary minerals noted in this unit.

2276 – 2304: No returns.

2304 – 2392 Trachyte: Light grey to pale greenish grey, medium grained porphyritic lava. The rock is composed of feldspars (alkali feldspar and plagioclase), pyroxene (augerine-augite) as primary minerals. Glass and amphiboles also are present in the rock. The rock matrix is dominated by laths of feldspar and zoned plagioclase were noted. The rock is altered. Wollastonite appears growing together with quartz at 2352 m. Some losses from 2346 to 2348 and 2366 to 2384 m. The unit comprises calcite, pyrite, clay minerals, actinolite, quartz and wollastonite as secondary minerals.

2392 – 2424 m Trachyte: Light grey to pale greenish grey in colour. The rock is fine to medium grained, porphyritic and moderately altered from 2392 to 2424 m. Though, unaltered medium to coarse grained rock mixed with the lava noted. In this unit clay minerals, pyrite, actinolite and quartz observed as secondary minerals.

2424 – 2438 m Tuff: Light green, fine grained, and altered rock. It less oxidized rock. Some cuttings show lineation in this unit. From 2428 to 2430 m tuff are mixed with trachyte cuttings, trachytic texture observed in this unit. Feldspar and prismatic mafic minerals noted as primary minerals. Actinolite was identified at 2430 m as alteration mineral. Cuttings at 2036 m missing. The alteration minerals are clay minerals, calcite, pyrite and actinolite.

2438 to 2446 m Trachyte: The unit is light dark grey in colour, fine grained rock. The rock has mafic minerals and feldspar as its primary minerals. Less calcite and pyrite are deposited. In this unit calcite, pyrite, actinolite and quartz observed as secondary minerals.

2446 – 2450 Trachyte: Light to dark grey to greenish grey, fine grained rock and altered. Feldspar, pyroxene, amphiboles and glass are the primary minerals in this rock. Fe-Ti oxides also present as recognized in thin section by its grey colour in reflected light. Undulating surface of quartz was noted in thin section, appears as alteration product of glass. The rock exhibits calcite, clay minerals, epidote and quartz as secondary minerals.

APPENDIX IV: Procedure for ICP-OES analysis

Samples were cleaned to remove foreign materials and remain with homogeneous samples. Then samples were grinded in agate mortar to a powder form. After grinding each sample was weighed in a graphite crucibles and mixed with Lithium metaborate flux ($LiBO_2$) at the ratio of 1 to 2, that means sample weighed at $0.1g \pm 0.001g$ and $LiBO_2$ at $0.2g \pm 0.001g$.

In order to be sure with the final results the instrument was calibrated and any drift during the analysis was monitored. In this case six standards were prepared and weighed. The three samples namely; K-1919, BIR-1 and RGM 1 each one was weighed at $0.1g \pm 0.001g$ and mixed with Lithium metaborate flux ($LiBO_2$) at $0.2g \pm 0.001g$.

The rest of the three samples; A-THO, B-THO and B-ALK each was weighed at $0.25g \pm 0.001g$ and mixed with $0.5g \pm 0.001g$ of Lithium metaborate flux ($LiBO_2$).

Then the samples were transferred and put in electric furnace and heated at 1000°C for at least 30 m where by each sample form a pellet. These pellets were given about 15 minutes to cool down.

Then each of the sample and standards (K – 1919, BIR -1 and RGM-1) was mixed with 30 ml of Complexion acid mixture (5% Conc HNO_3, 1.33% HCl and 1.33% Semi saturated oxalic acid) in the bottle. The mixed samples with acid were taken to the shaker machine and shaken for at least 3hours however the aim was to make sure there is total/complete dissolution. However, the other three standards (A-THO, B-THO and B-ALK) was mixed with 75 ml of Complexion acid mixture (5% Conc HNO_3, 1.33% HCl and 1.33% Semi saturated oxalic acid). Before analysis the reference (REF) was prepared by mixing 33% of A-THO, B-THO and B-ALK dissolution for the essence of monitoring drift during analysis.

After these procedures the prepared samples were taken for ICP – OES analysis. The three standards (K – 1919, BIR -1 and RGM-1) were run first to calibrate the instrument (Spectro Ciros 500 ICP-OES equipment).

To monitor fluctuation or drifting of the instrument during the analysis the reference (REF) was employed. Also REF was used at the start of the analysis and after every ten samples so that instrument reproducibility in multiple analyses to be monitored. The analysis was done at 2 ml sample per minute with argon plasma. After obtaining the raw data on major elements and trace elements then were corrected and normalised to 100%. Trace elements were converted to ppm.

APPENDIX V: Procedure for X-ray diffractometer analysis

The selected samples were placed in crucibles, 1/5 sample then 3/4 water and then shaken for 4 hrs in a shaker machine to separate the phyllo-silicates from the rock matrix.

The samples were then placed into a clean test-tube, when finished, the samples were mounted on thin films on a glass plate and allowed to dry at room temperature overnight.

The samples were run in range 2-14^0 for a time of about 15 minutes on the XRD machine.

After drying they were placed in a desiccator which contain glycol solution and left in at room temperature for about 24hours. The glycolated samples were then run in the XRD machine.

The next step was put into an oven and heated to about 550^{0}C for one hour and allowed to cool. The analysis was done using Bruker AXS, D8 Focus Diffractometer at ISOR, Icelandic GeoSurvey. The results are found in Tables 3 and 4.

Well MW-03

58139/MW-03 1940m OMH - Start: 2.000 ° - End: 14.000 ° - Step: 0.020 ° - Step time: 1. s - Anode: Cu - Generator kV: 40 kV - Generator mA: 40 mA - Company: IPX - Creation: 10.12.2015 09:11:27
58186/MW-03 1940m GLY - Start: 2.000 ° - End: 14.000 ° - Step: 0.020 ° - Step time: 1. s - Anode: Cu - Generator kV: 40 kV - Generator mA: 40 mA - Company: IPX - Creation: 15.12.2015 09:57:57
58231/MW-03 1940m HIT - Start: 2.000 ° - End: 14.000 ° - Step: 0.020 ° - Step time: 1. s - Anode: Cu - Generator kV: 40 kV - Generator mA: 40 mA - Company: IPX - Creation: 18.12.2015 12:55:55
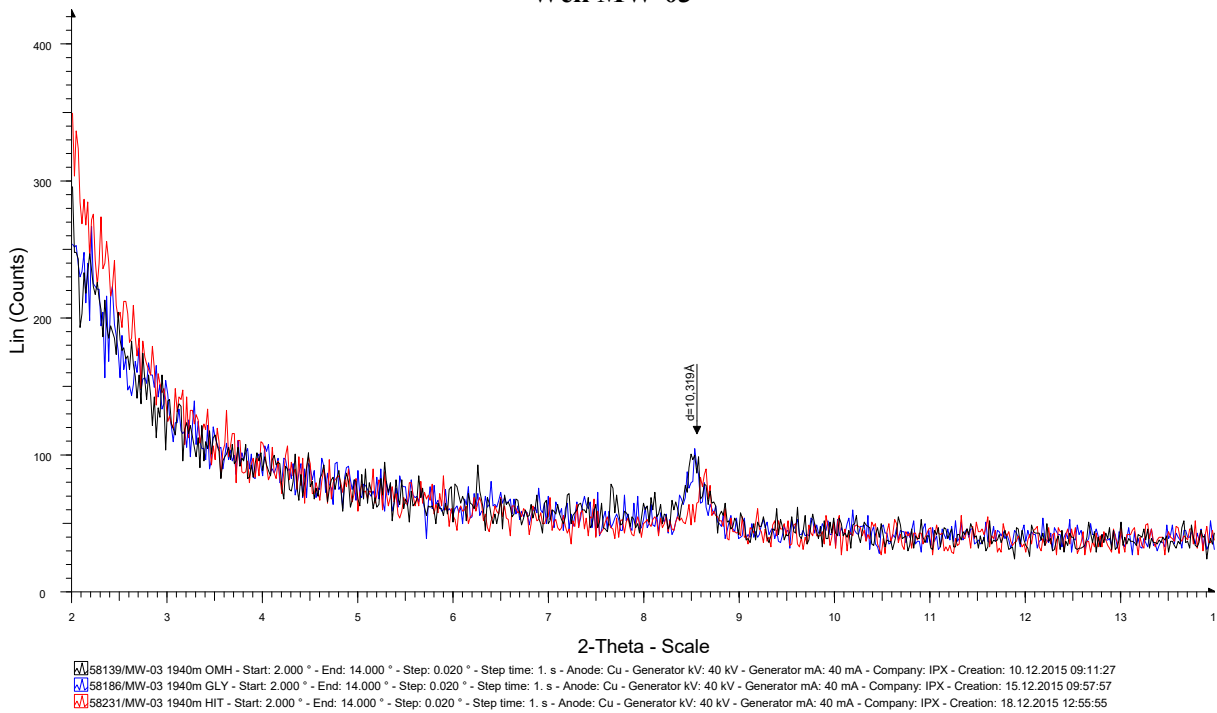
FIGURE 1: Diffractogram for illite at 1940 m in MW-03 with peak at 10.319 Å
in untreated, glycolated and heated sample

58134/MW-03 1462m OMH - Start: 2.000 ° - End: 14.000 ° - Step: 0.020 ° - Step time: 1. s - Anode: Cu - Generator kV: 40 kV - Generator mA: 40 mA - Company: IPX - Creation: 9.12.2015 16:21:19
58181/MW-03 1426m GLY - Start: 2.000 ° - End: 14.000 ° - Step: 0.020 ° - Step time: 1. s - Anode: Cu - Generator kV: 40 kV - Generator mA: 40 mA - Company: IPX - Creation: 14.12.2015 16:25:19
58226/MW-03 1462m HIT - Start: 2.000 ° - End: 14.000 ° - Step: 0.020 ° - Step time: 1. s - Anode: Cu - Generator kV: 40 kV - Generator mA: 40 mA - Company: IPX - Creation: 18.12.2015 11:48:54
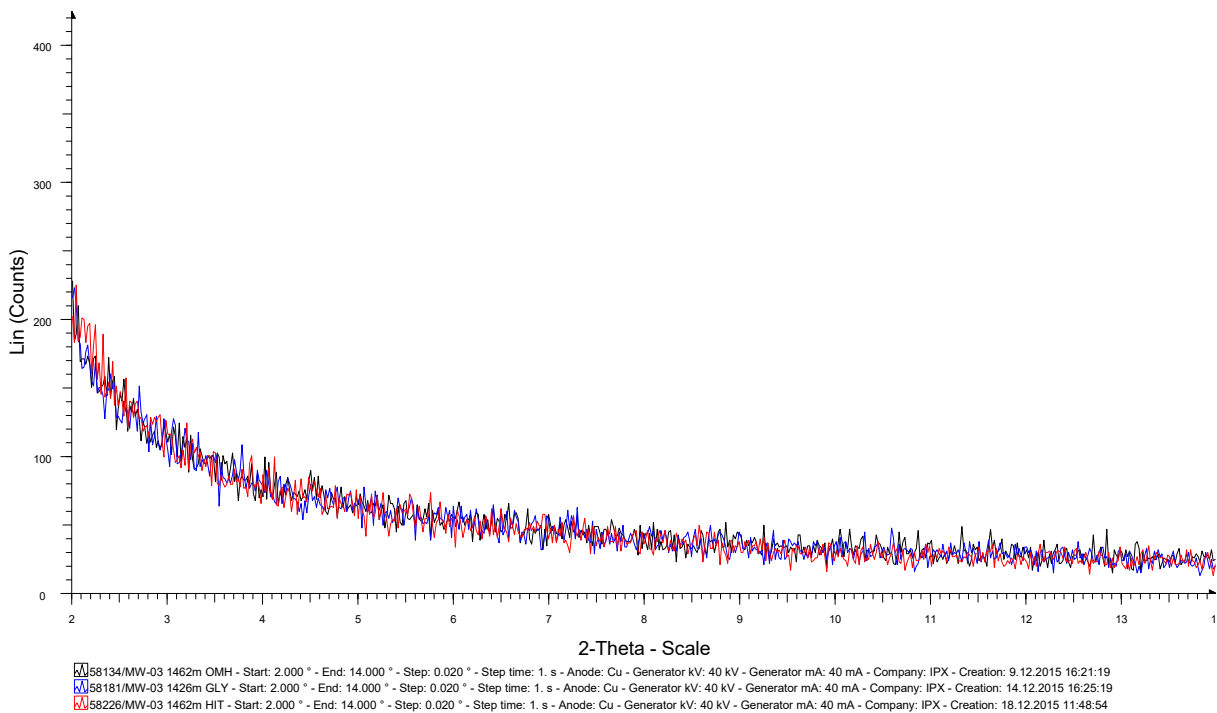
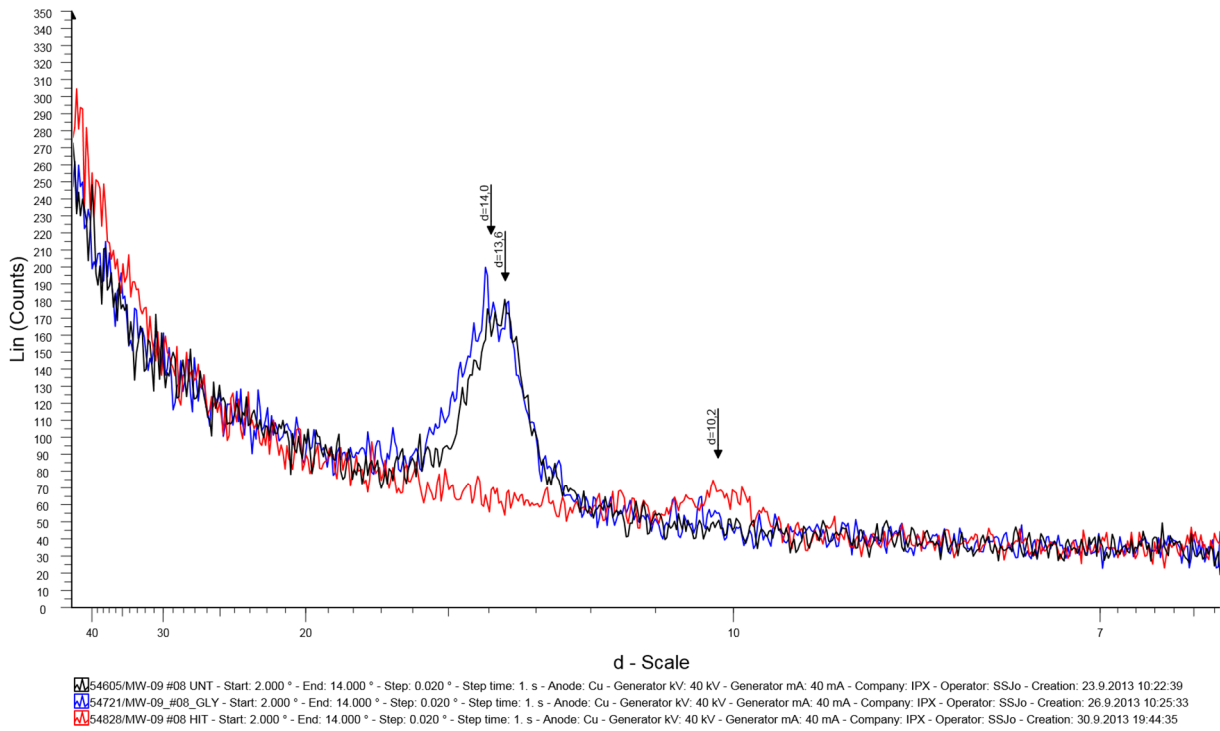FIGURE 2: No clay at 1462 m in well MW-03

Well MW-09

FIGURE 3: Diffractogram for smectite at 820 m in MW-09 with peak at in 13.6 Å untreated, 14 Å in glycolated and when heated the peak at 10.2 Å (from Lopeyok, 2013)
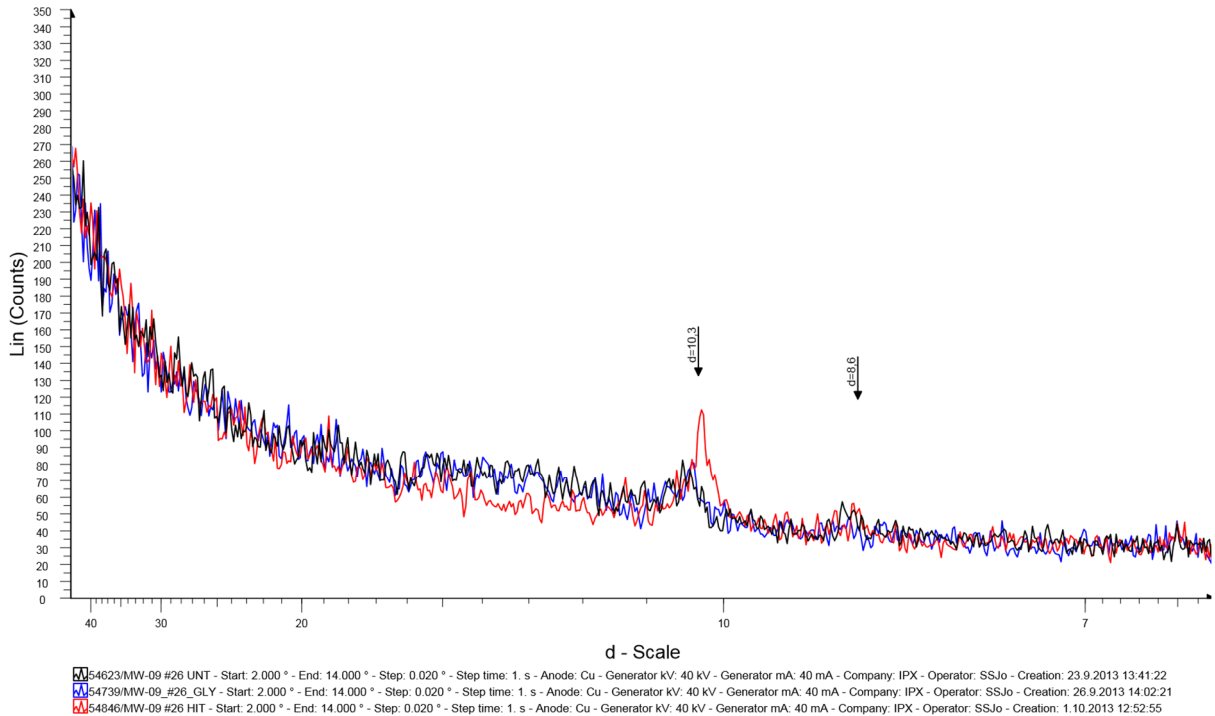

FIGURE 4: Diffractogram for smectite at 1946 m in MW-09 with peak at 10.3Å in untreated, glycolated and when heated (from Lopeyok, 2013)
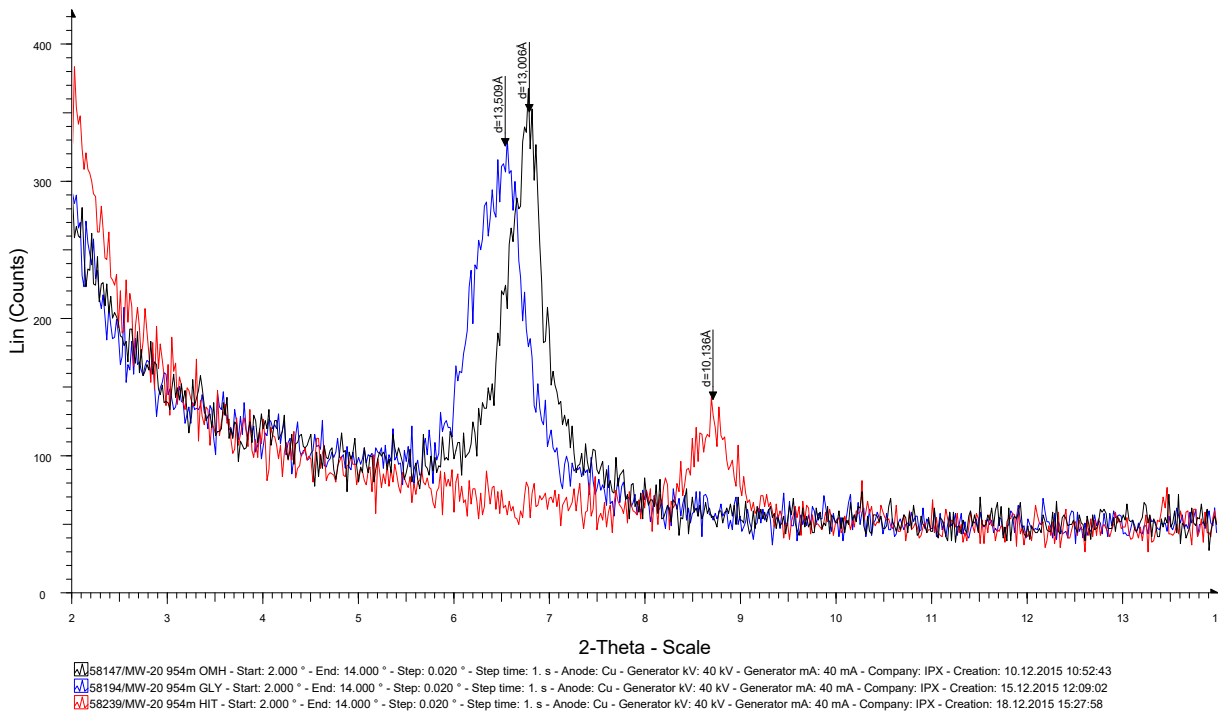
FIGURE 5: Diffractogram for smectite at 954 m in MW-20 with peak at 13.006 Å in untreated, 13.509 Å in glycolated and when heated the peak at 10.136 Å
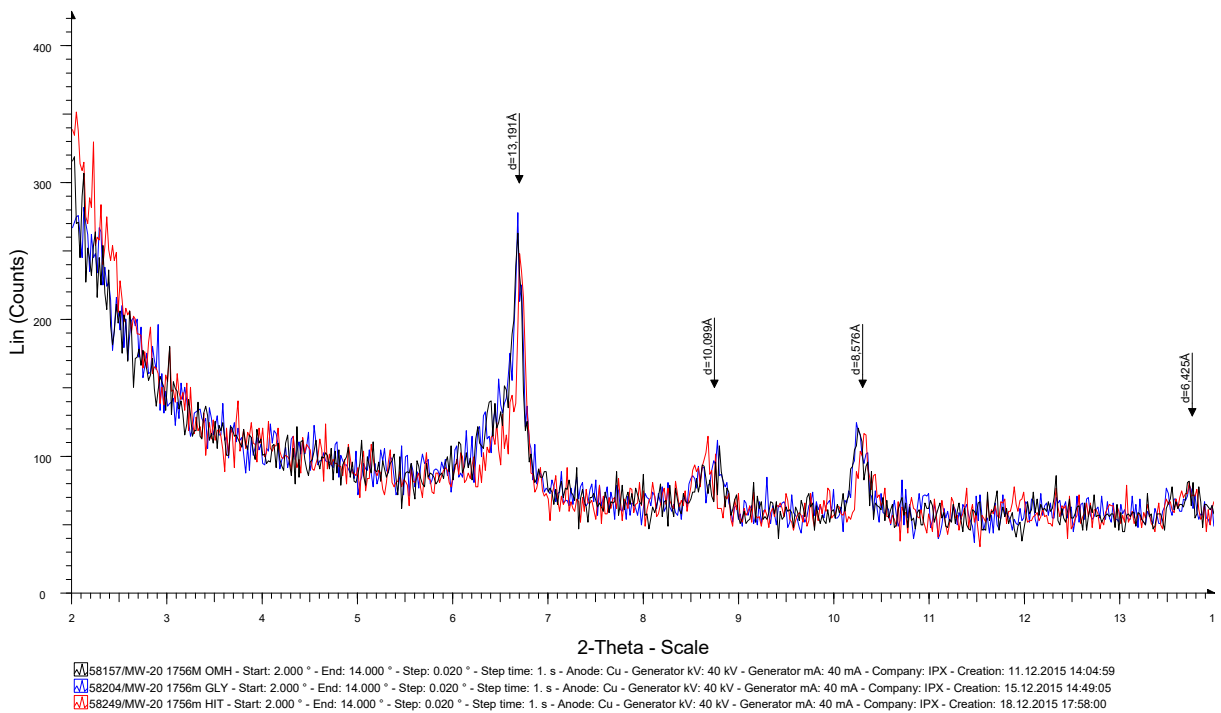

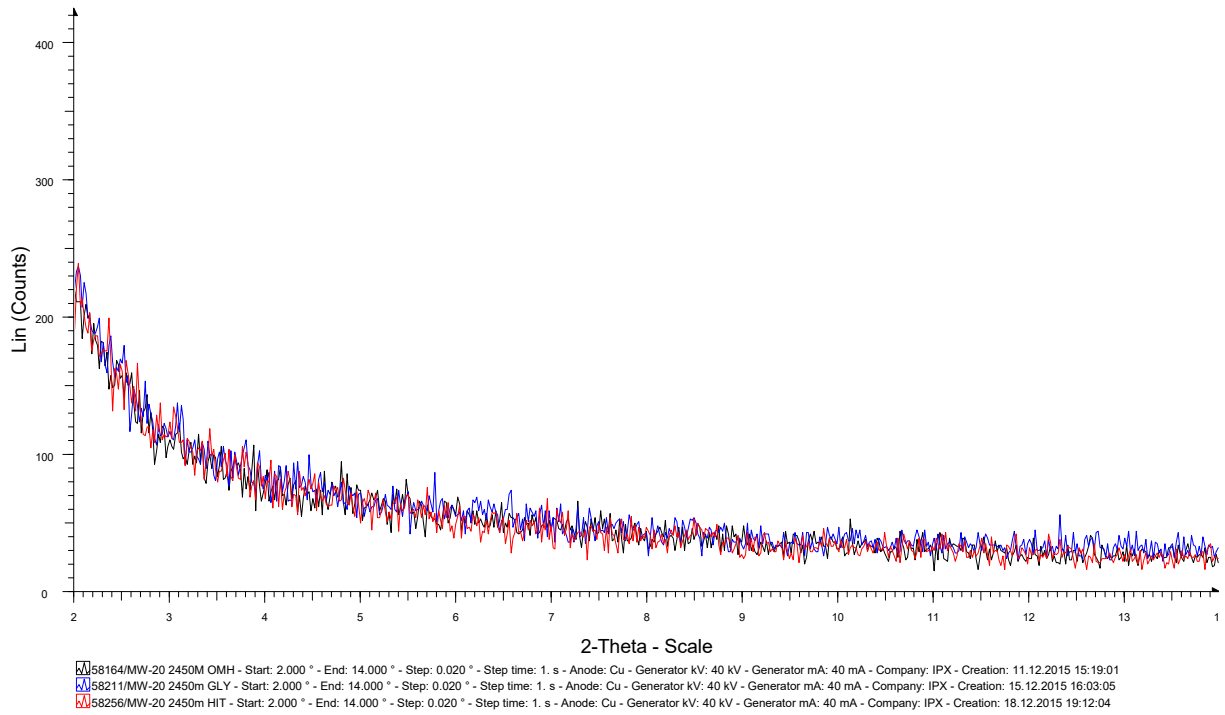FIGURE 6: Diffractogram for chlorite and illite at 1754 m in MW-20; chlorite with peak at 13.191 Å in untreated, glycolated and heated sample. Illite with peak at 10.136 Å

FIGURE 7: No clay at 2450 m in well MW-20